

## Supporting Information for

### Synthesis, biological activity, and binding modes of novel guanidino-containing neonicotinoid derivatives

Jiayang Li,<sup>1</sup> Jing Miao,<sup>1</sup> Peibo Liang,<sup>1</sup> Yiyang Wang,<sup>1</sup> Xingyue Zhou,<sup>1</sup> Huizhe  
Lu,<sup>1</sup> Yanhong Dong,<sup>1</sup> and Jianjun Zhang<sup>1,\*</sup>

<sup>1</sup>*Department of Applied Chemistry, China Agricultural University, Beijing 100193,  
China.*

#### Corresponding authors

Jianjun Zhang: [zhangjianjun@cau.edu.cn](mailto:zhangjianjun@cau.edu.cn)

#### Contents

The Spectra of <sup>1</sup> H, <sup>13</sup> C, and HRMS.....	2-53
Supporting Information.....	54-57



Fig S1. <sup>1</sup>H, <sup>13</sup>C spectra of 4a

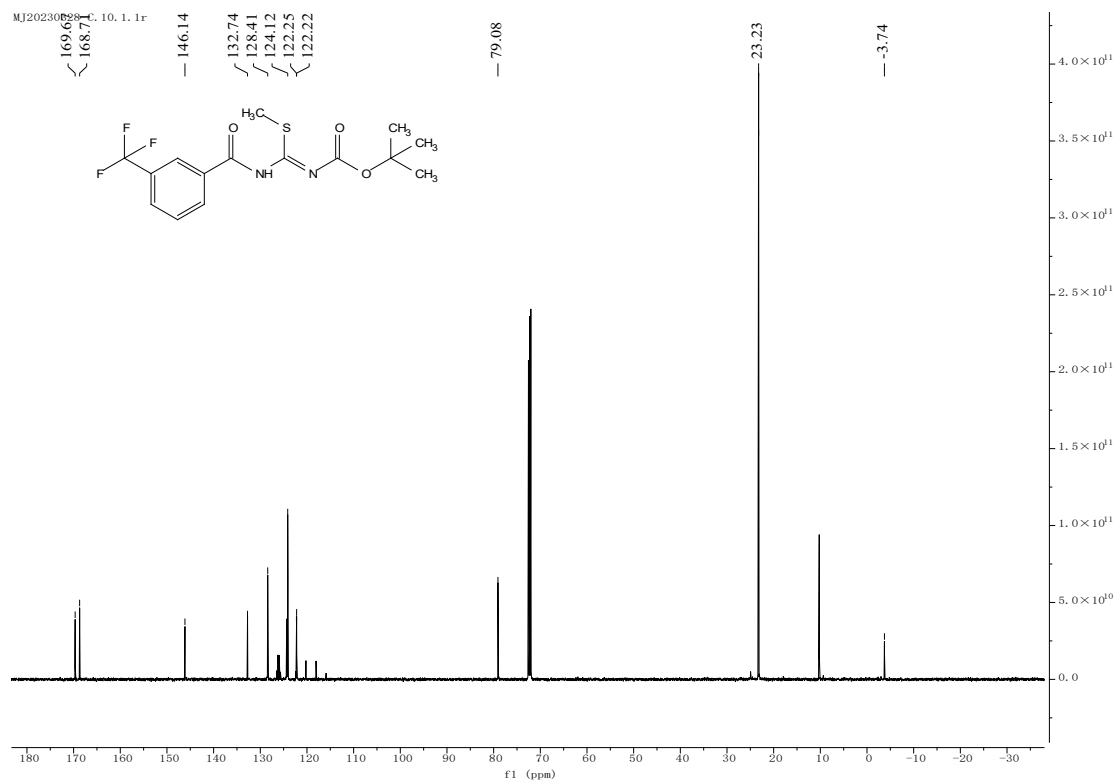
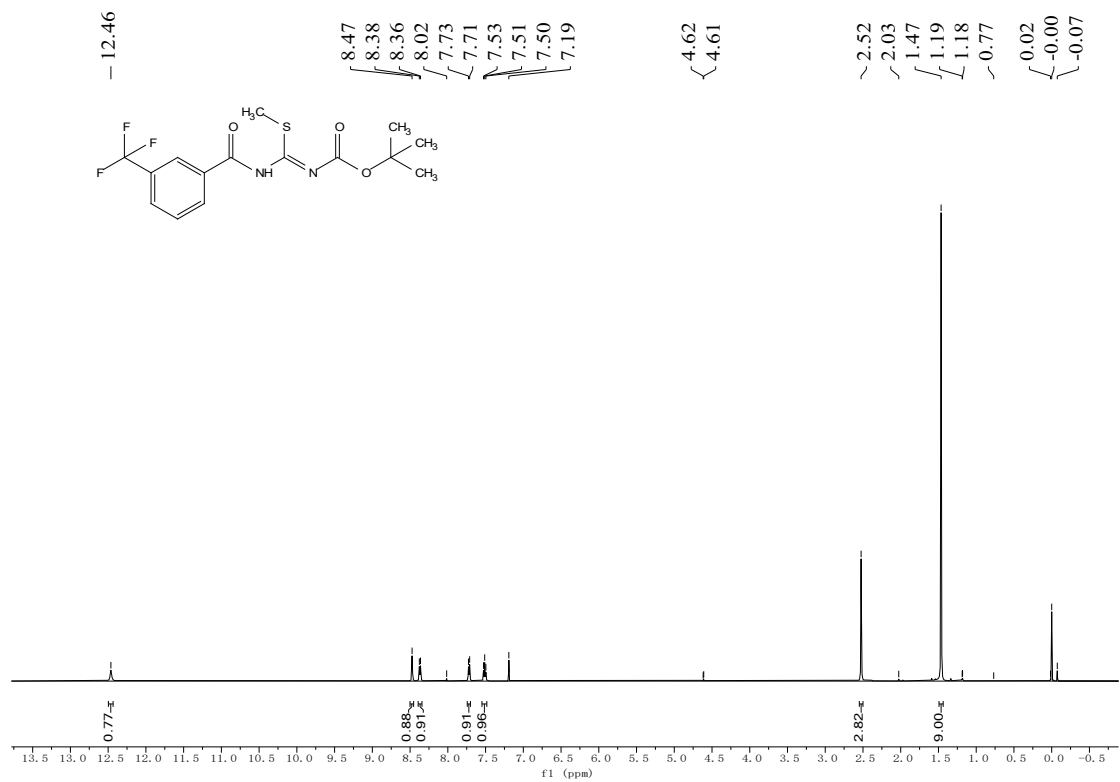


Fig S2. <sup>1</sup>H, <sup>13</sup>C spectra of **4c**

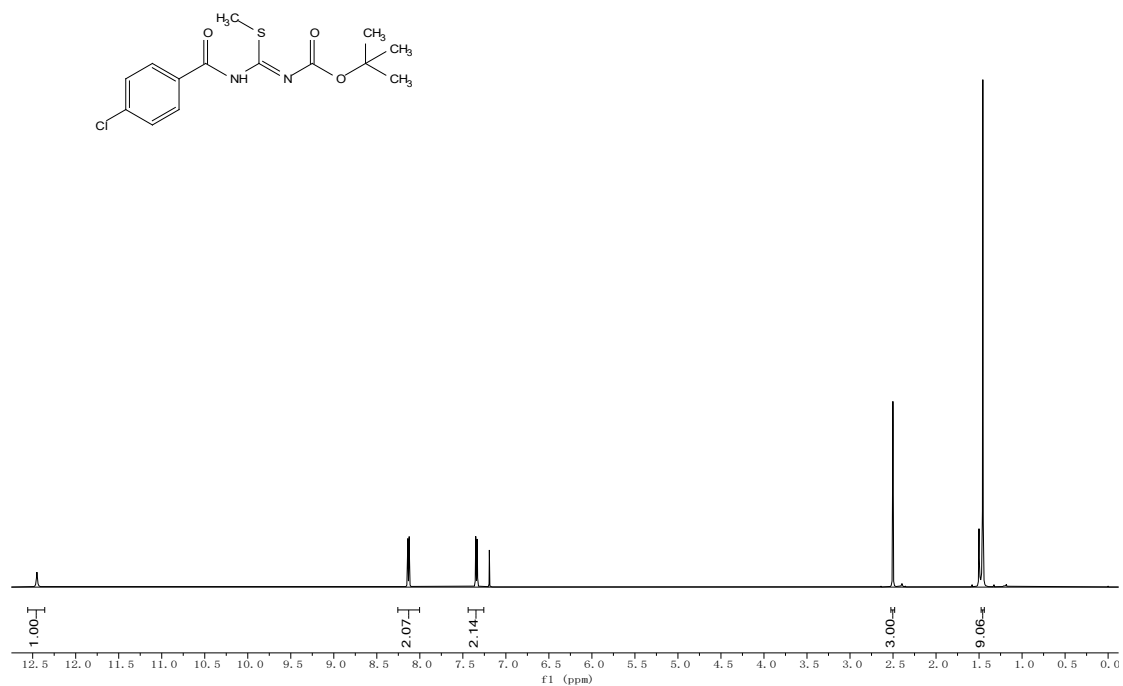
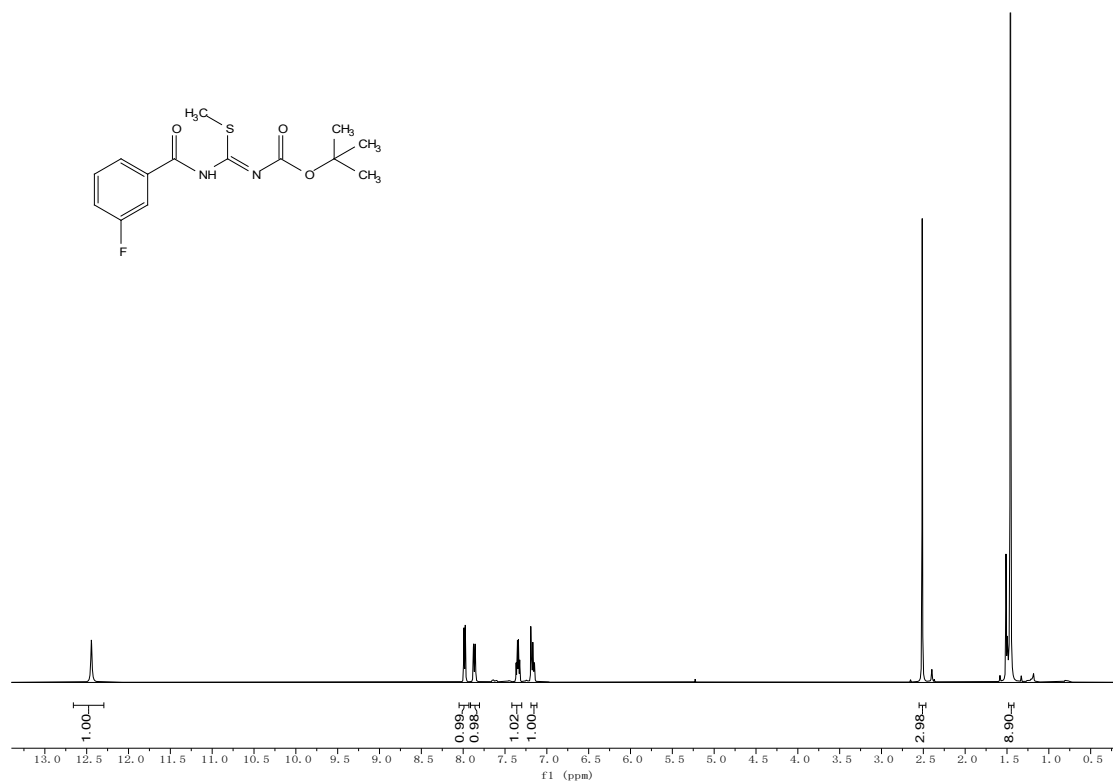


Fig S3. <sup>1</sup>H, <sup>13</sup>C spectra of 4d



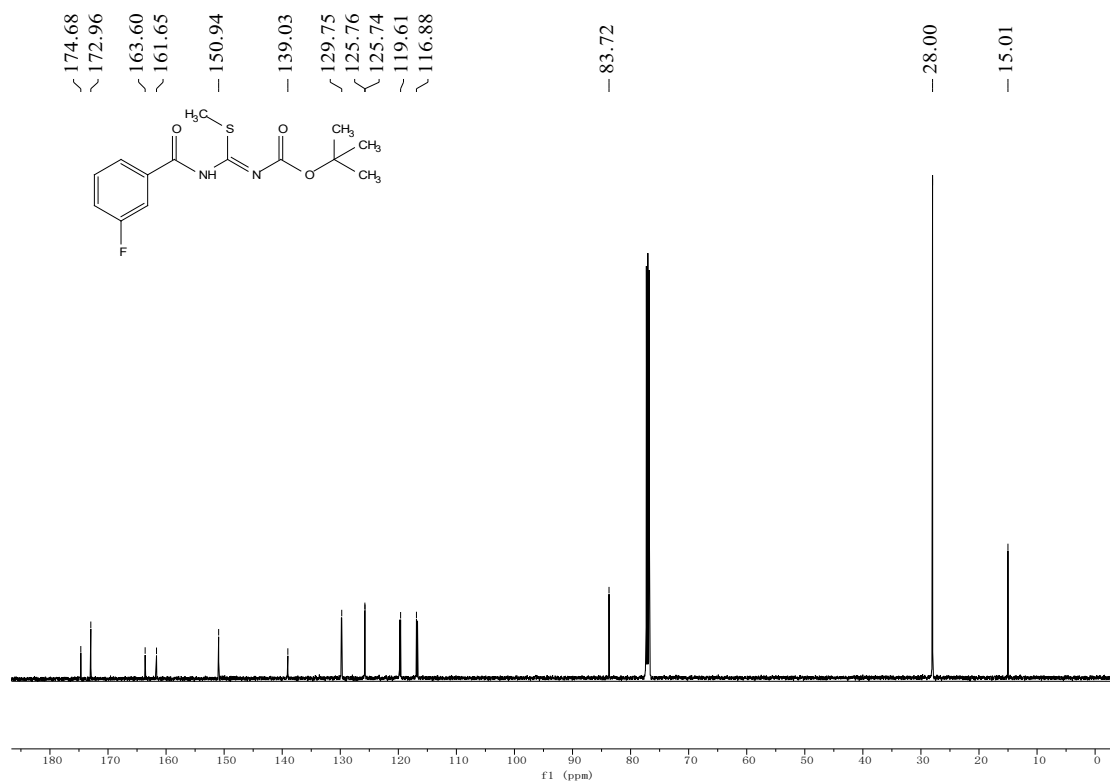
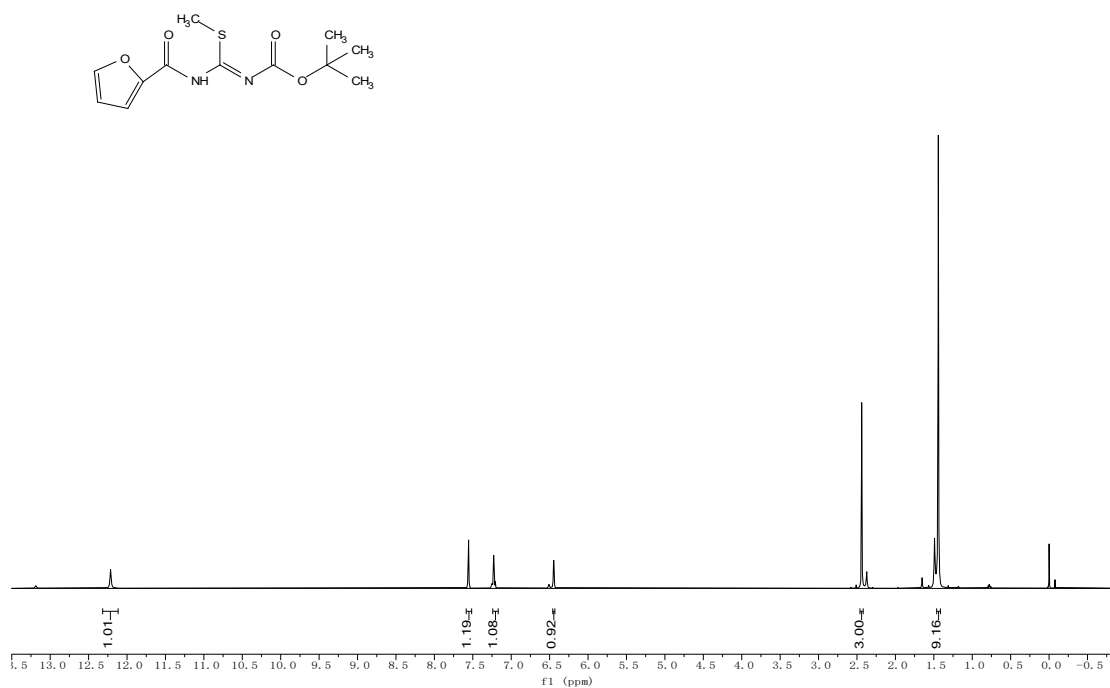


Fig S4. <sup>1</sup>H, <sup>13</sup>C spectra of 4e



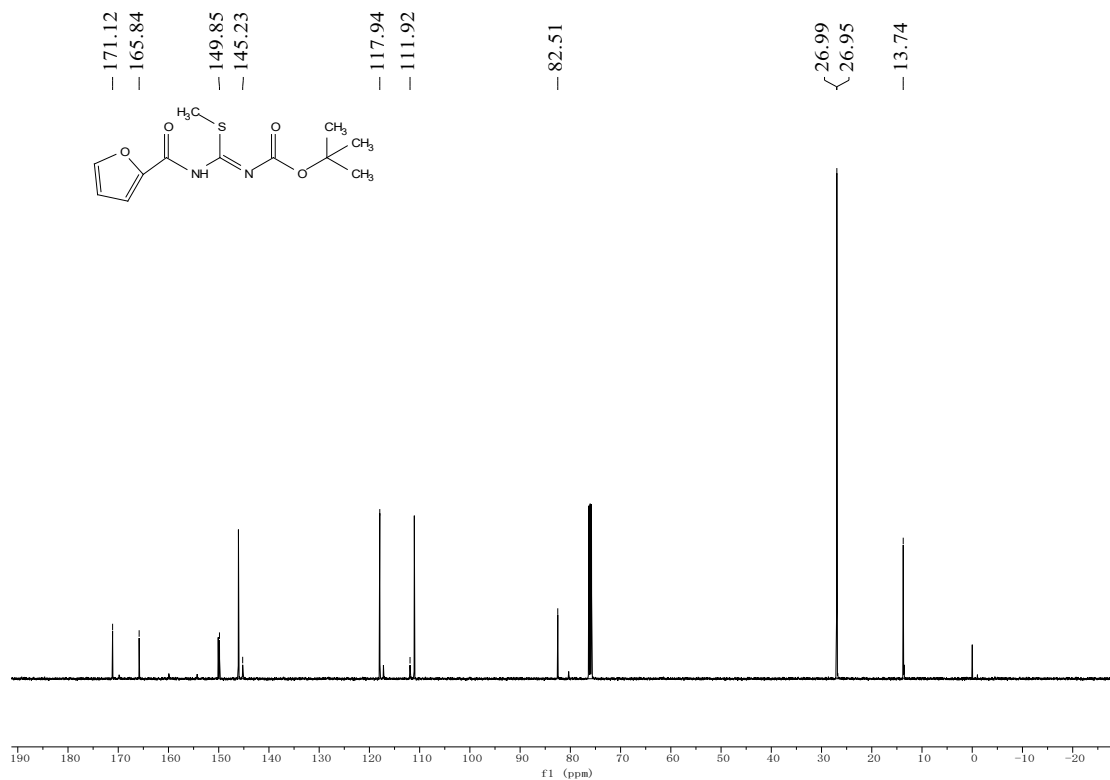
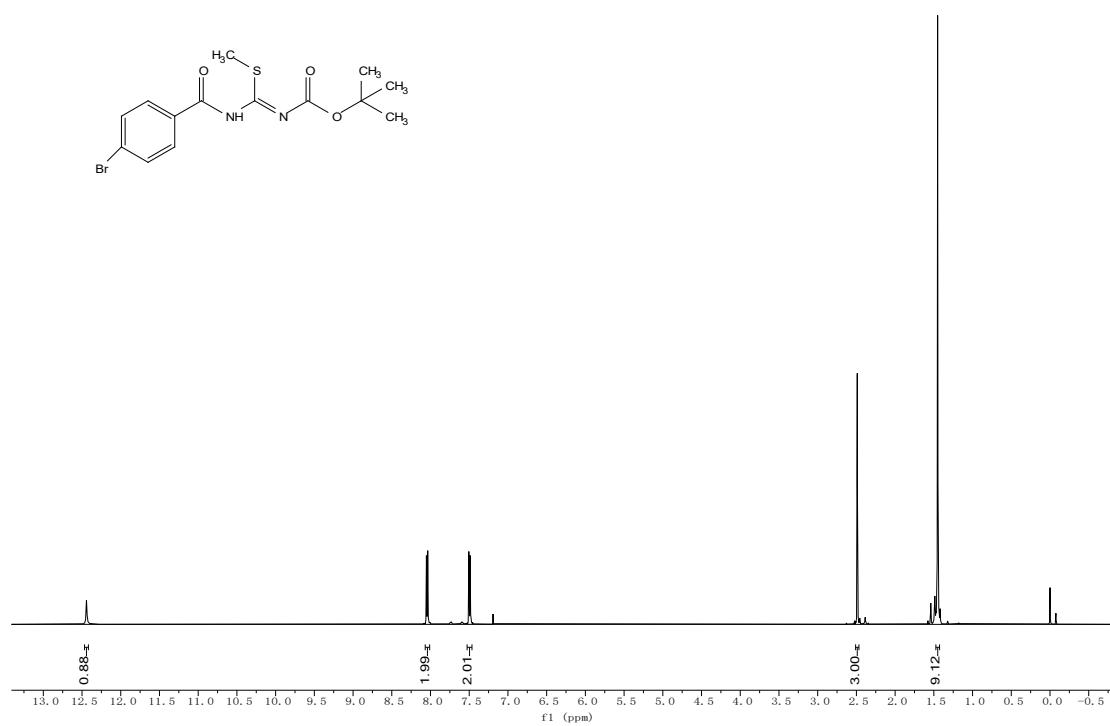


Fig S5. <sup>1</sup>H, <sup>13</sup>C spectra of **4g**



MJ-7-DU1XU-C, 10, 1, 1r

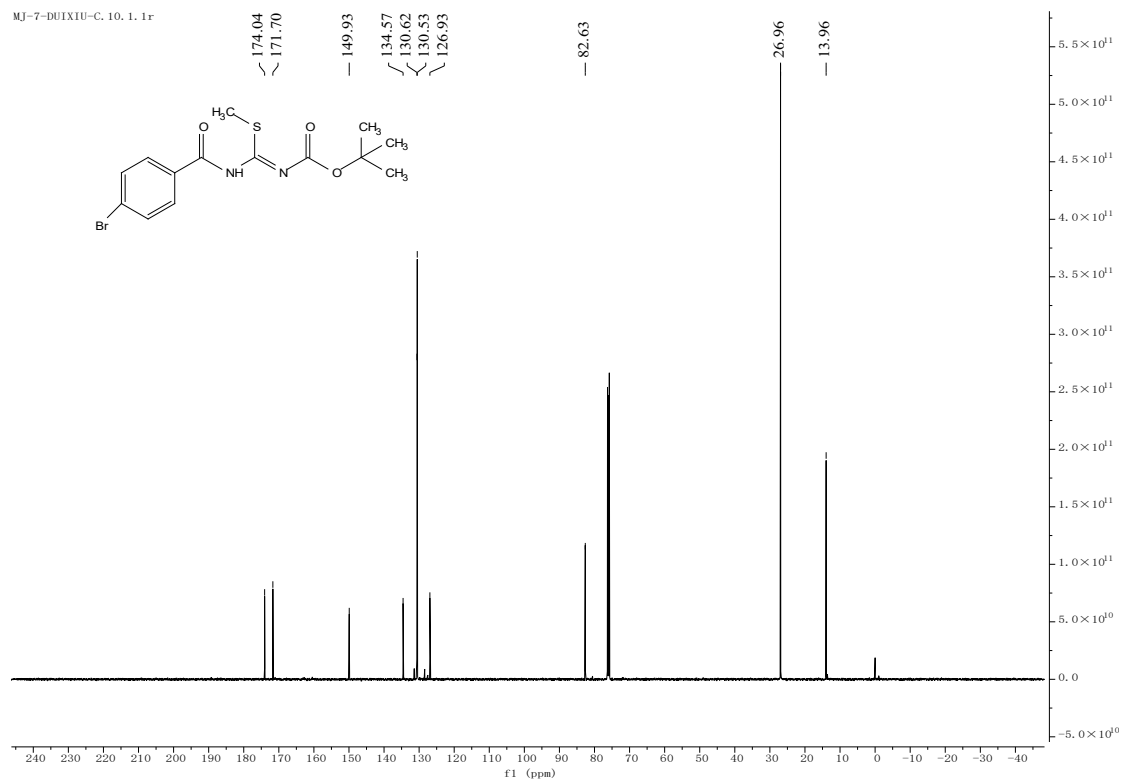
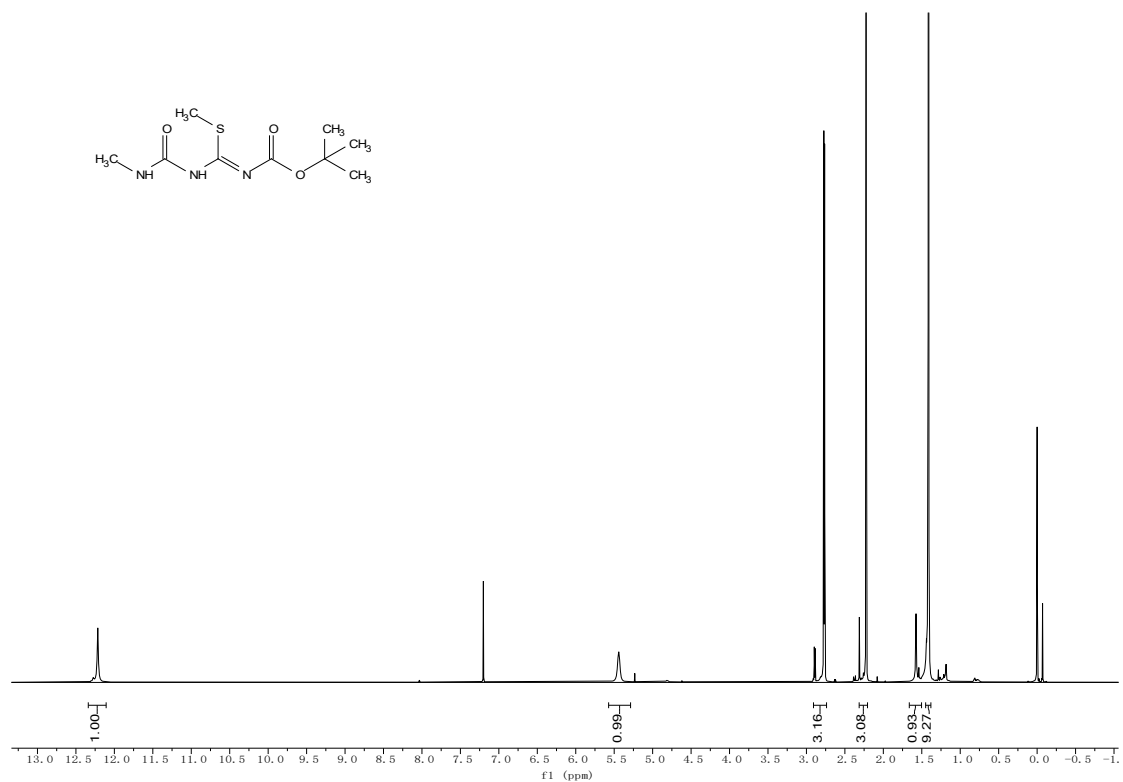


Fig S6.  $^1\text{H}$ ,  $^{13}\text{C}$  spectra of 4h



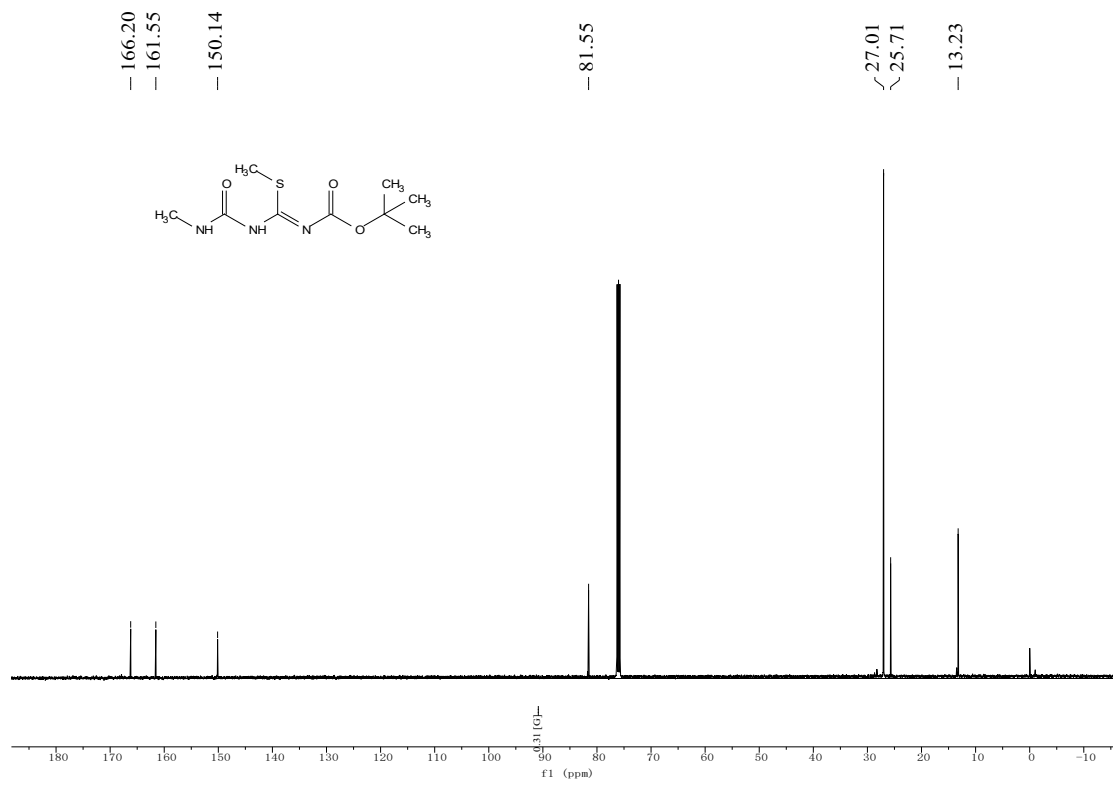
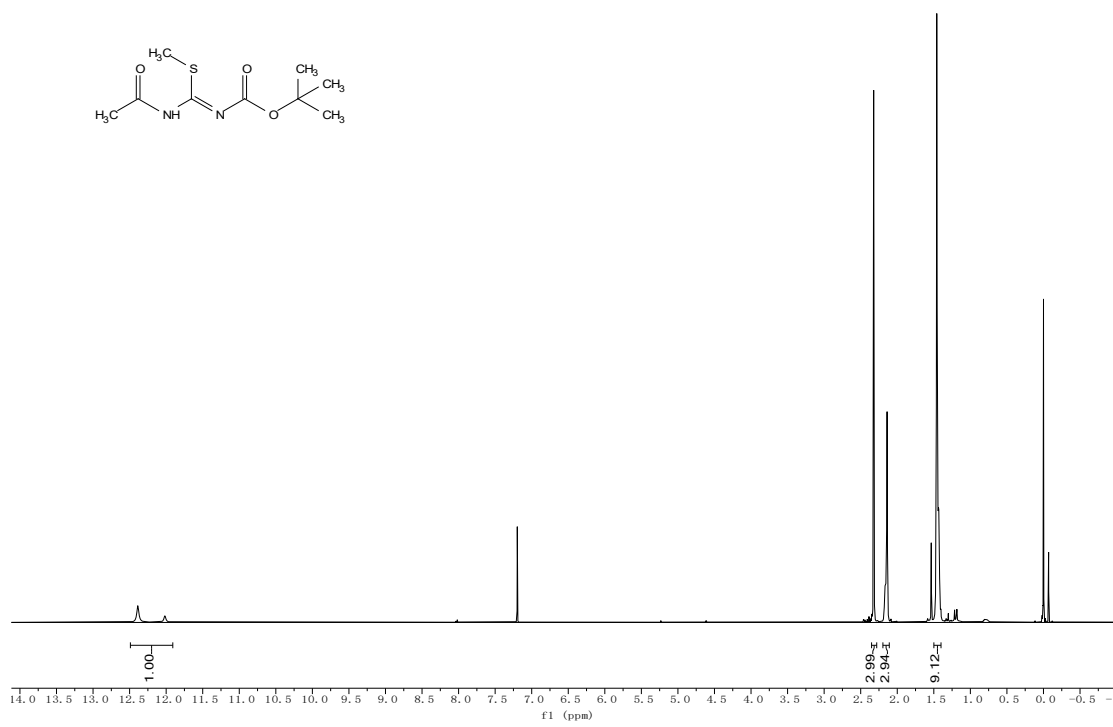


Fig S7.  $^1\text{H}$ ,  $^{13}\text{C}$  spectra of 4i





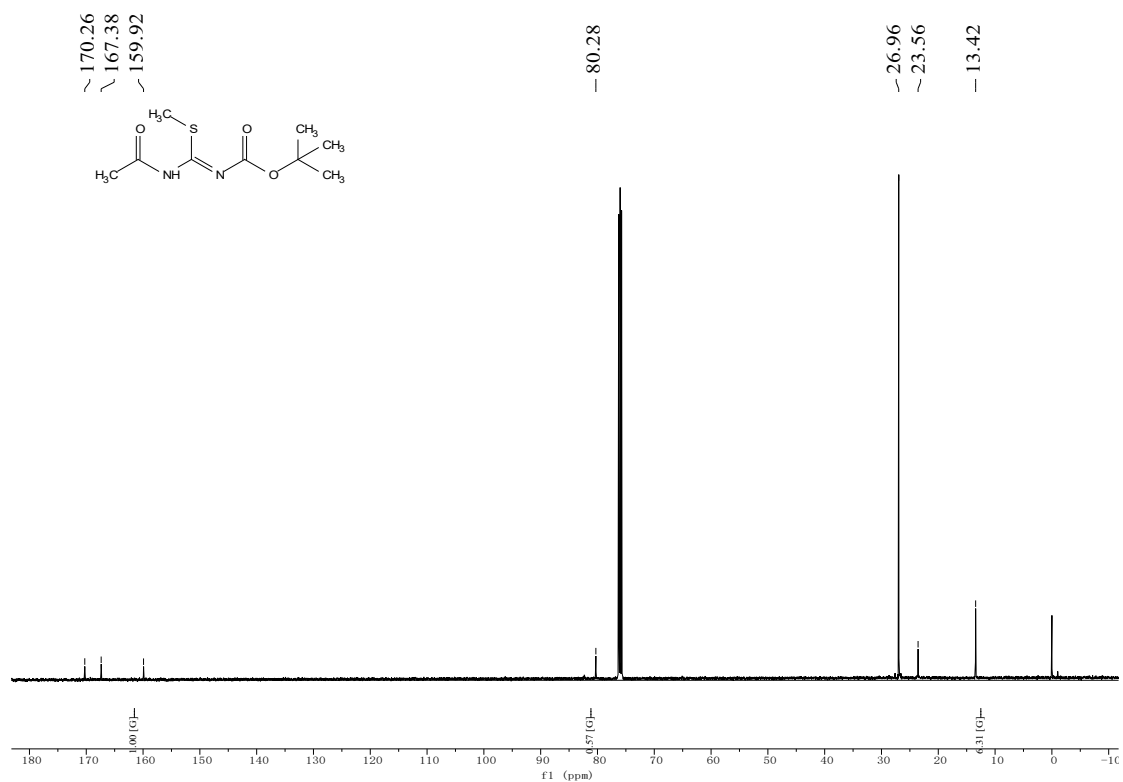
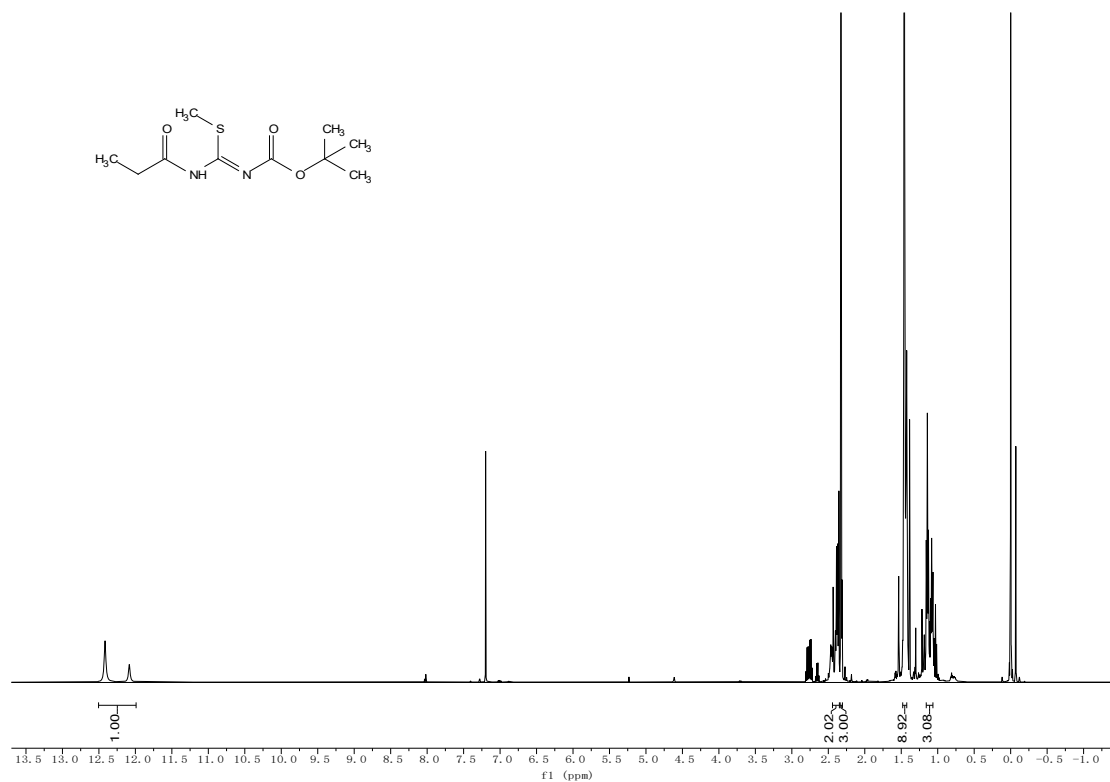


Fig S9.  $^1\text{H}$ ,  $^{13}\text{C}$  spectra of 4j



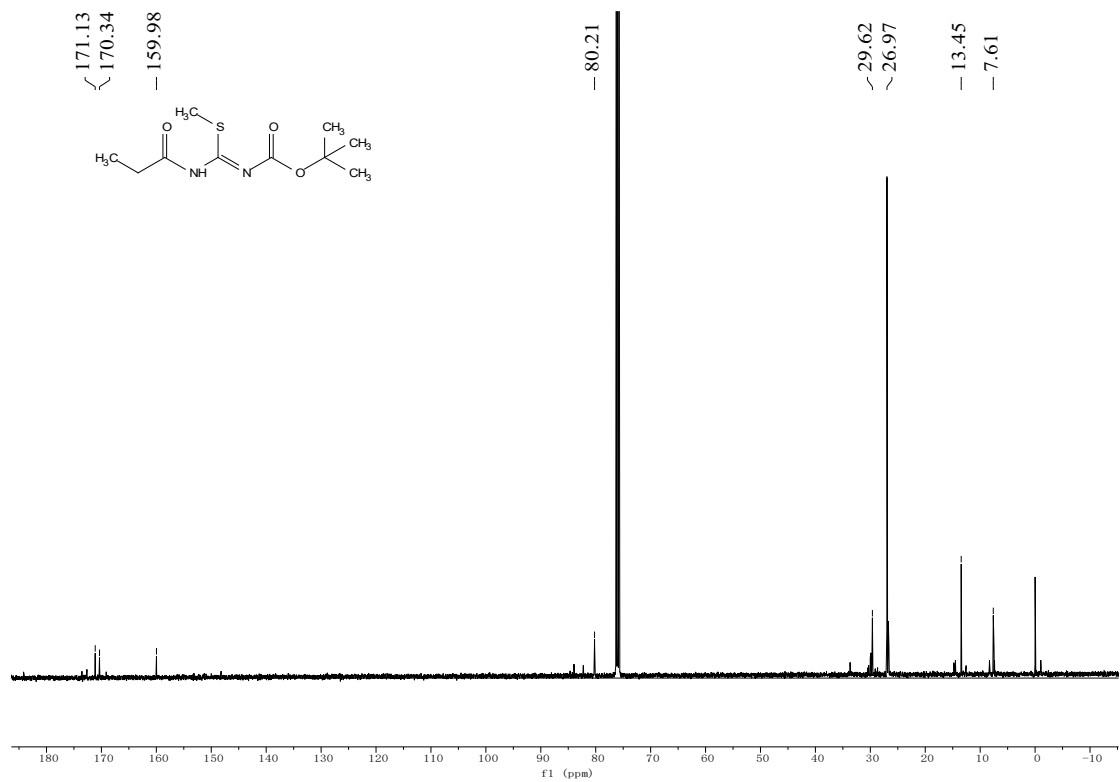
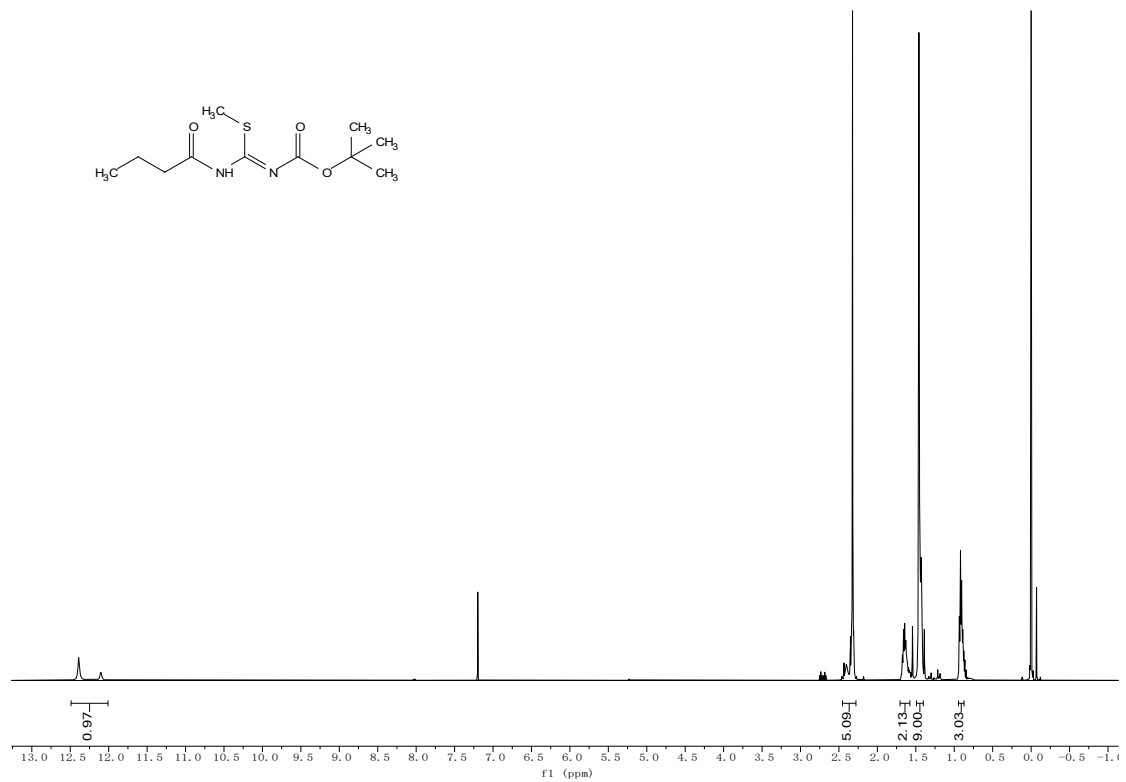


Fig S10. <sup>1</sup>H, <sup>13</sup>C spectra of 4k



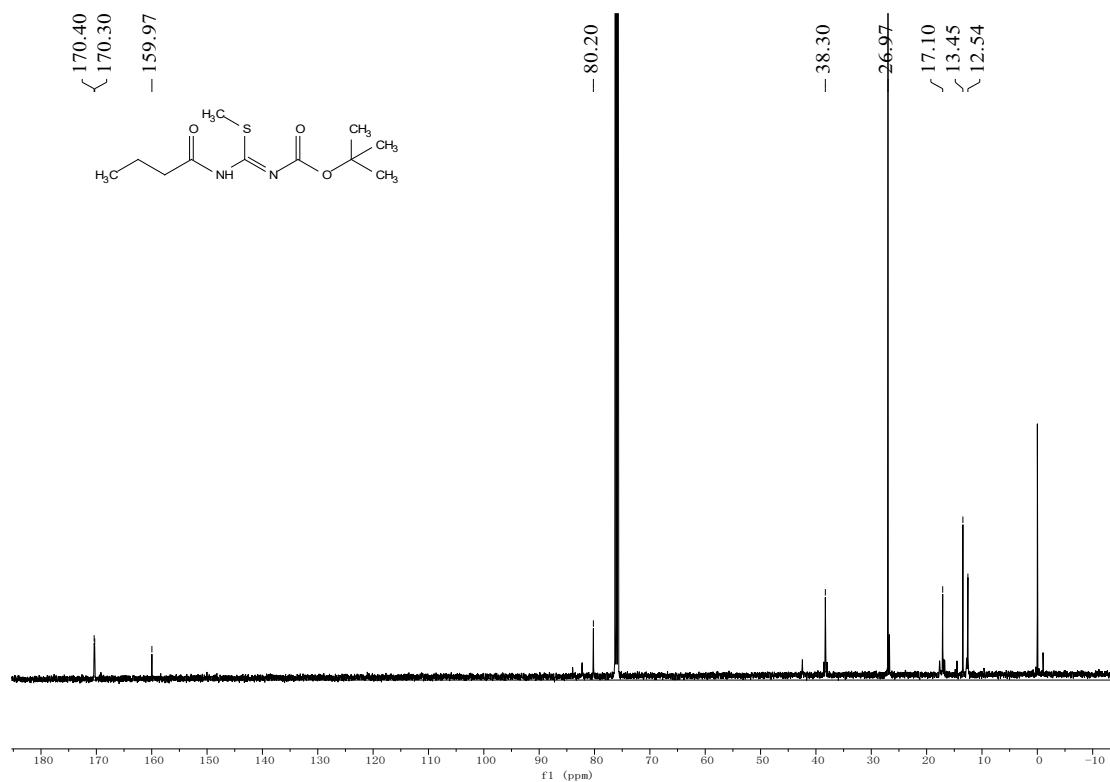


Fig S11.  $^1\text{H}$ ,  $^{13}\text{C}$  spectra of 4l

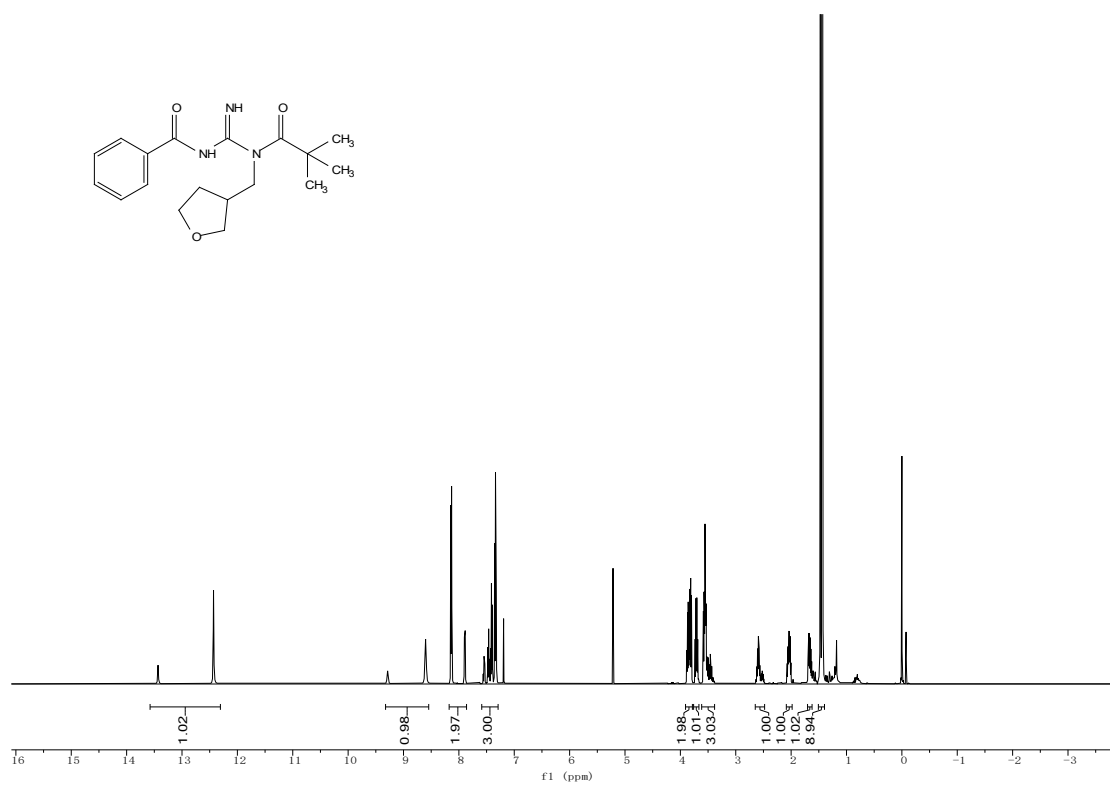
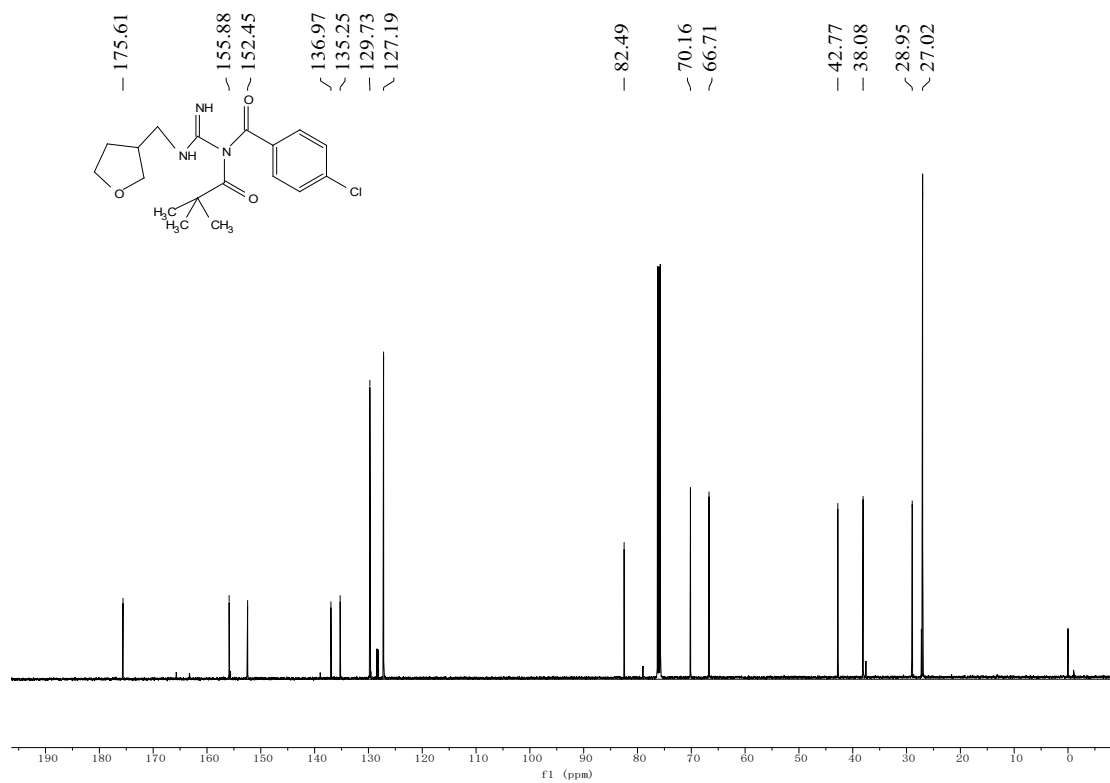
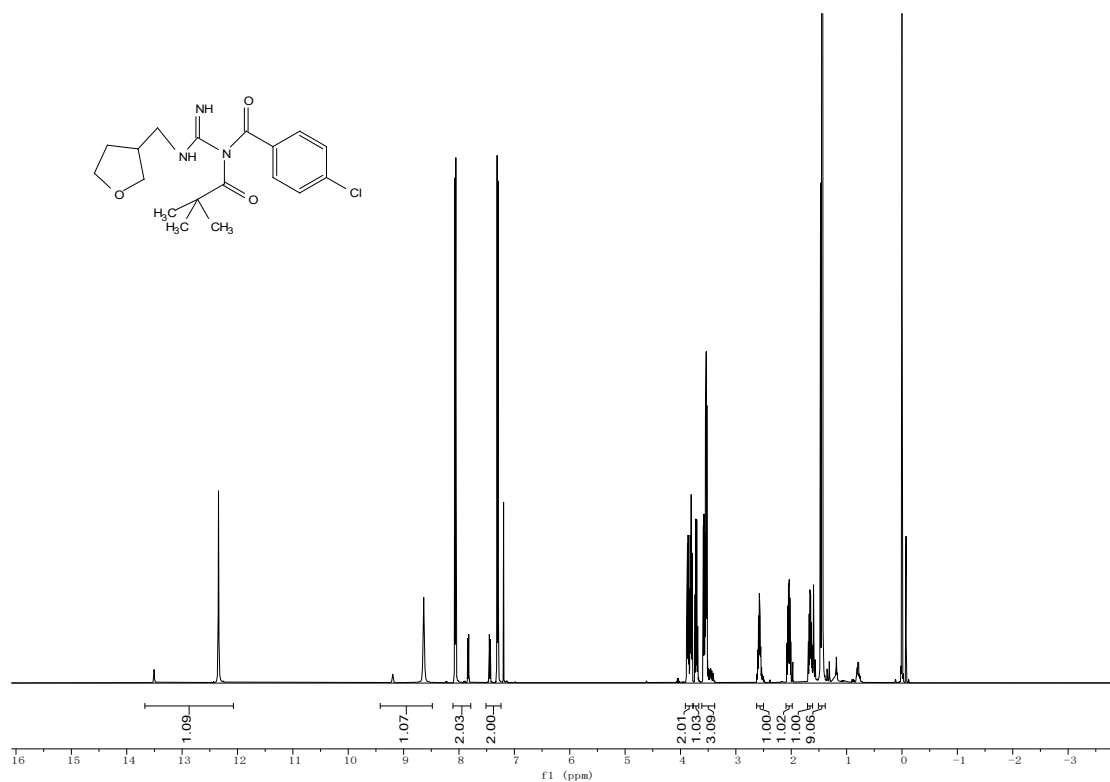


Fig S12.  $^1\text{H}$ ,  $^{13}\text{C}$  spectra of 6a





**Fig S14.** <sup>1</sup>H, <sup>13</sup>C spectra of **6d**

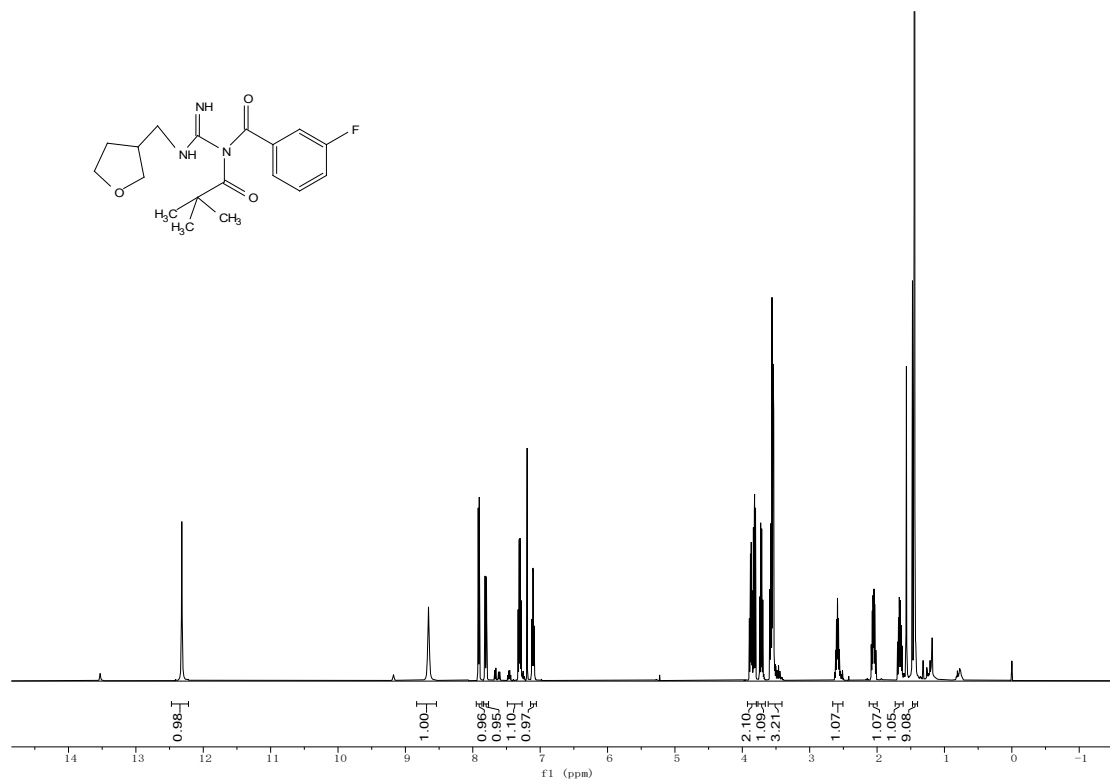
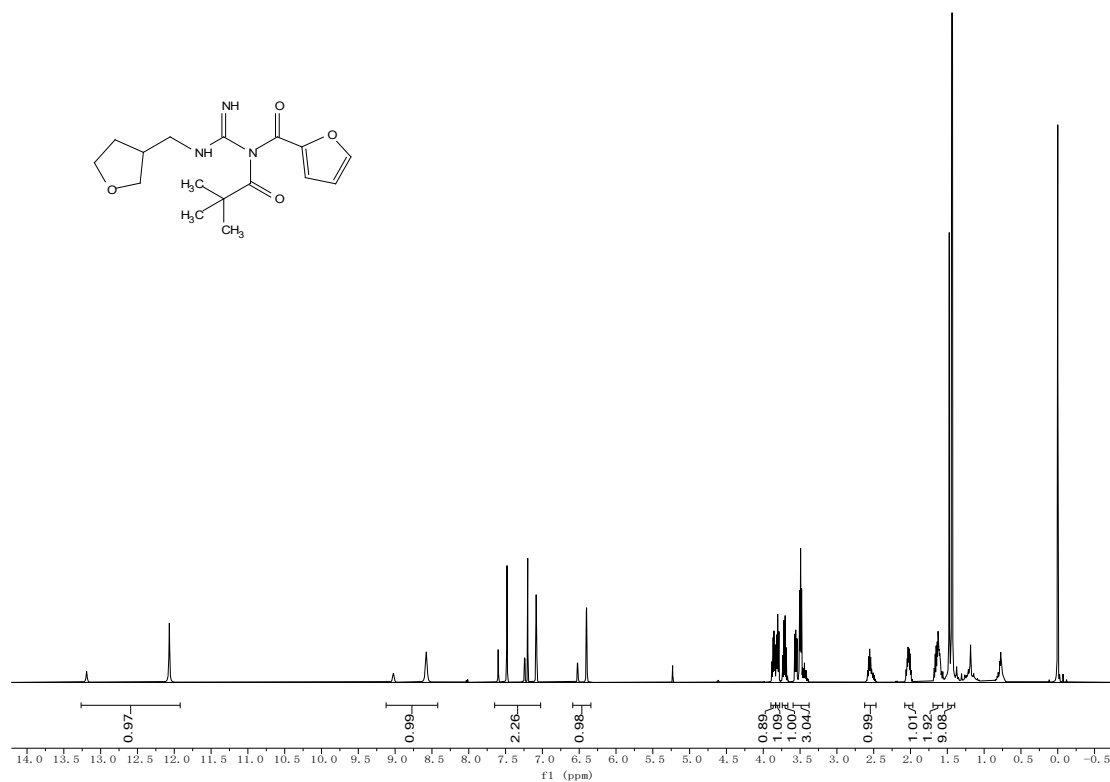
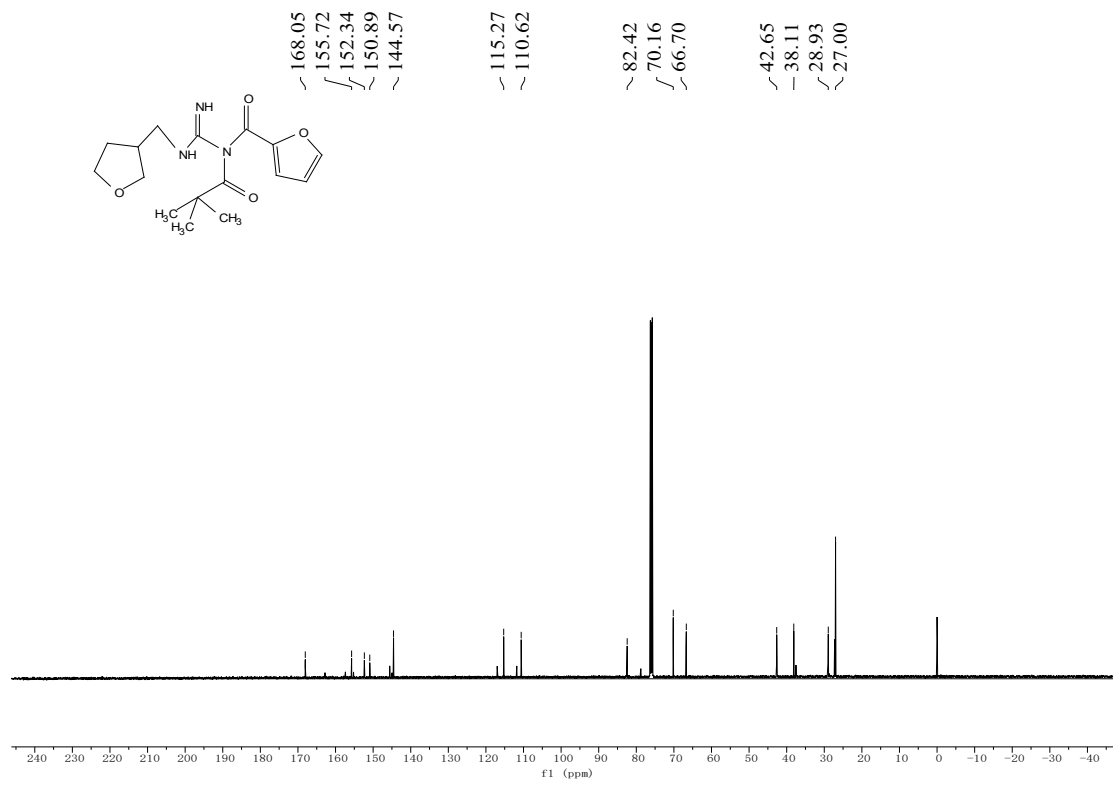
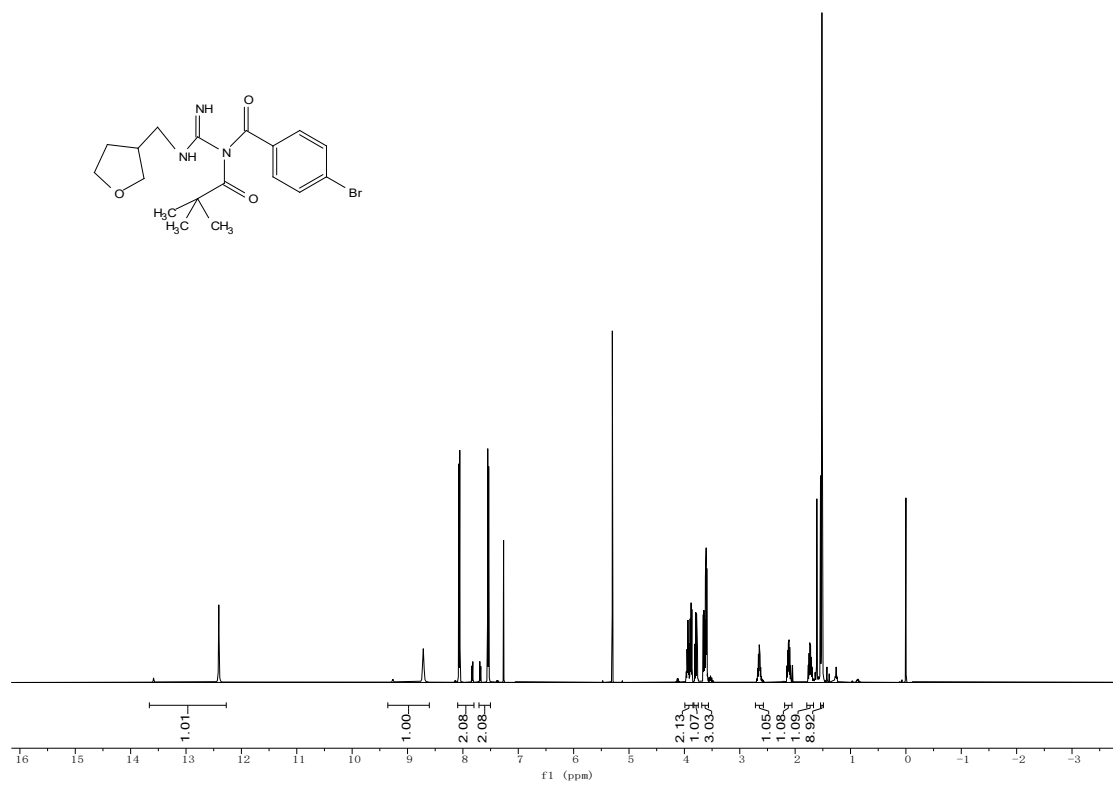


Fig S15. <sup>1</sup>H, <sup>13</sup>C spectra of 6e





**Fig S16.**  $^1\text{H}$ ,  $^{13}\text{C}$  spectra of **6g**



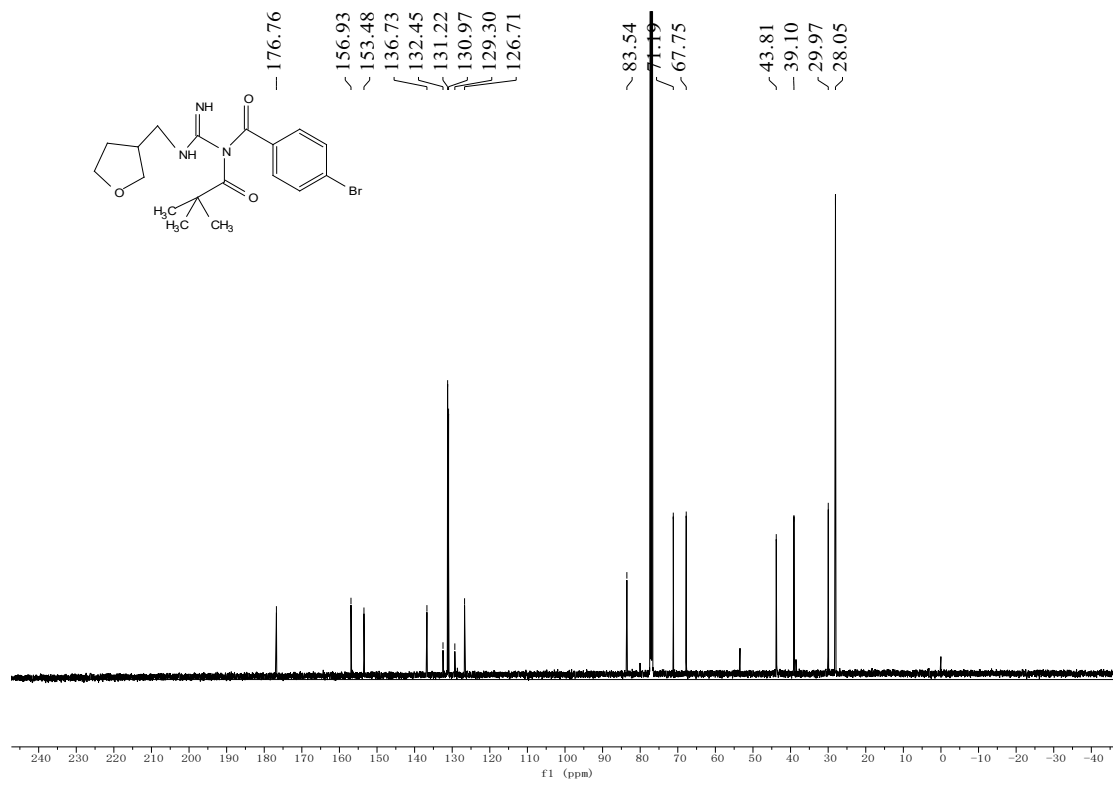
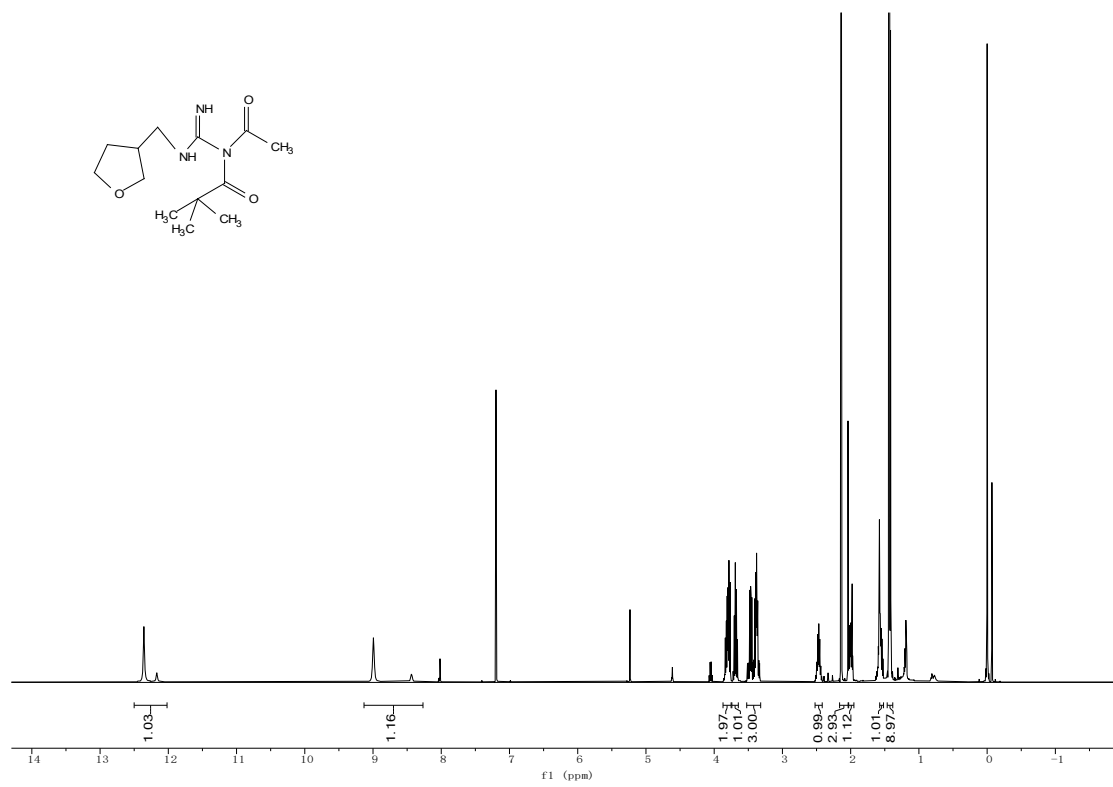


Fig S17. <sup>1</sup>H, <sup>13</sup>C spectra of 6h





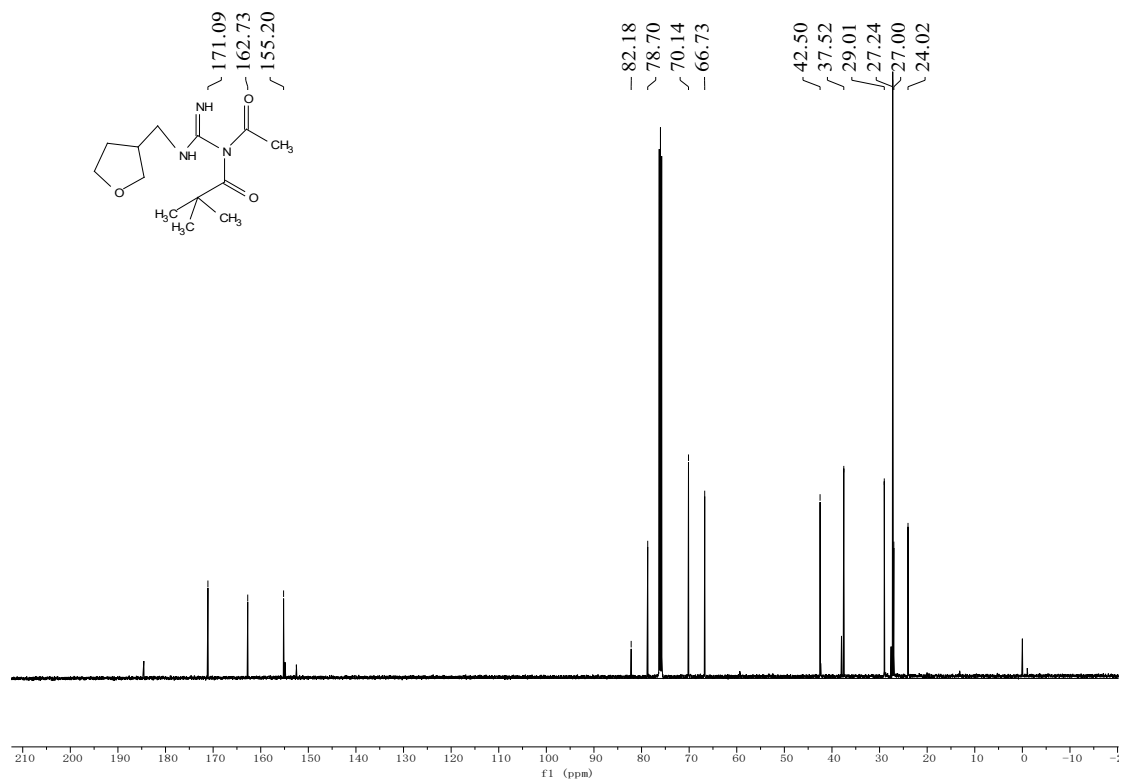
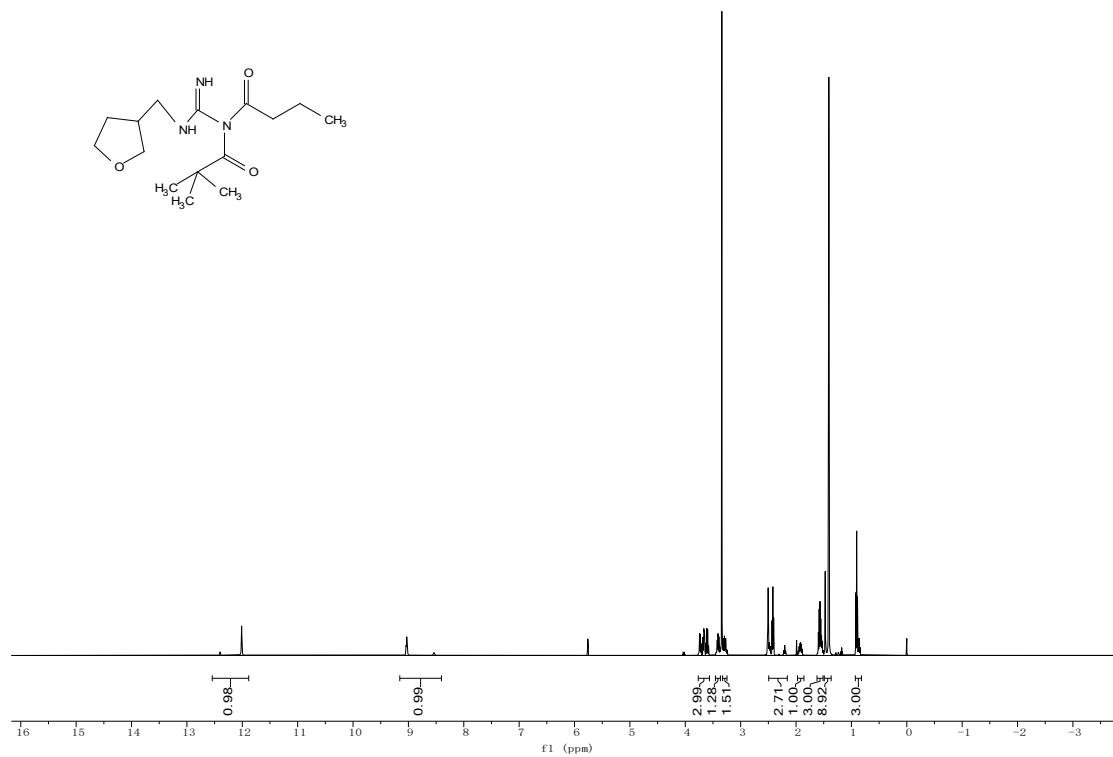


Fig S18. <sup>1</sup>H, <sup>13</sup>C spectra of 6J



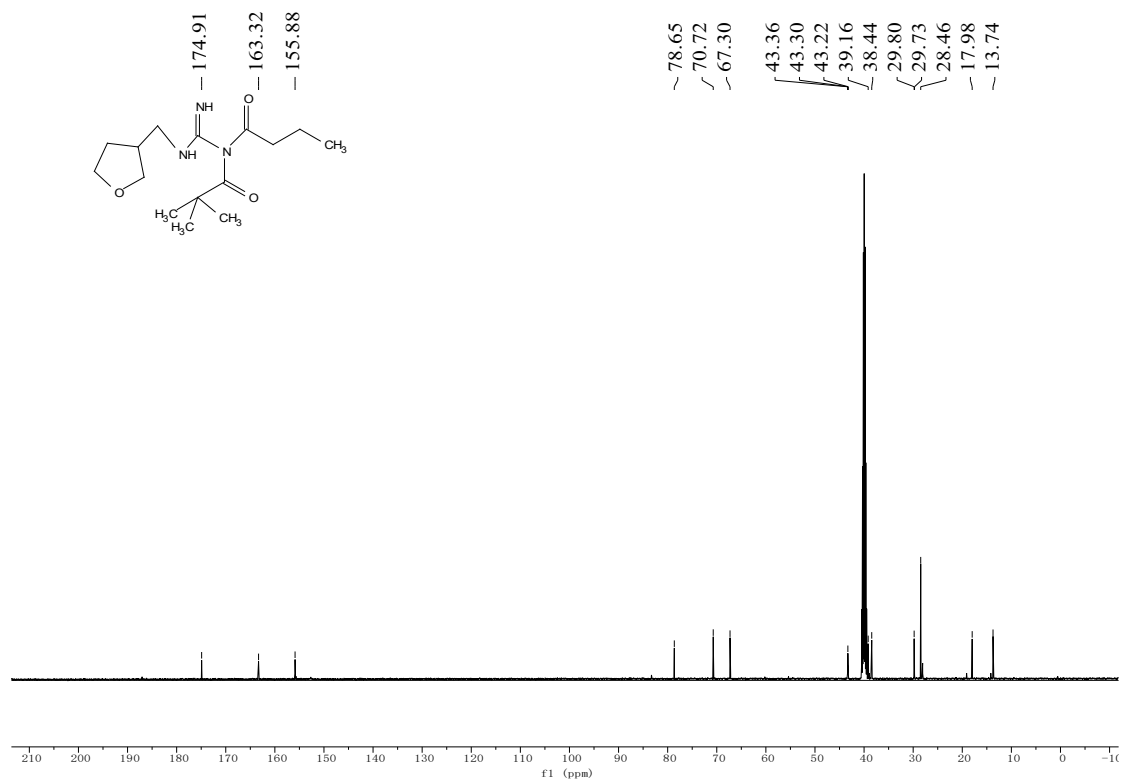
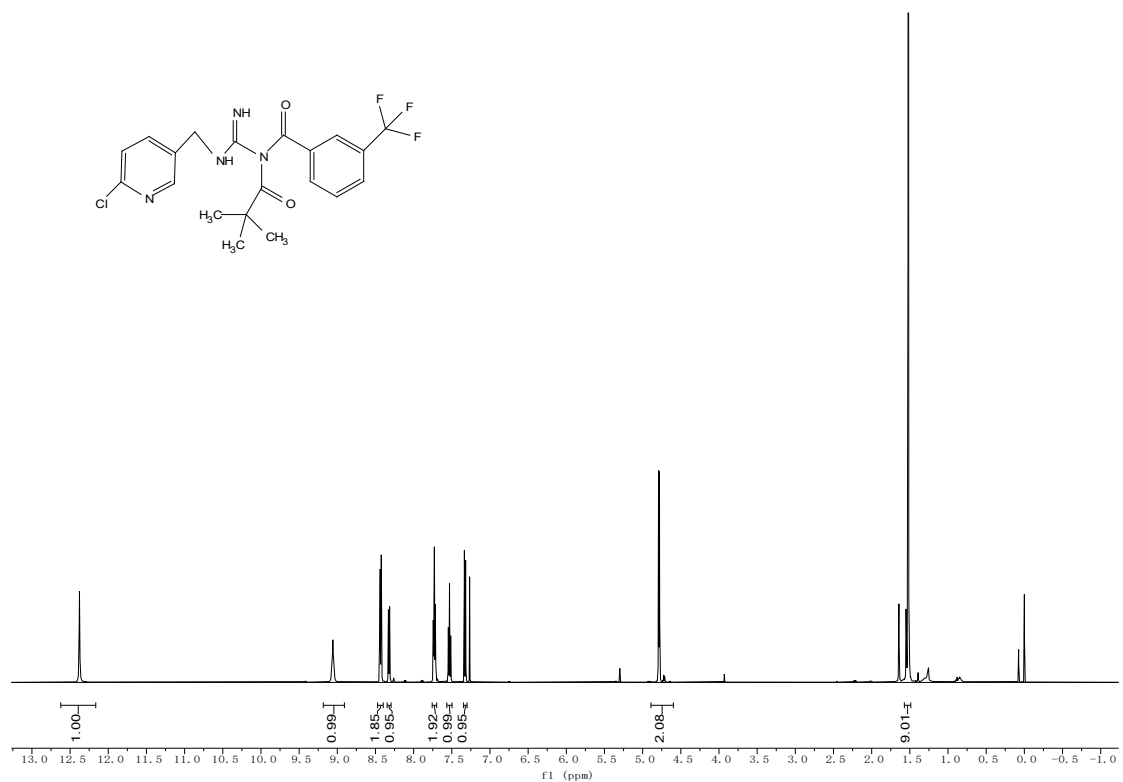


Fig S19.  $^1\text{H}$ ,  $^{13}\text{C}$  spectra of 6k



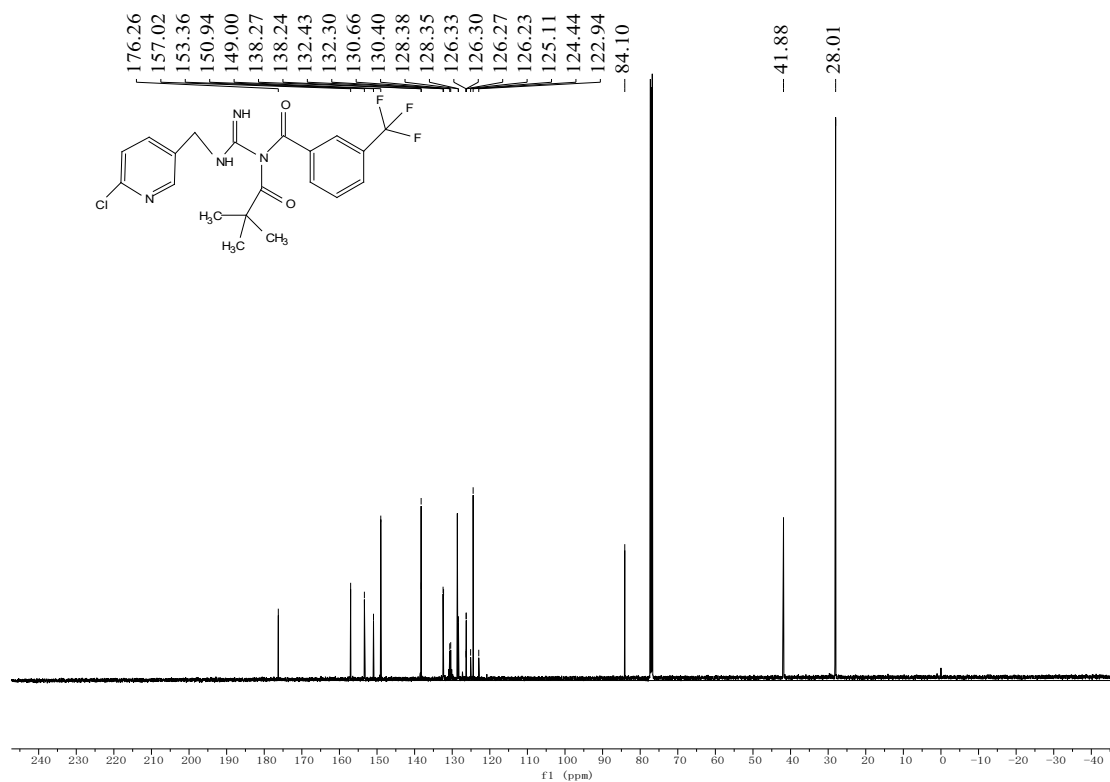


Fig S20. <sup>1</sup>H, <sup>13</sup>C spectra of 6l

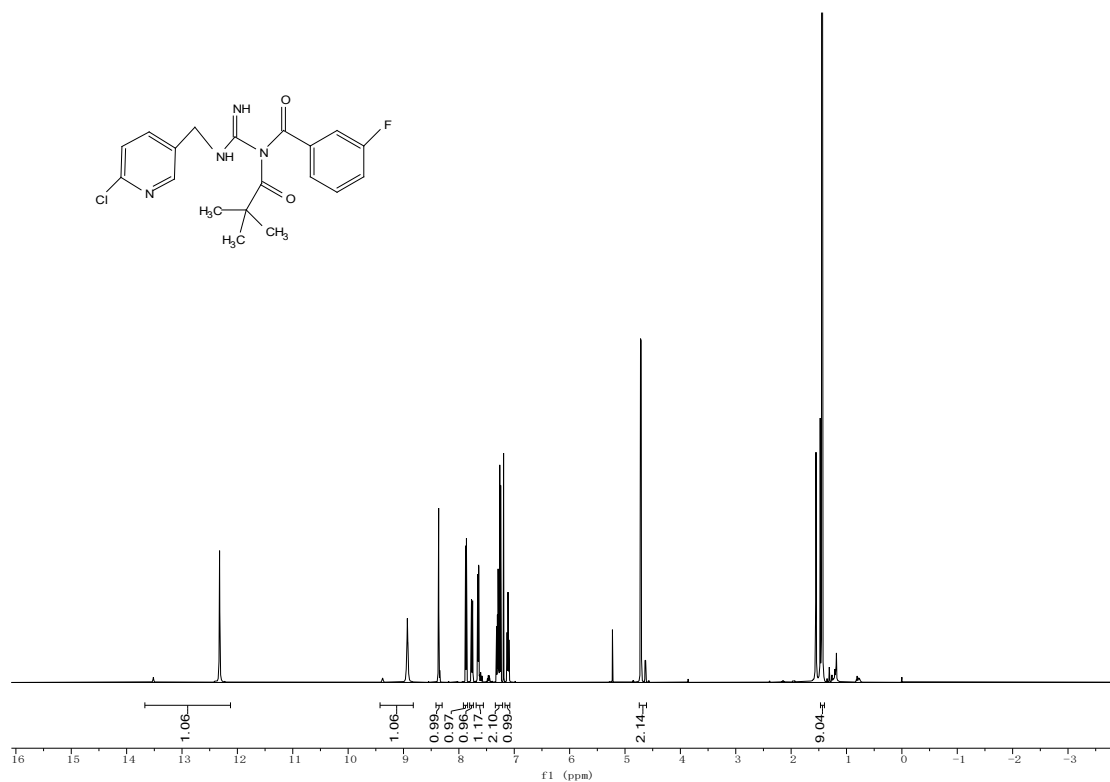
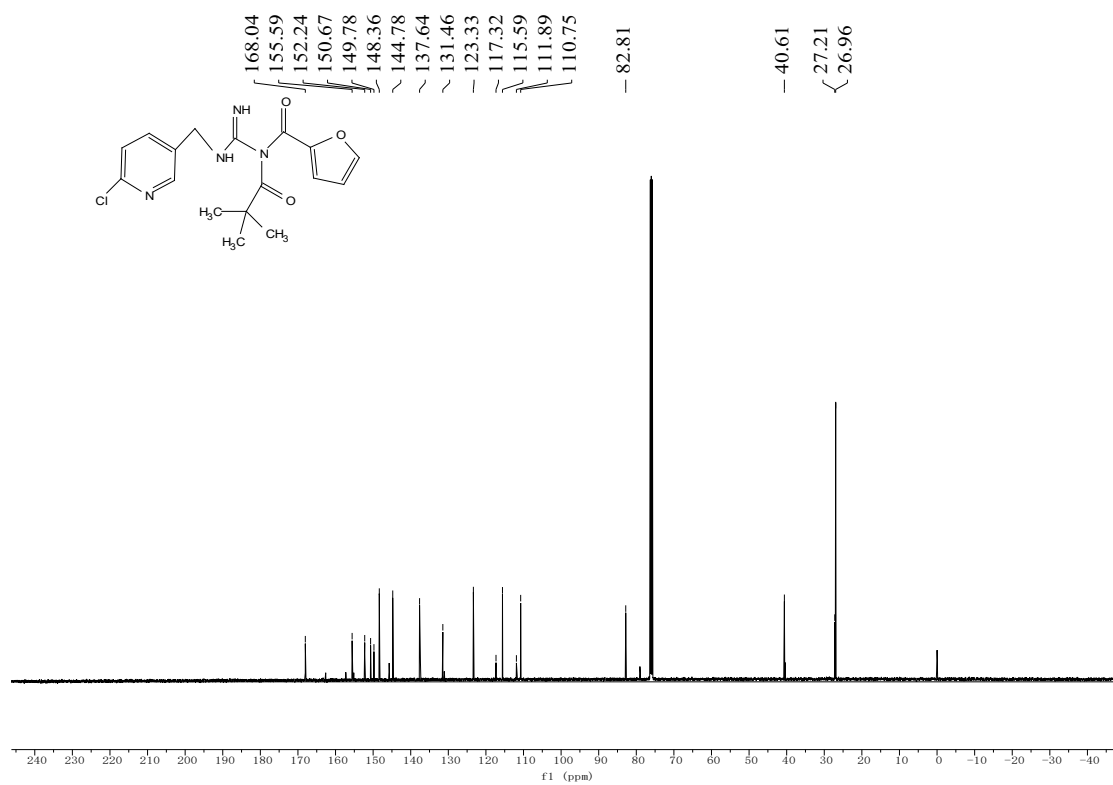
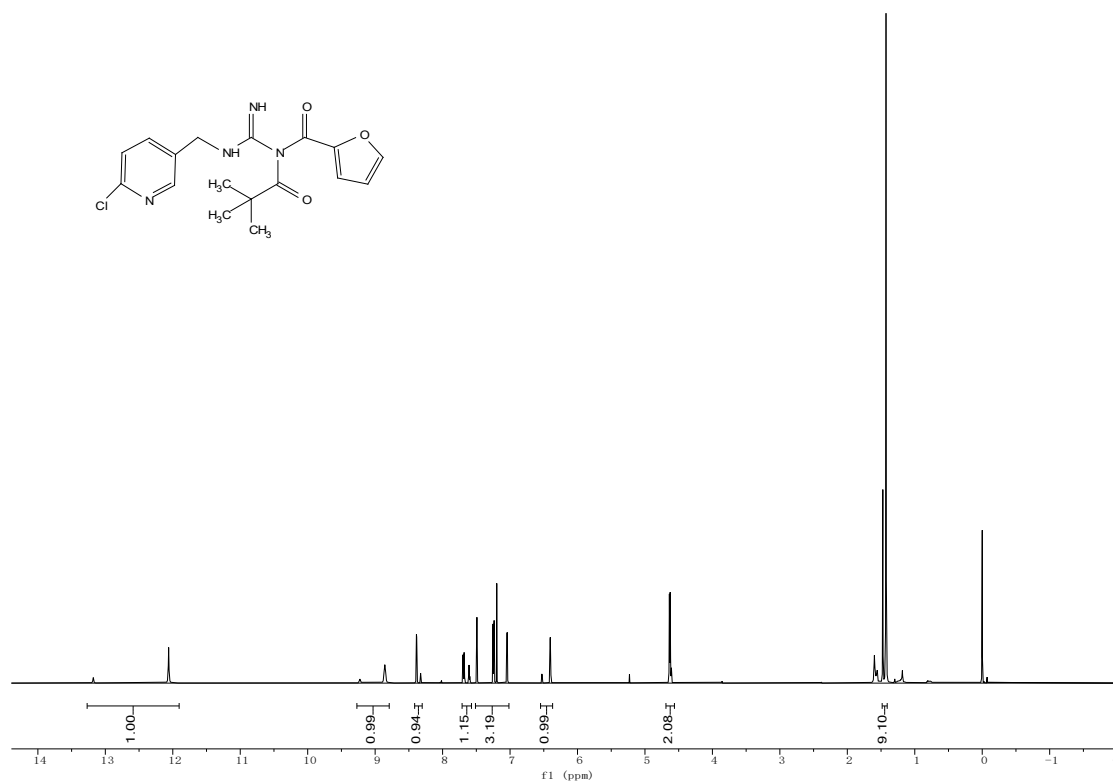
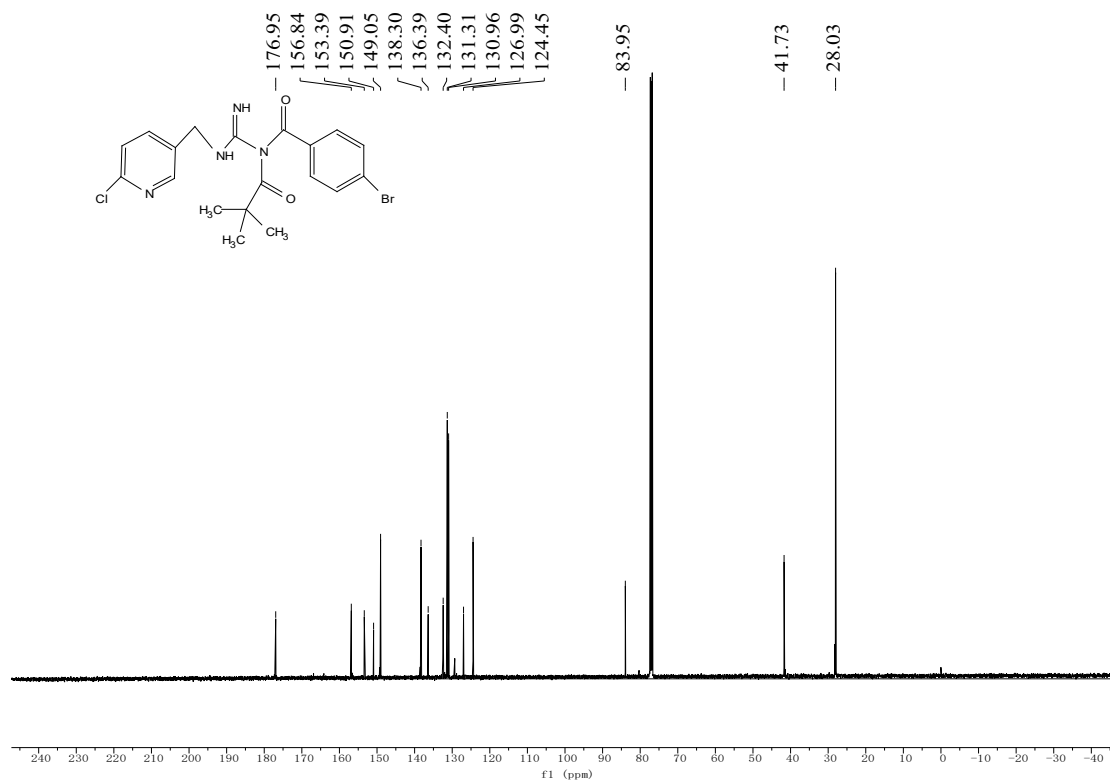
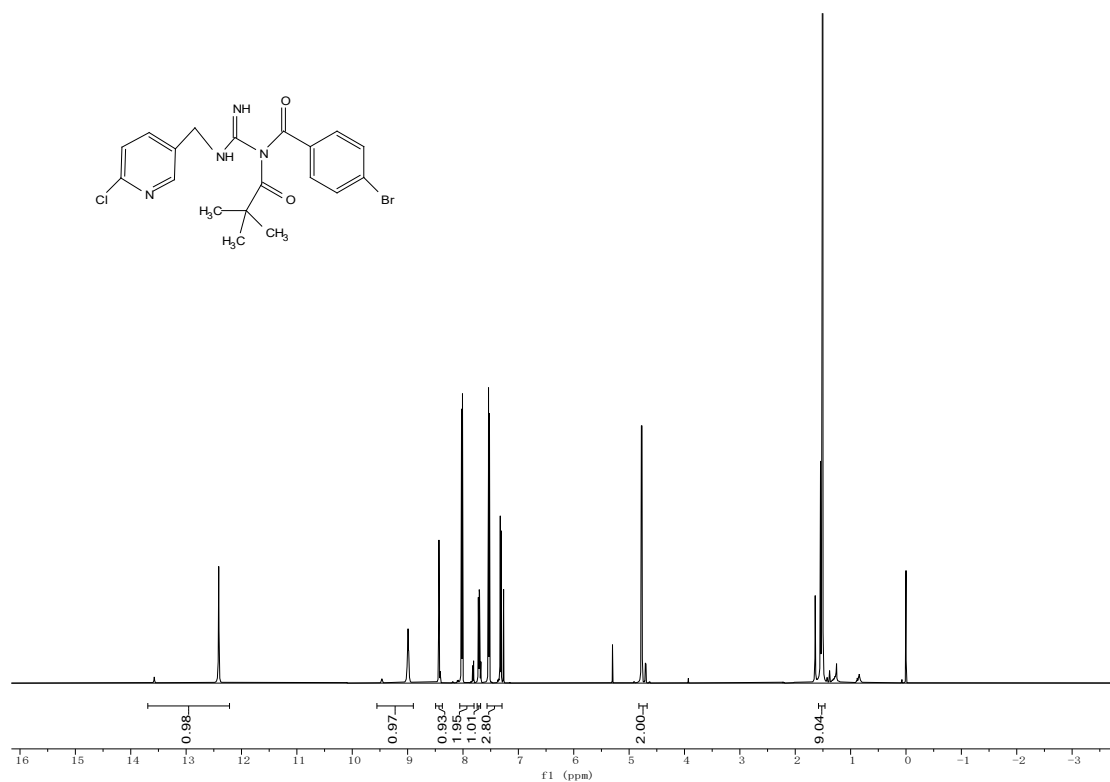


Fig S21. <sup>1</sup>H, <sup>13</sup>C spectra of 6m



**Fig S22.** <sup>1</sup>H, <sup>13</sup>C spectra of **6n**



**Fig S23.** <sup>1</sup>H, <sup>13</sup>C spectra of 60

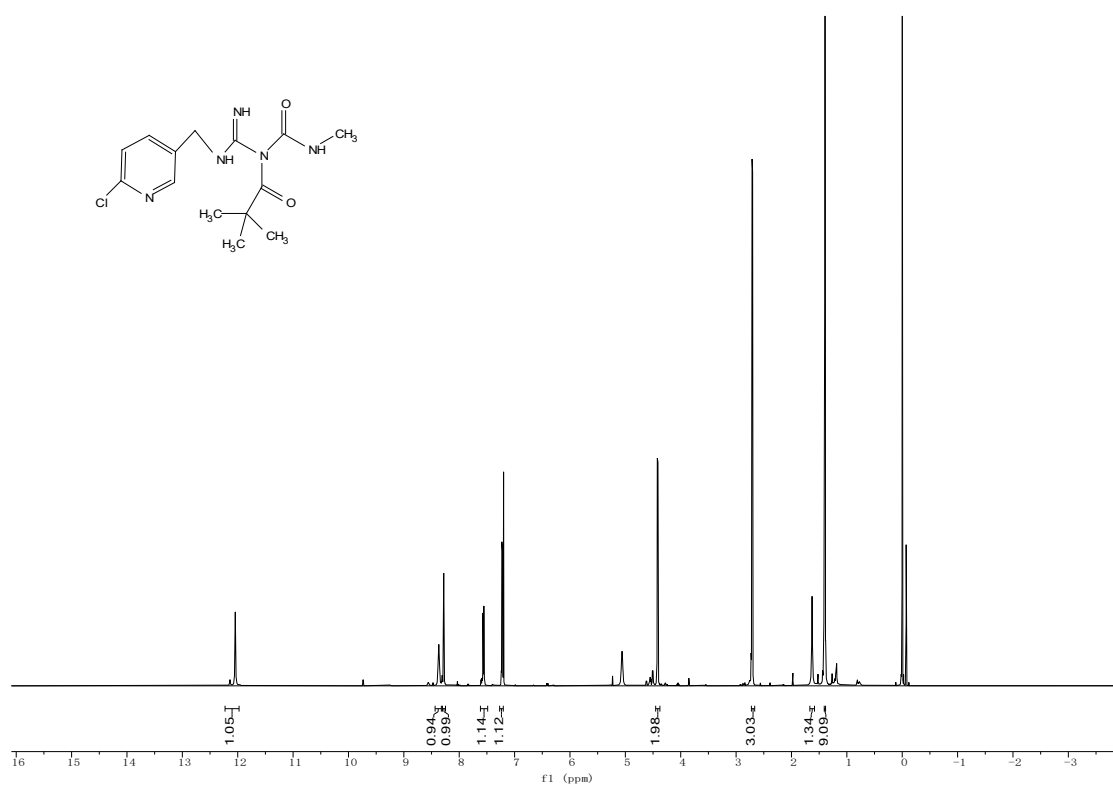
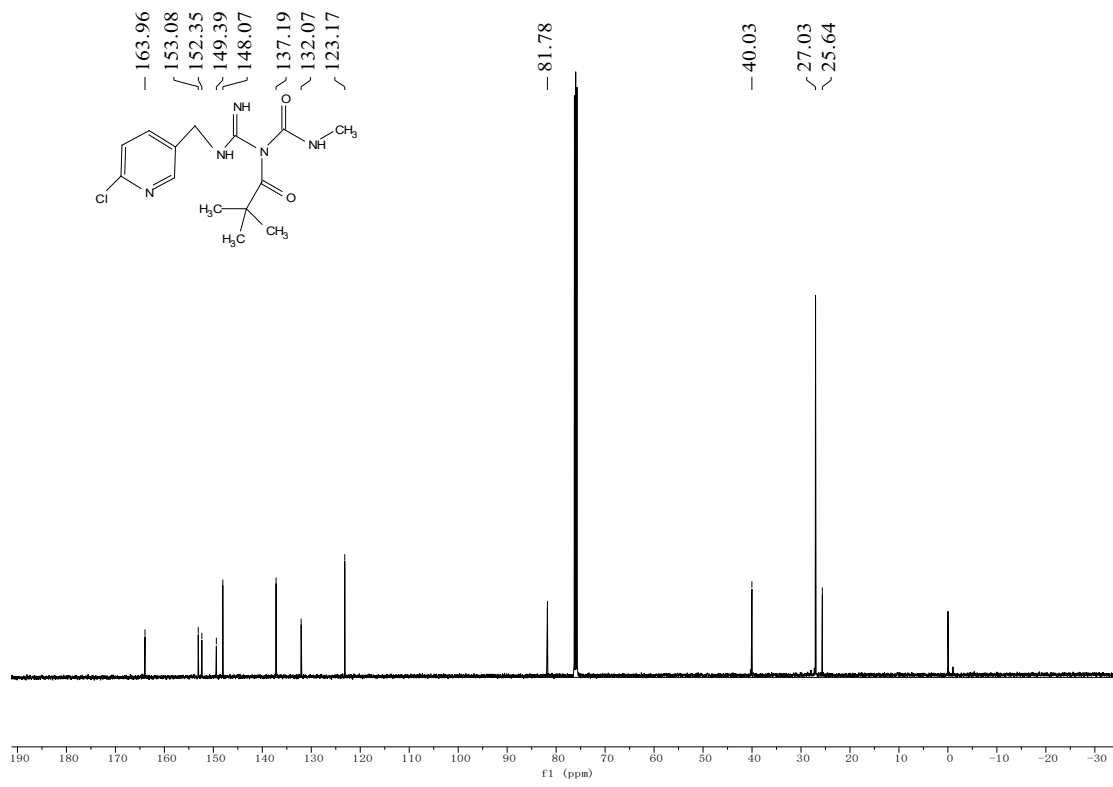


Fig S24. <sup>1</sup>H, <sup>13</sup>C spectra of 6p

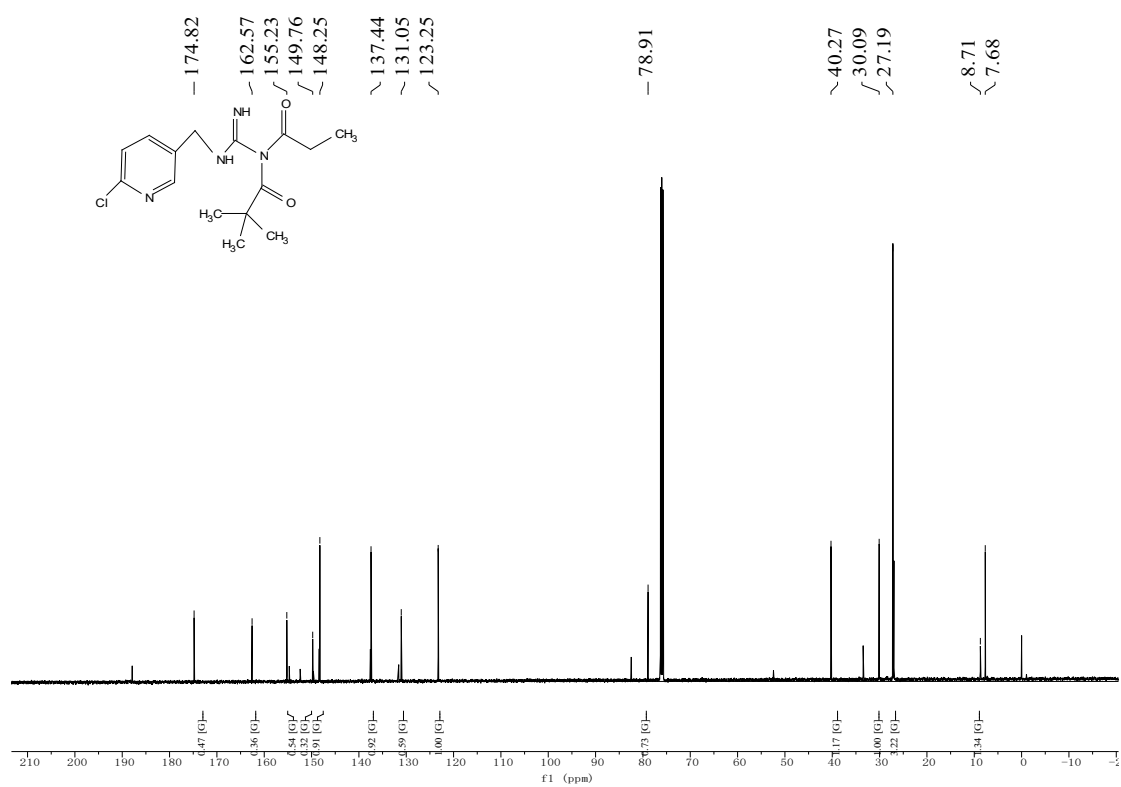
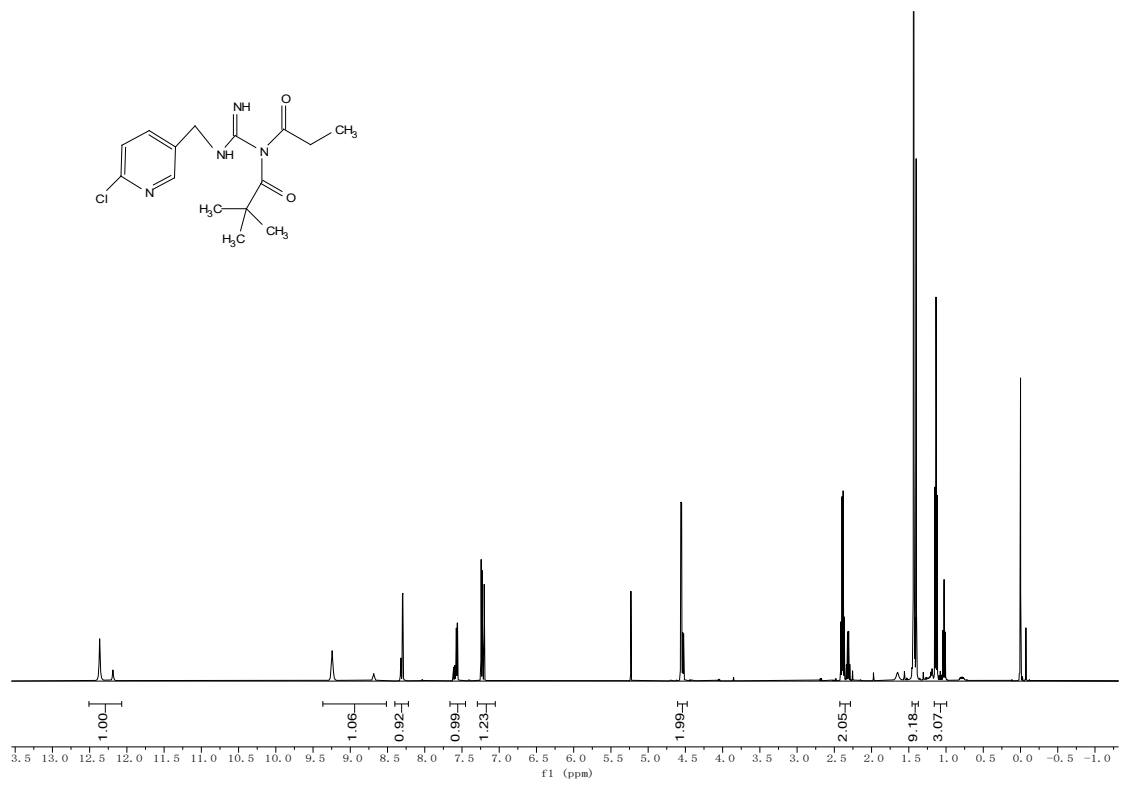


Fig S25. <sup>1</sup>H, <sup>13</sup>C spectra of 6r

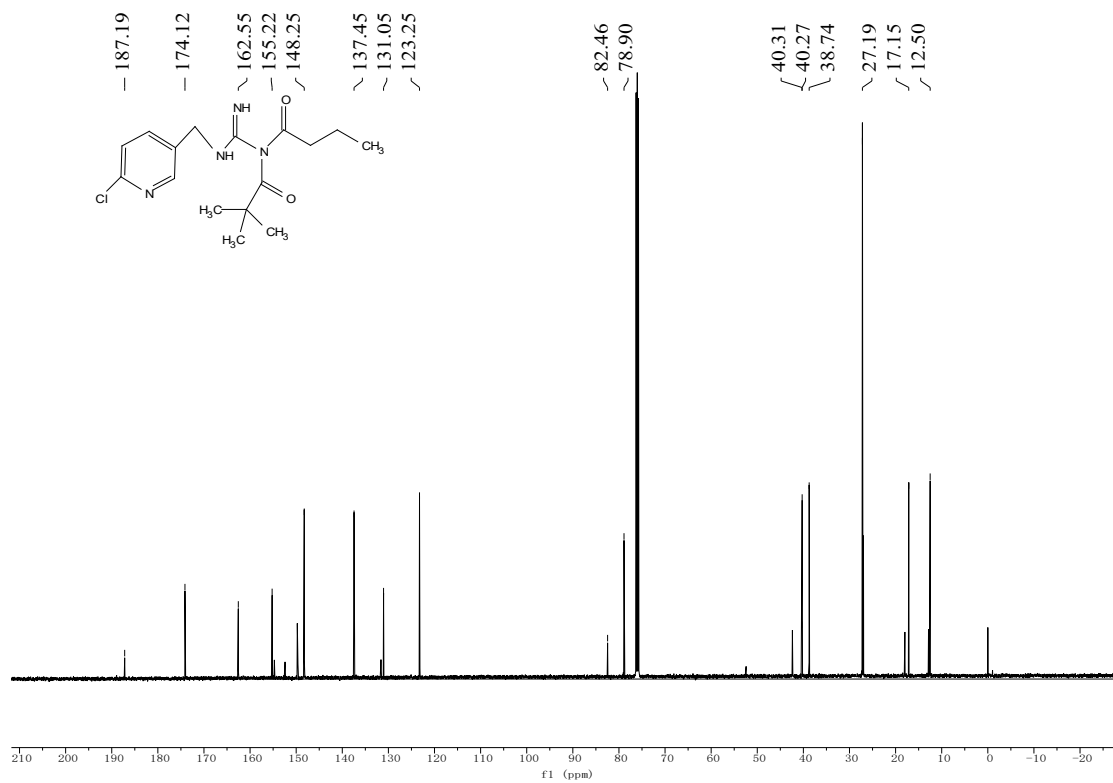
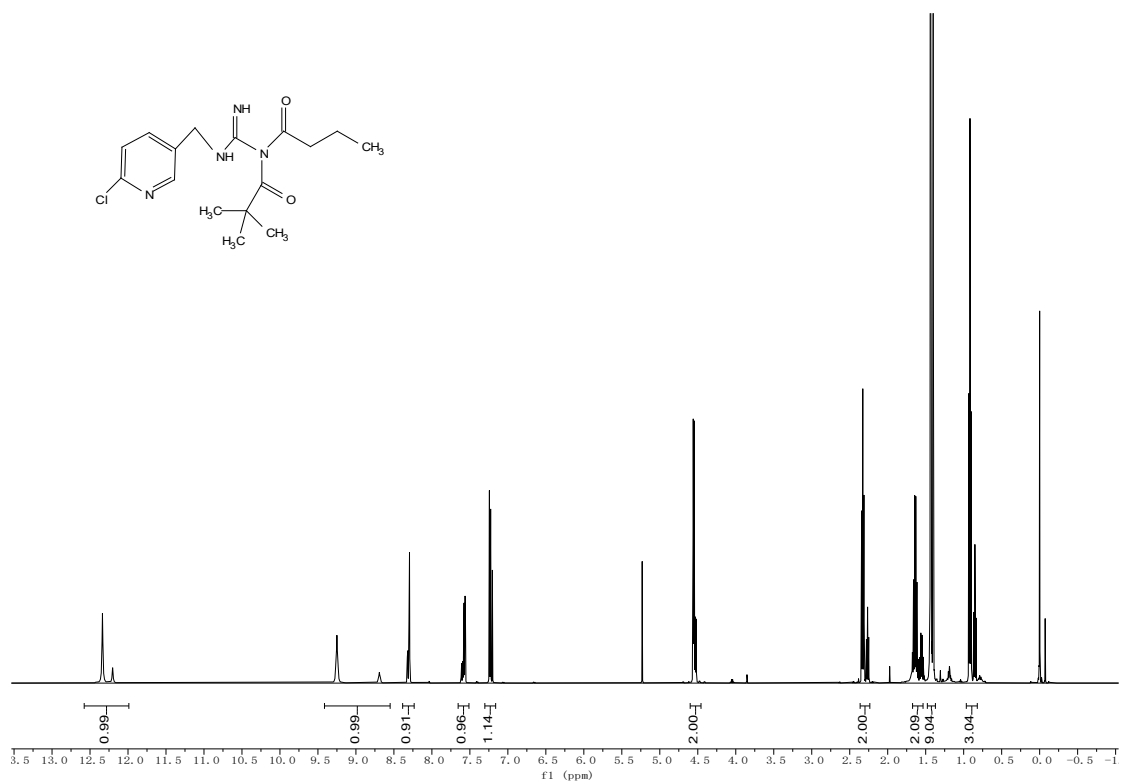
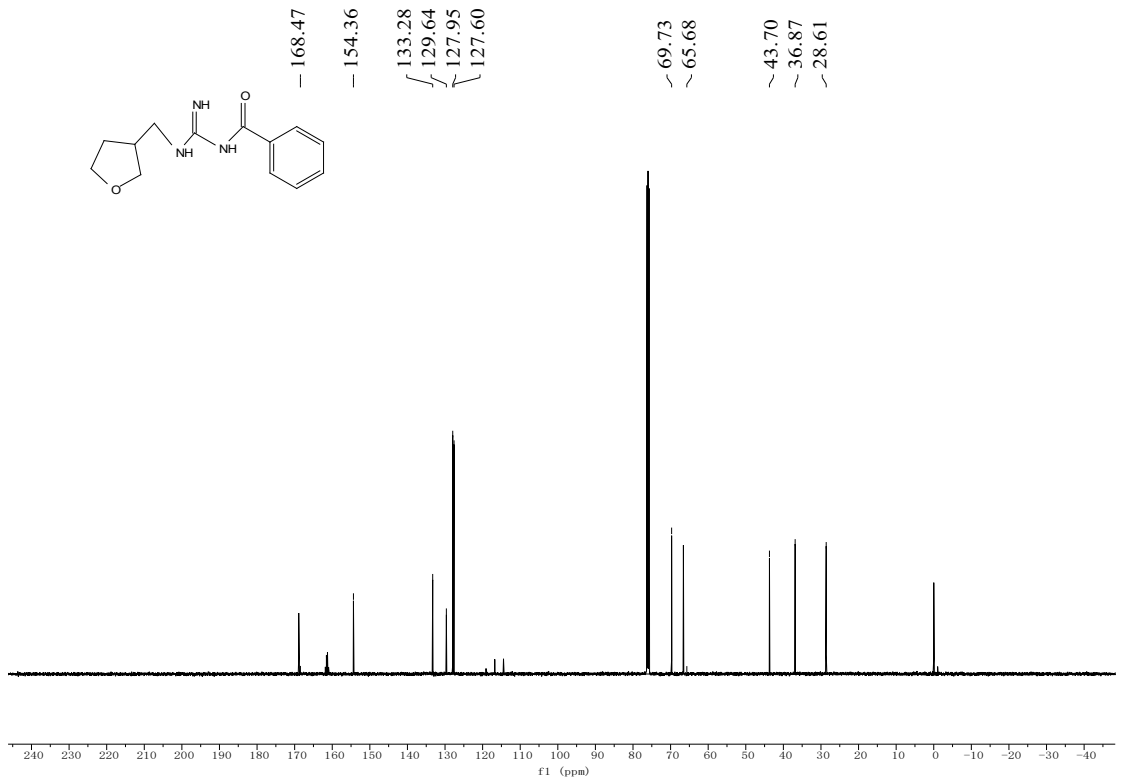
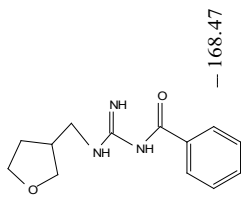
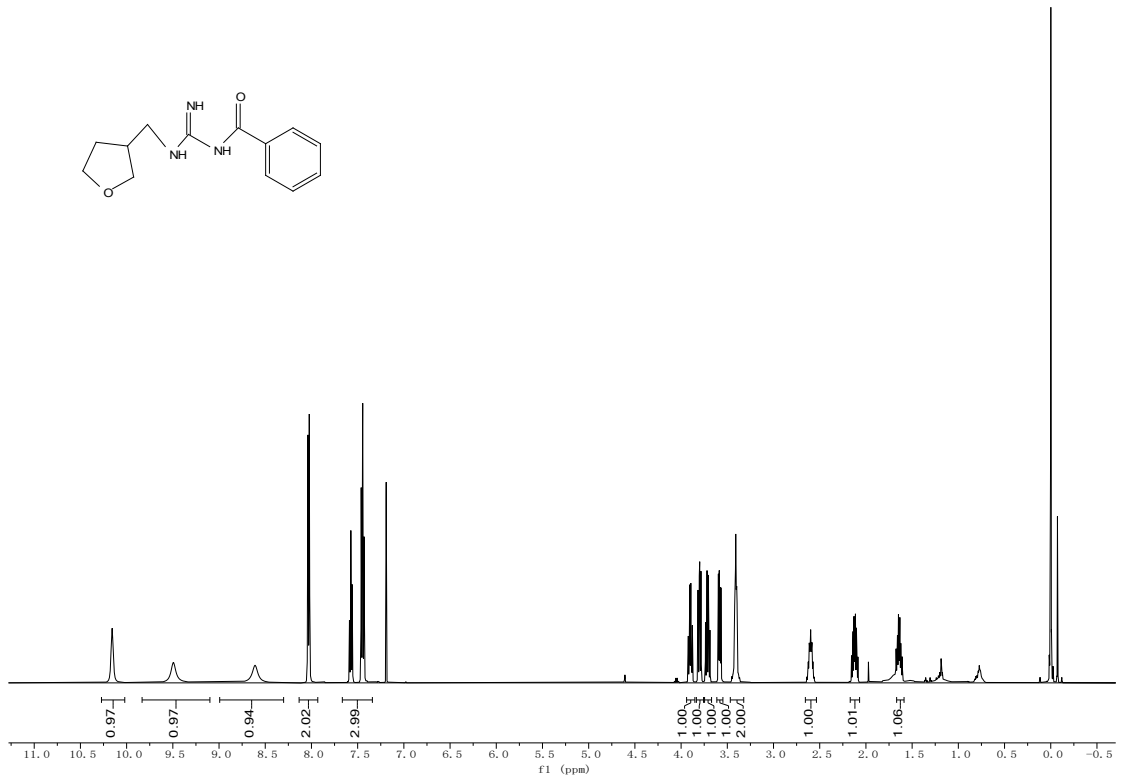
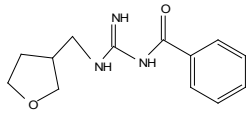


Fig S26. <sup>1</sup>H, <sup>13</sup>C spectra of 6s





LJY-3 #69 RT: 0.68 AV: 1 NL: 1.00E9  
T: FTMS + p ESI Full ms [170.0000-2500.0000]

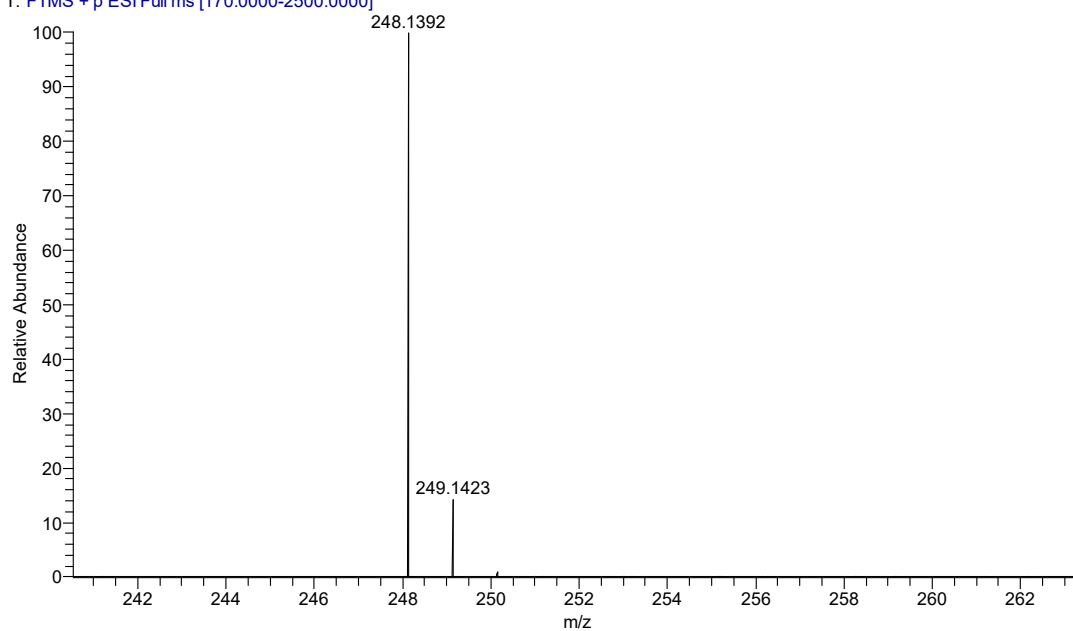
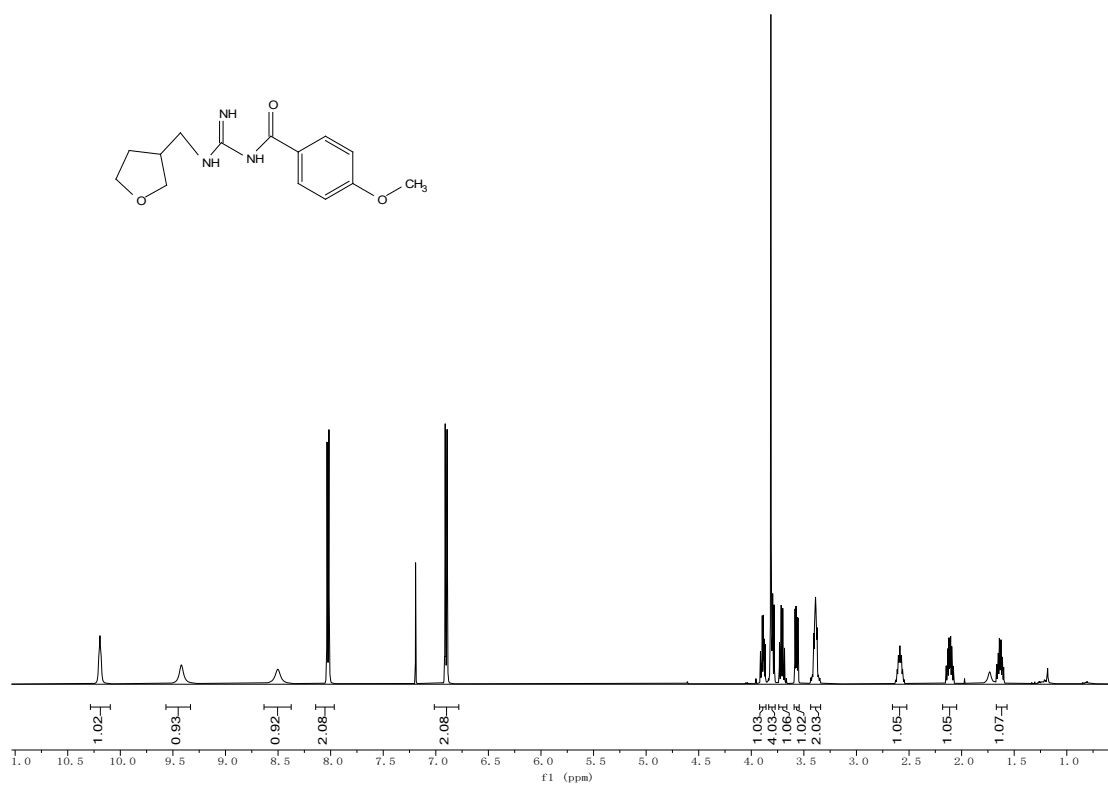
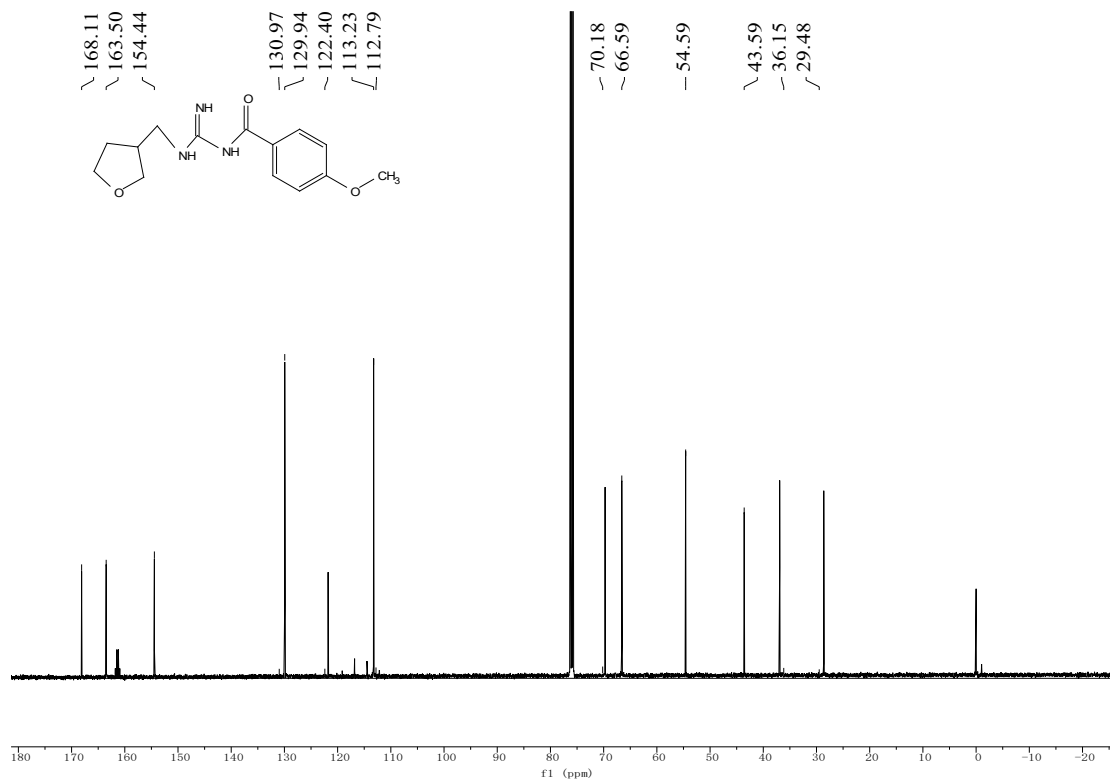
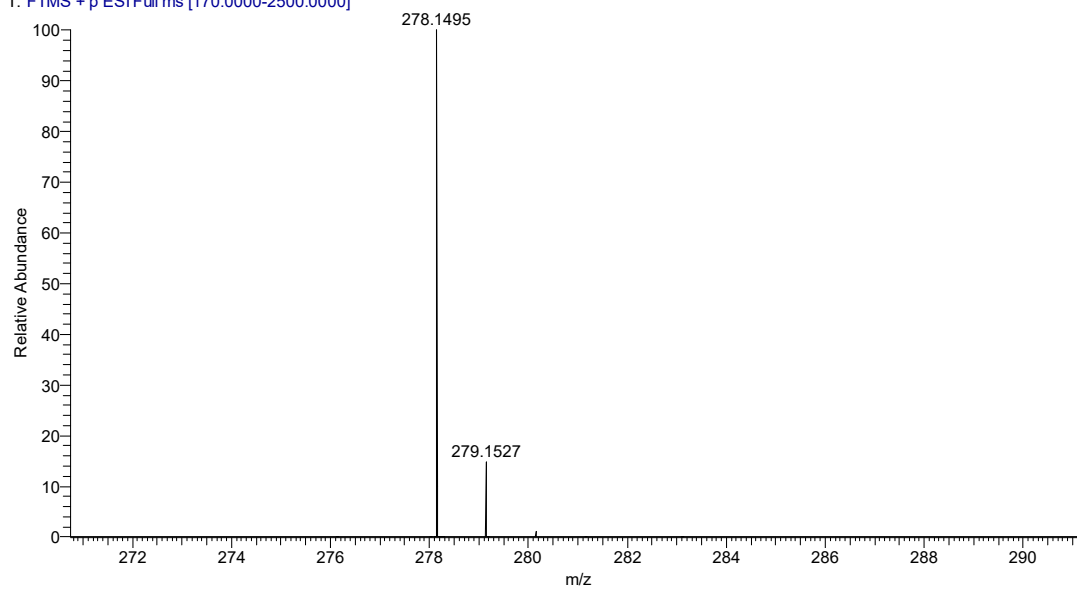


Fig S27.  $^1\text{H}$ ,  $^{13}\text{C}$  spectra of 7a

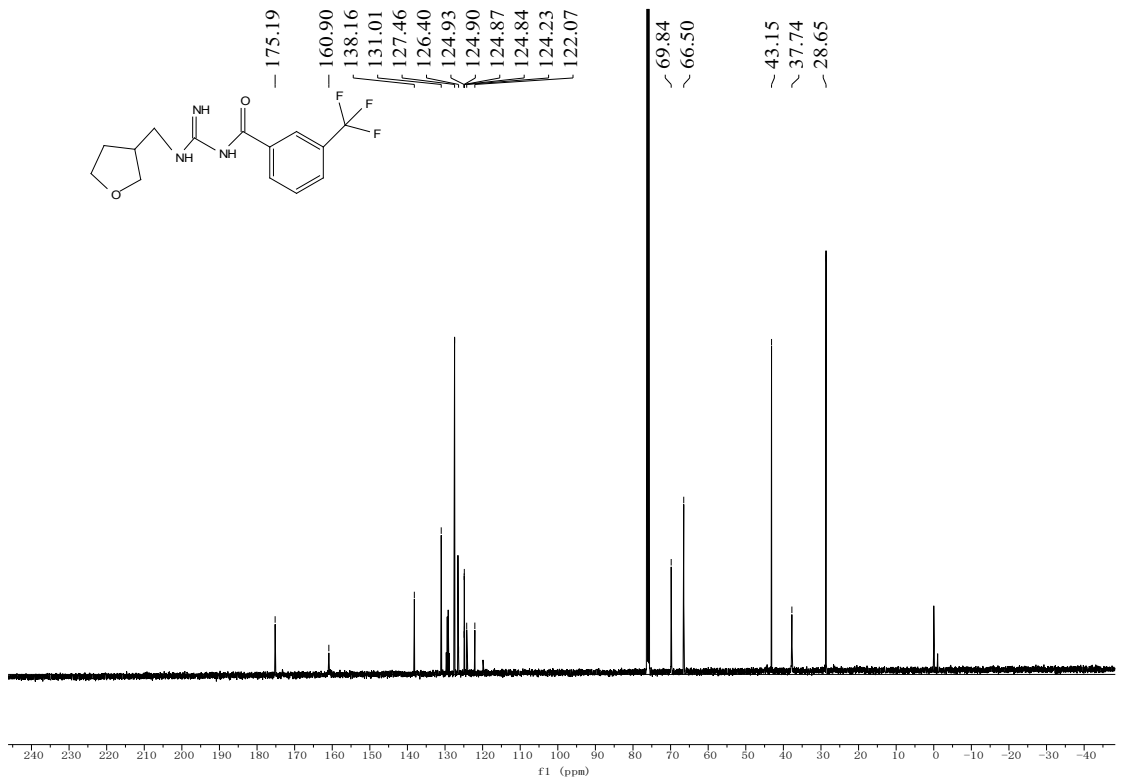
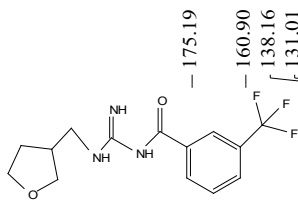
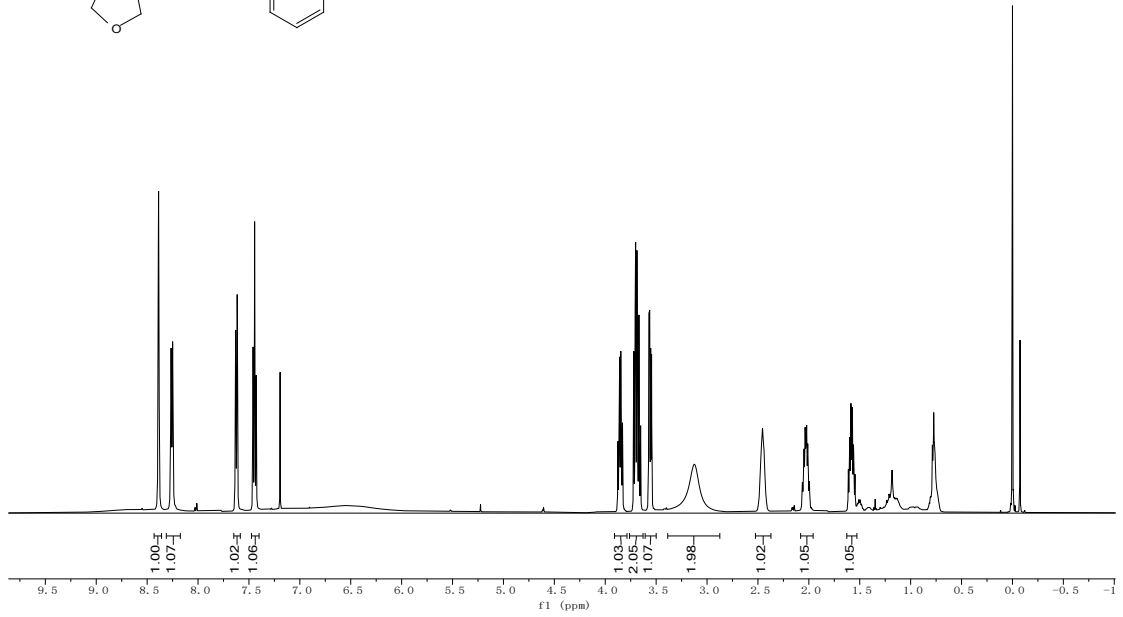
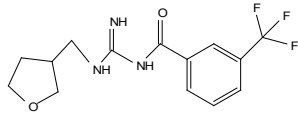




LJY-17 #53 RT: 0.53 AV: 1 NL: 1.07E10  
 T: FTMS + p ESI Full ms [170.0000-2500.0000]



**Fig S28.** <sup>1</sup>H, <sup>13</sup>C spectra of **7b**



LJY-4 #61 RT: 0.61 AV: 1 NL: 2.25E10  
T: FTMS + p ESI Full ms [170.0000-2500.0000]

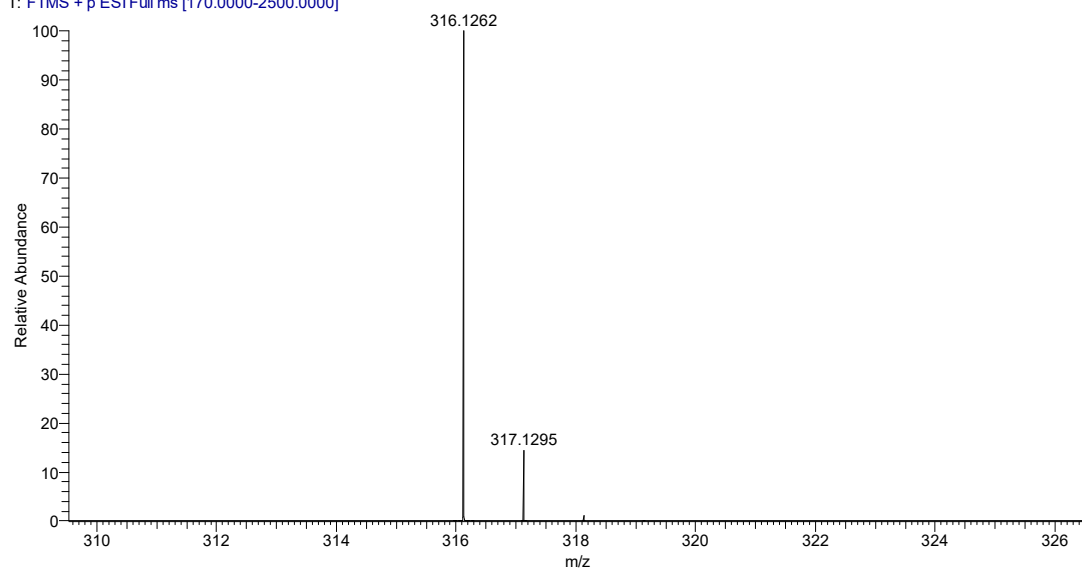
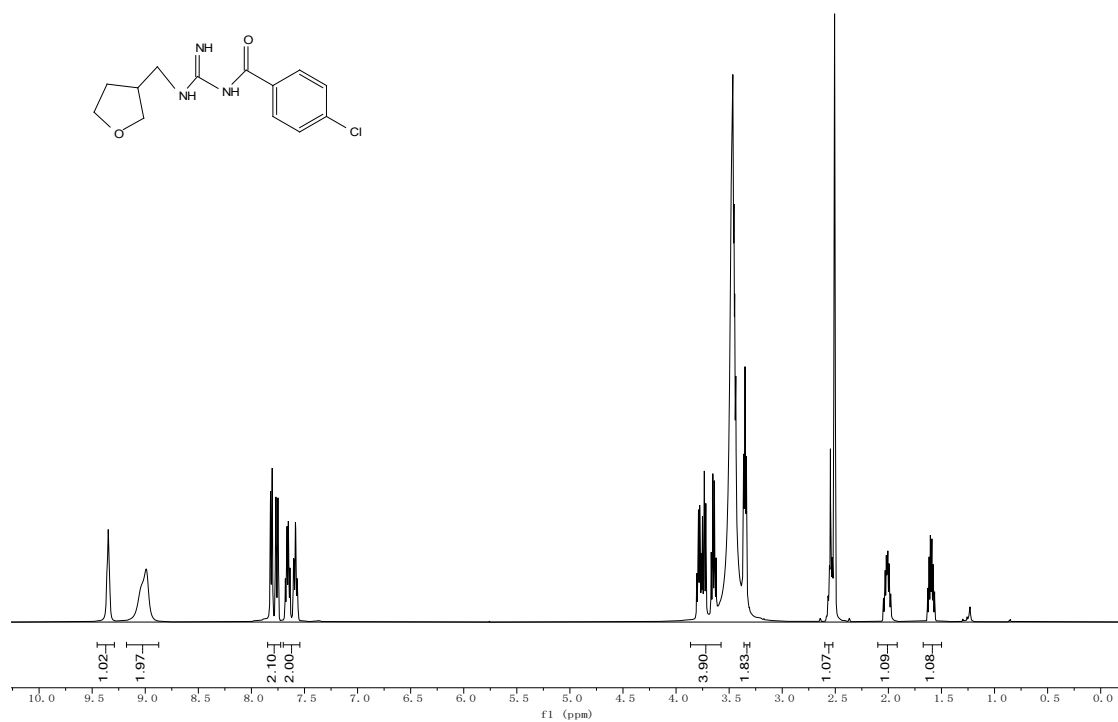
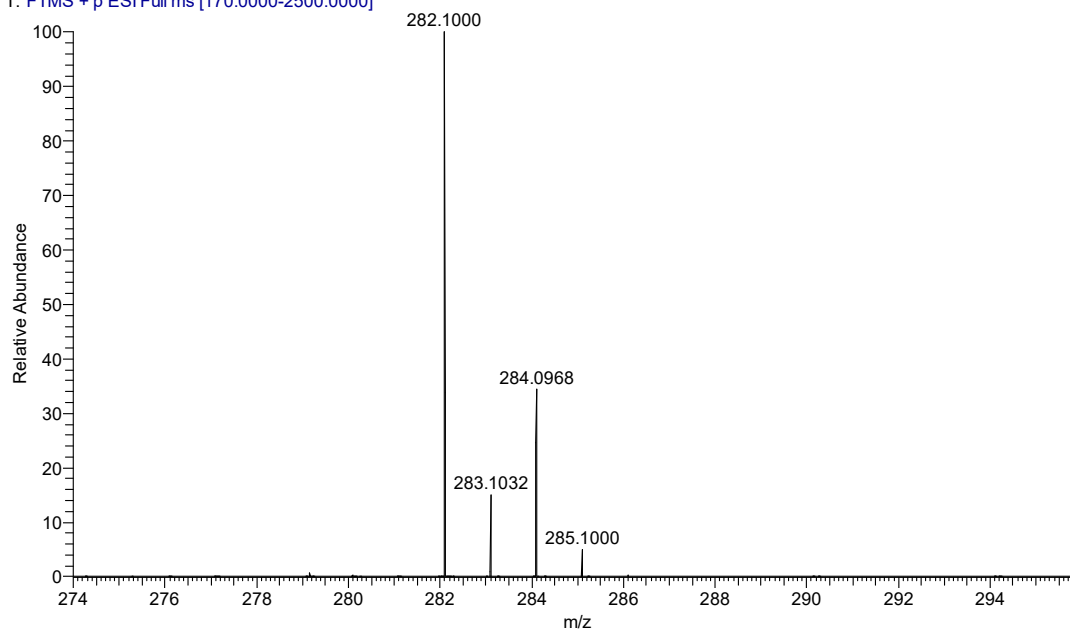


Fig S29.  $^1\text{H}$ ,  $^{13}\text{C}$  spectra of **7c**

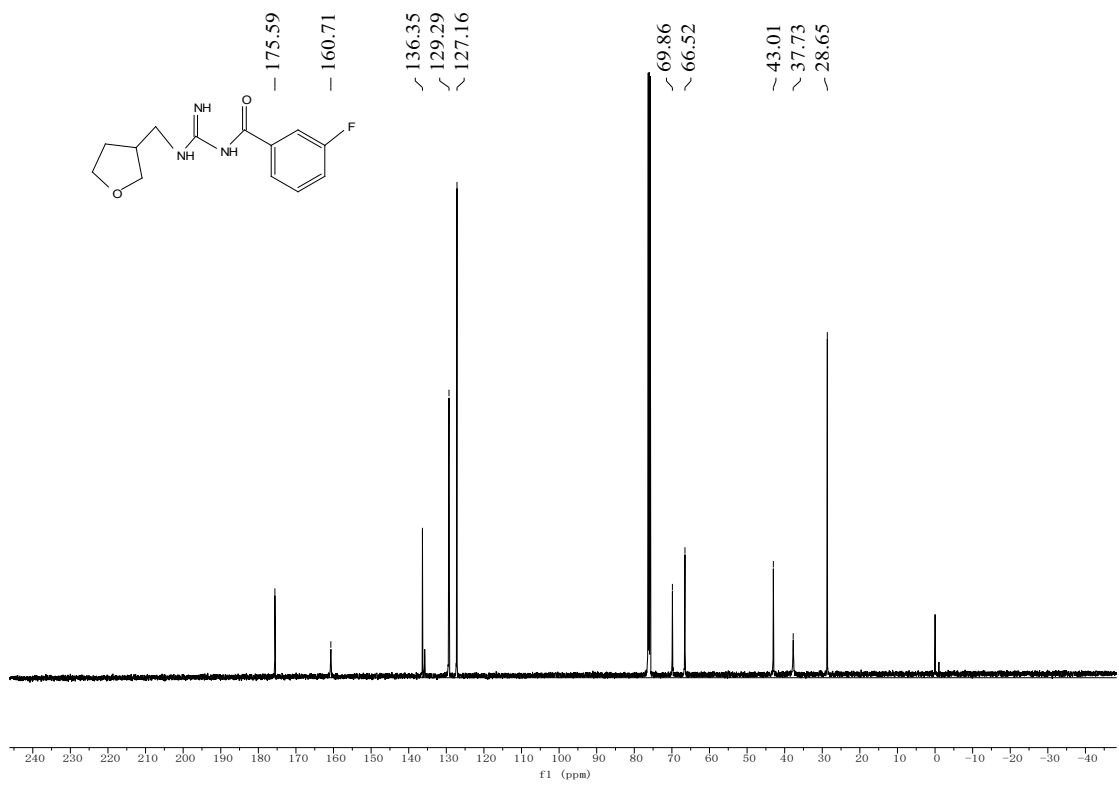
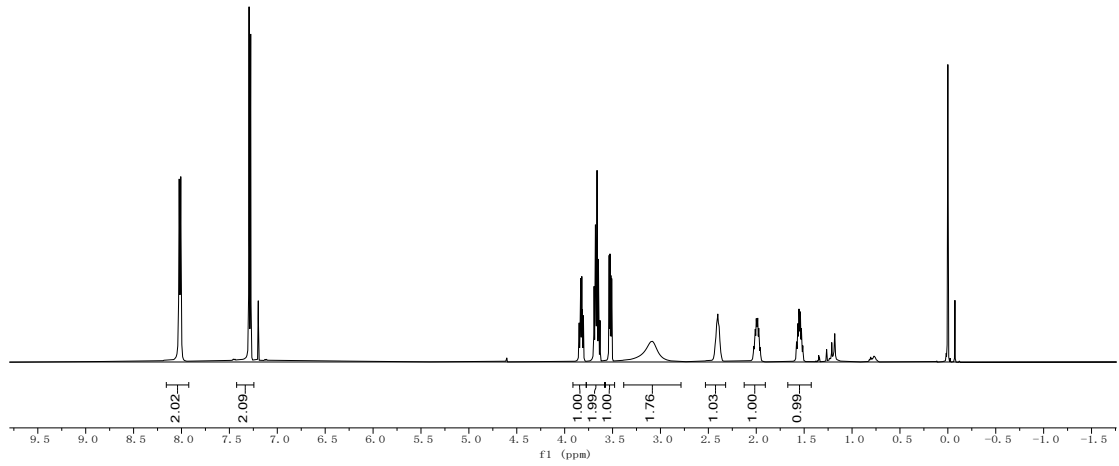
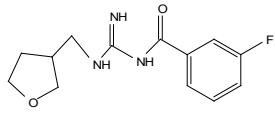




LJY-10 #71 RT: 0.70 AV: 1 NL: 7.42E8  
 T: FTMS + p ESI Full ms [170.0000-2500.0000]



**Fig S30.**  $^1\text{H}$ ,  $^{13}\text{C}$  spectra of **7d**



LJY-12 #55 RT: 0.55 AV: 1 NL: 1.10E10  
T: FTMS + p ESI Full ms [170.0000-2500.0000]

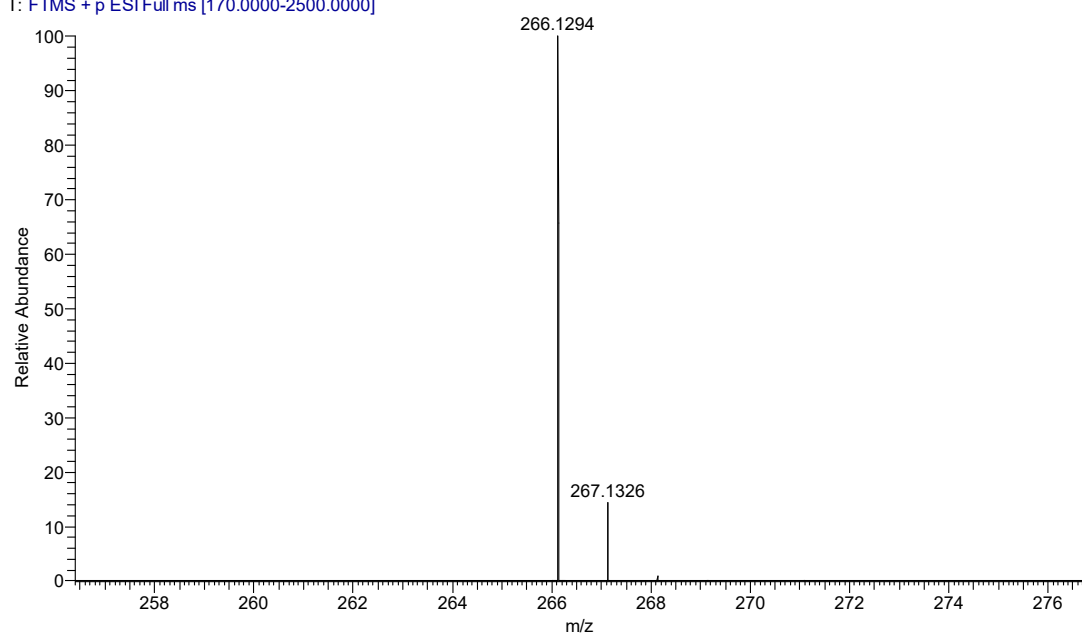
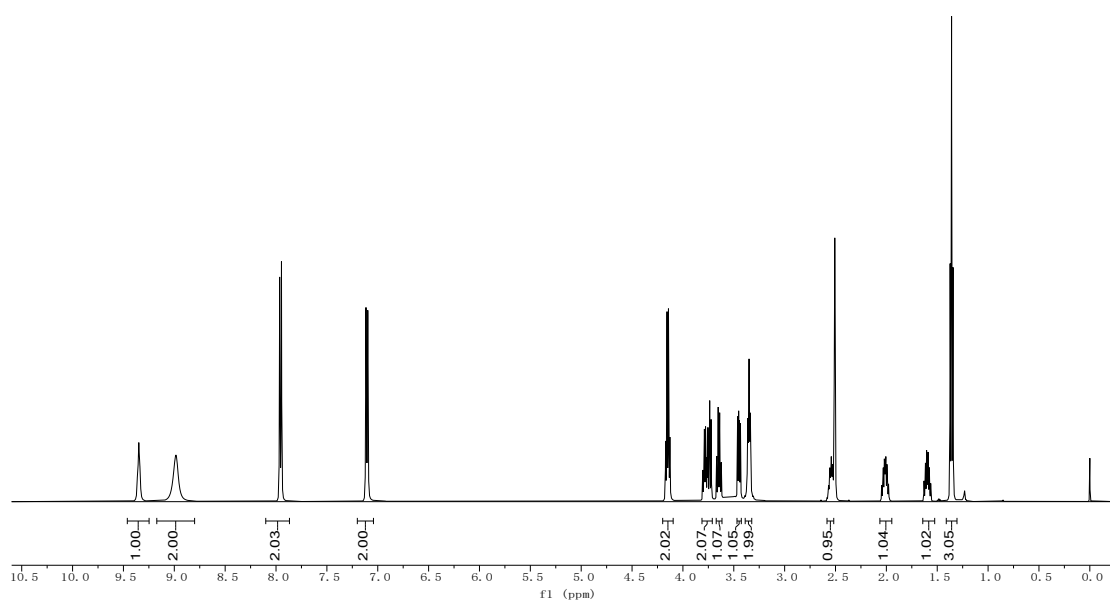
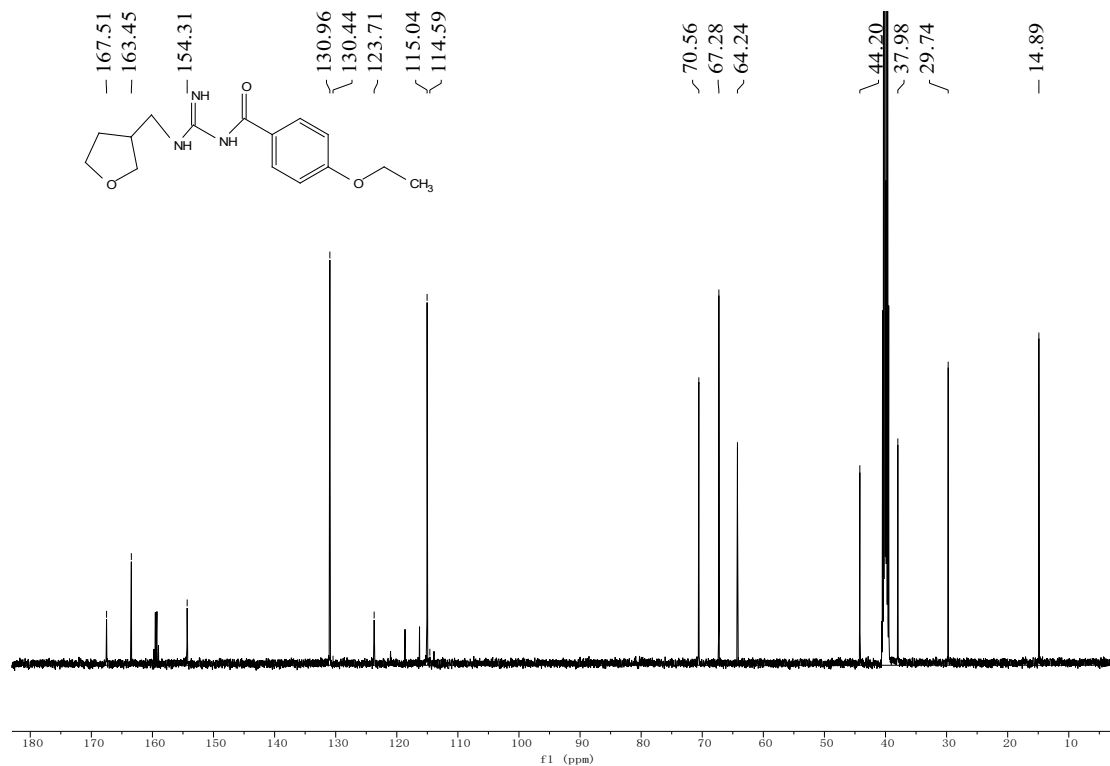


Fig S31.  $^1\text{H}$ ,  $^{13}\text{C}$  spectra of **7e**







LJY-15 #55 RT: 0.54 AV: 1 NL: 1.17E10  
 T: FTMS + p ESI Full ms [170.0000-2500.0000]

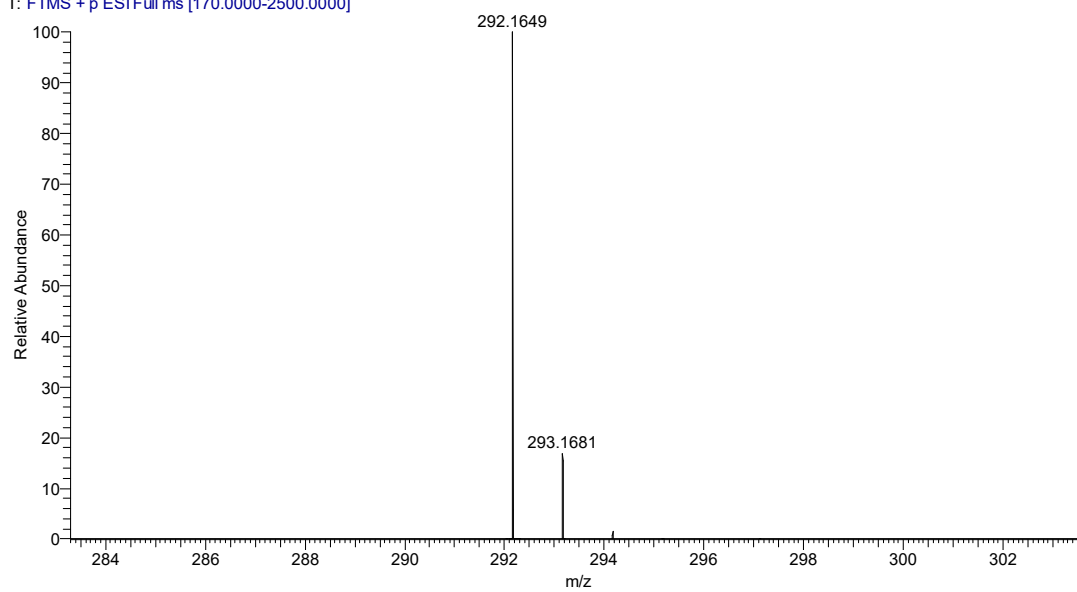
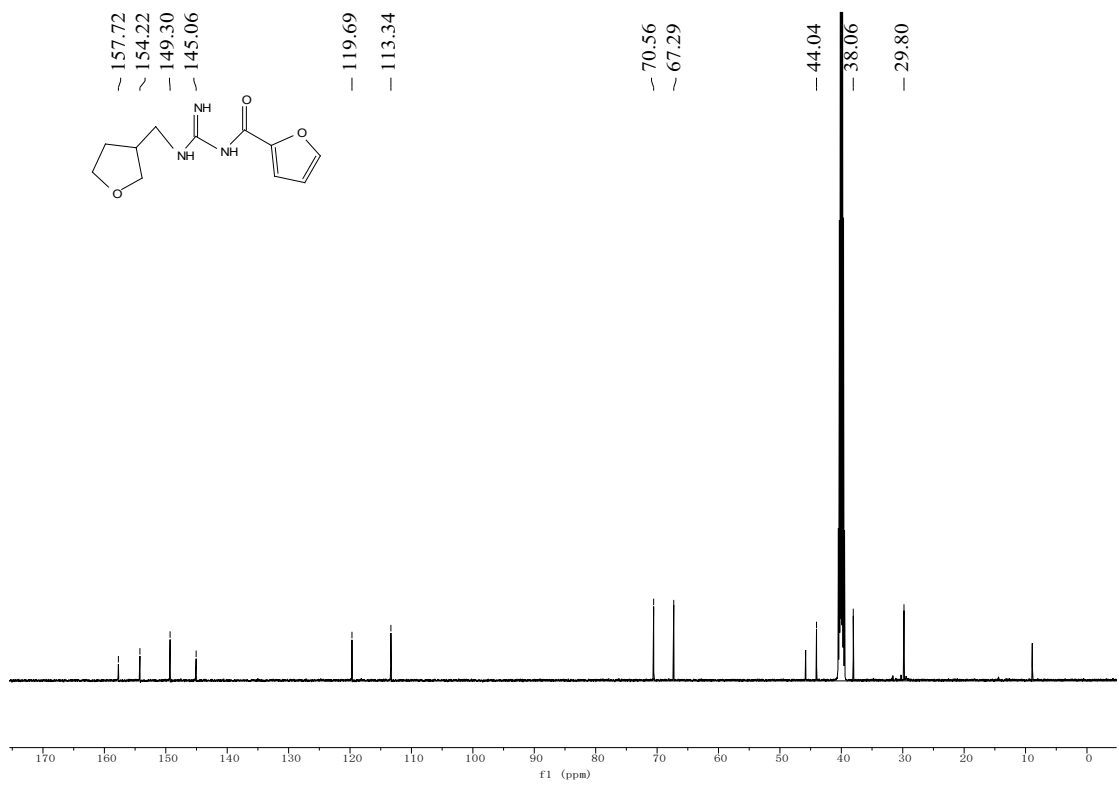
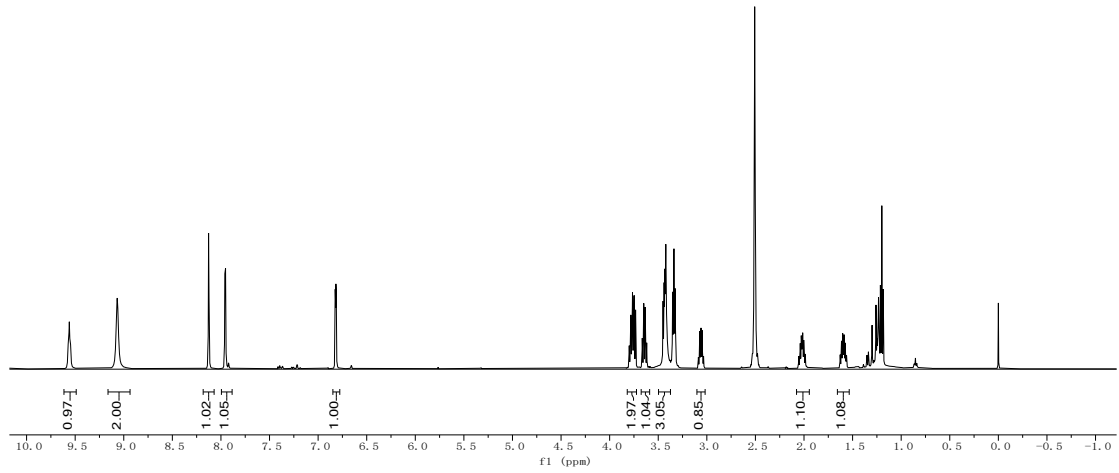
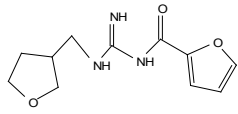


Fig S32. <sup>1</sup>H, <sup>13</sup>C spectra of 7f



LJY-FN2

Pos\_LJY-FN2 171 (0.980) AM (Cen,4, 80.00, Ar,10000.0,0.00,0.00); Cm (171)

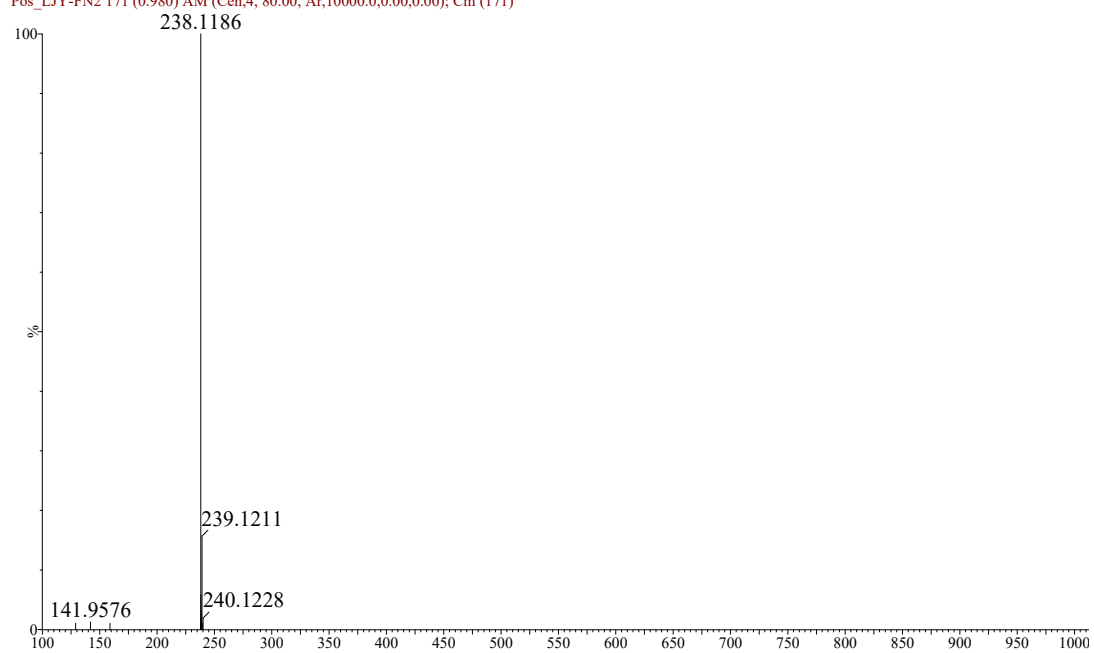
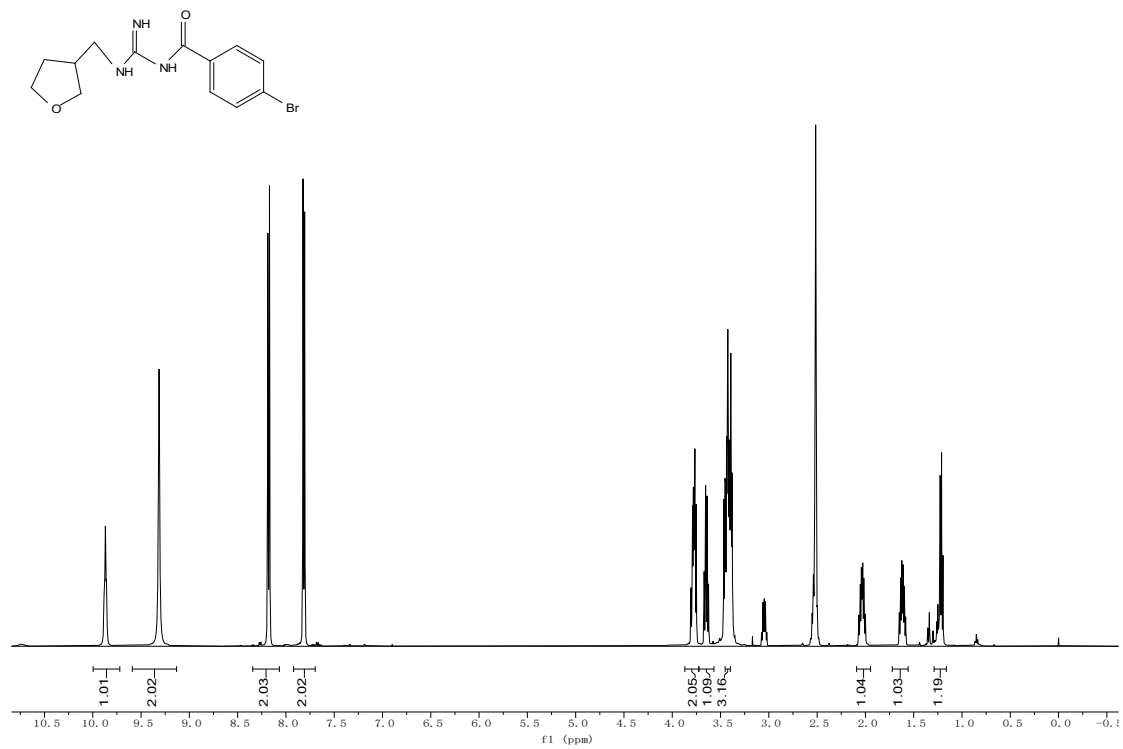
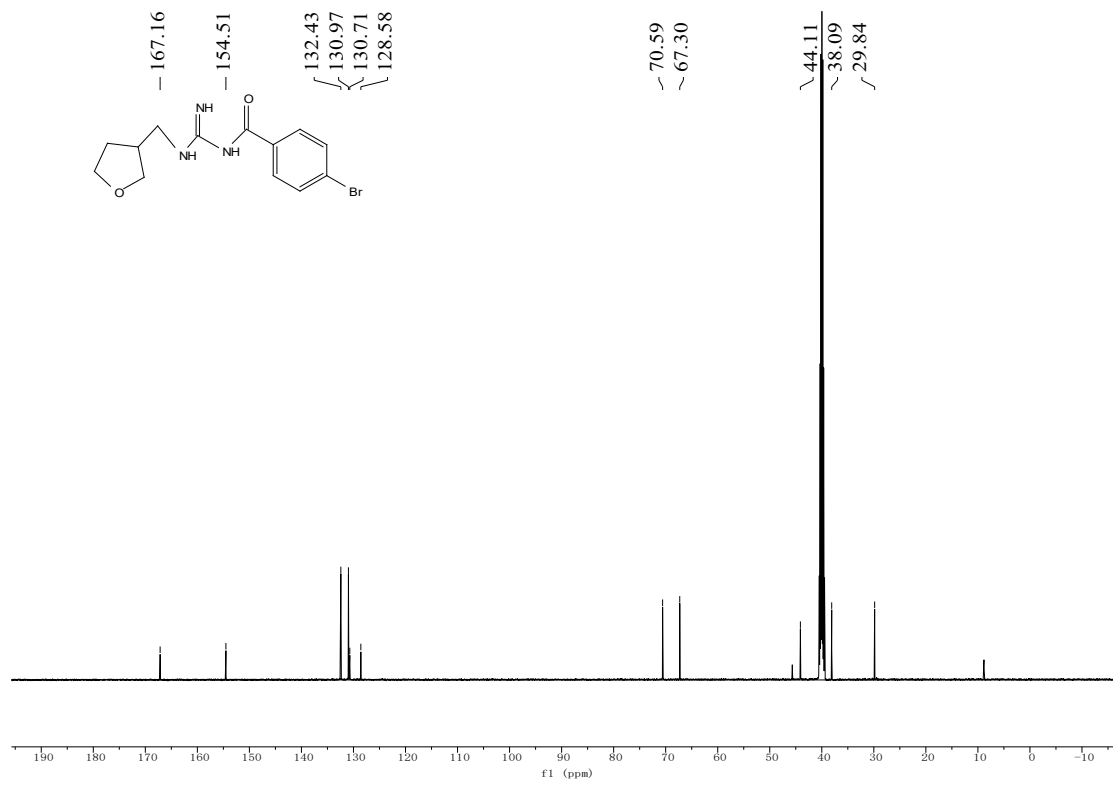


Fig S33.  $^1\text{H}$ ,  $^{13}\text{C}$  spectra of 7g





LJY-BF

Pos\_LJY-BF 307 (1.739) AM (Cen,4, 80.00, Ar,10000.0,0.00,0.00); Cm (307:308)

1: TOF MS ES+  
7.50e6

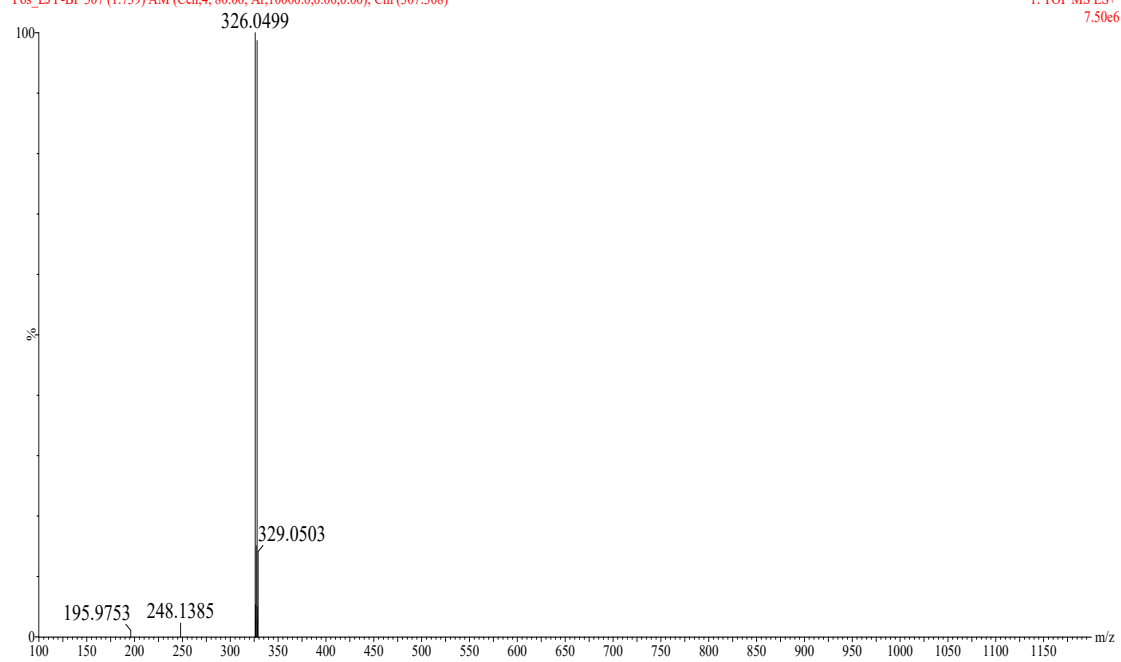
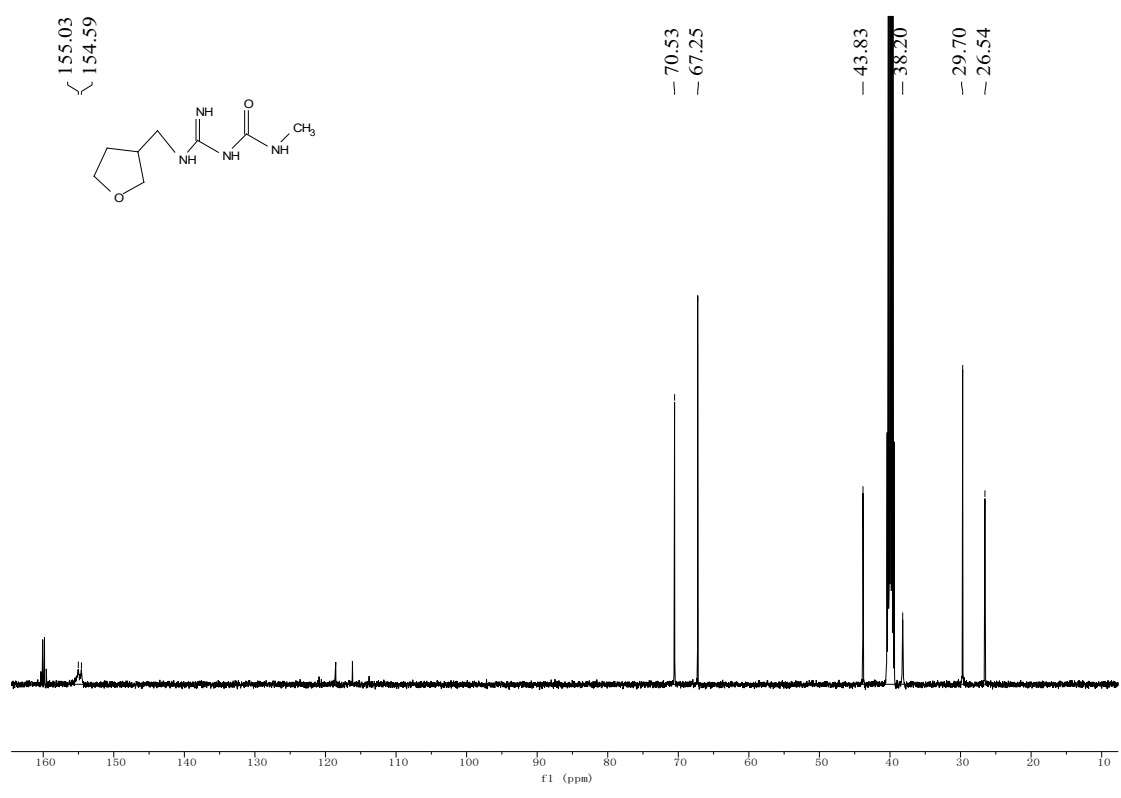
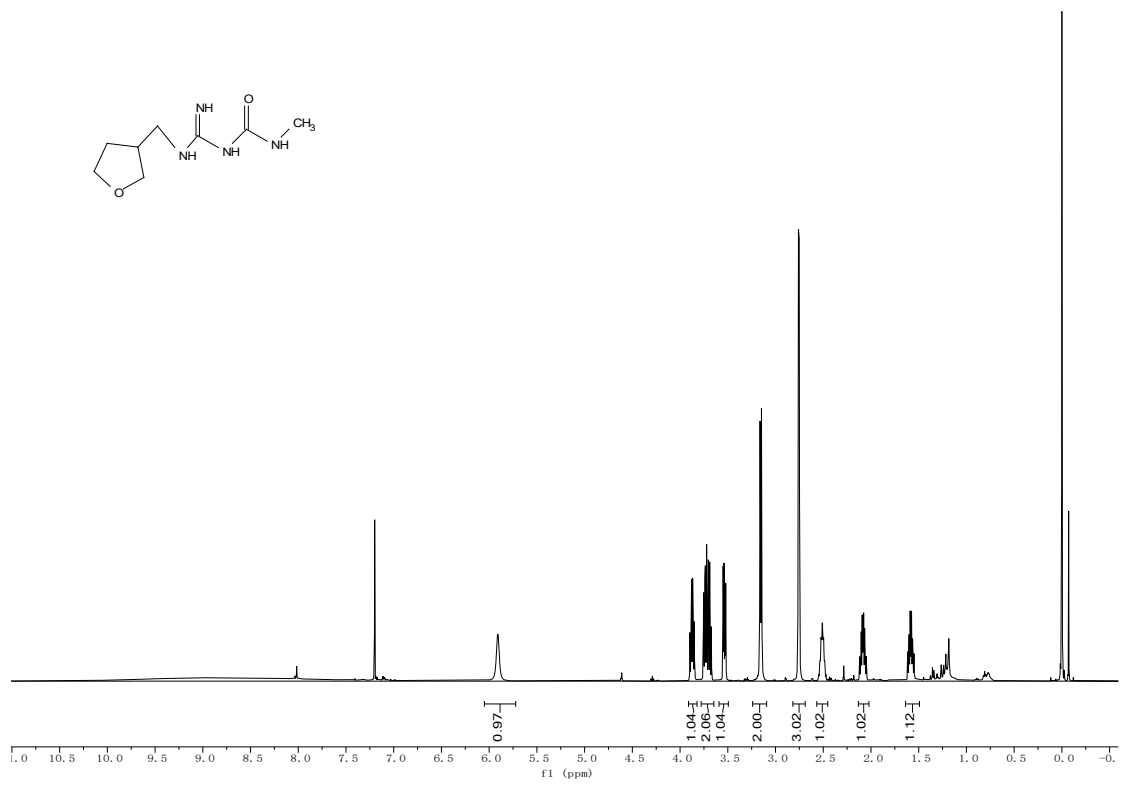


Fig S34. <sup>1</sup>H, <sup>13</sup>C spectra of 7h



LJY-1 #55 RT: 0.54 AV: 1 NL: 4.20E9  
T: FTMS + p ESI Full ms [170.0000-2500.0000]

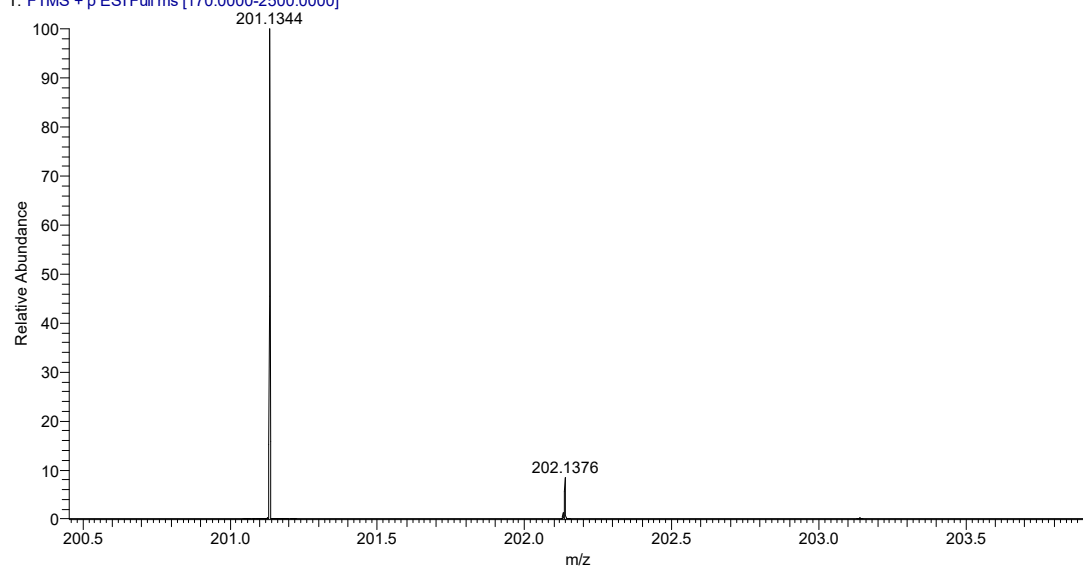
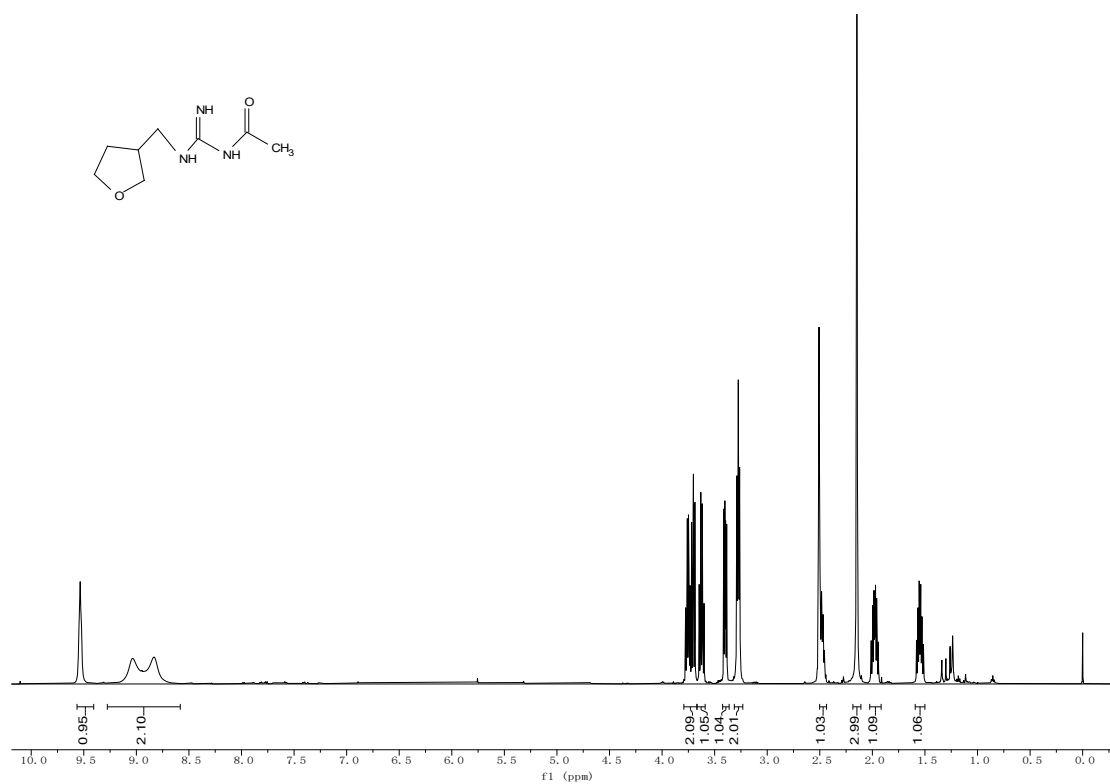
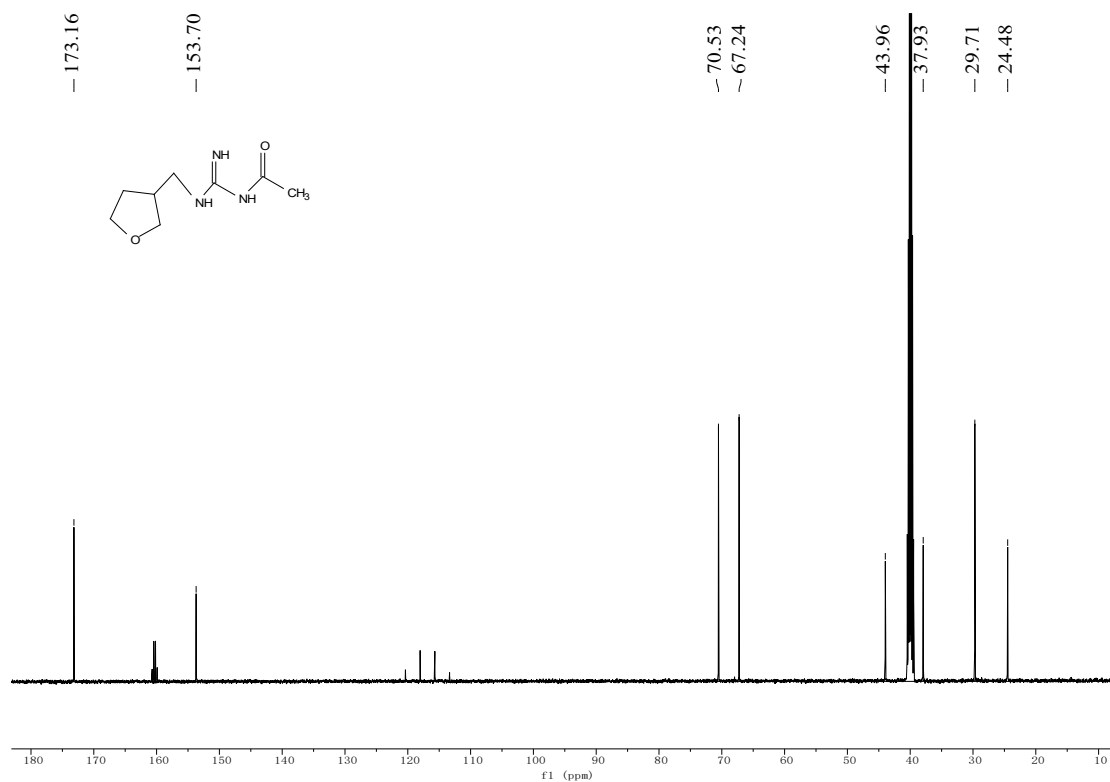


Fig S35.  $^1\text{H}$ ,  $^{13}\text{C}$  spectra of **7i**





LJY-19 #51 RT: 0.51 AV: 1 NL: 4.52E9  
T: FTMS + p ESI Full ms [170.0000-2500.0000]

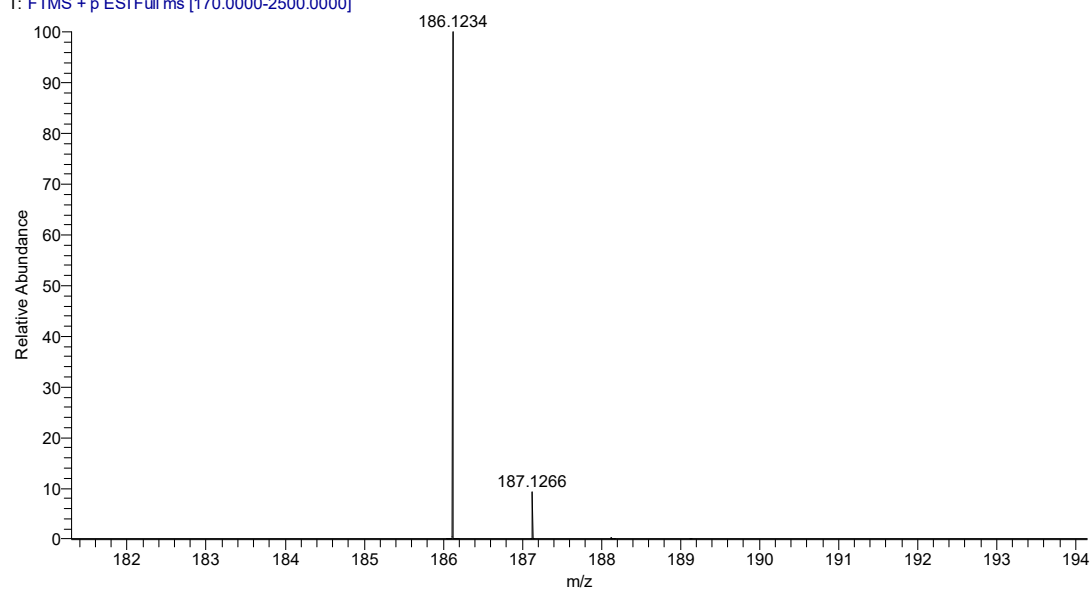
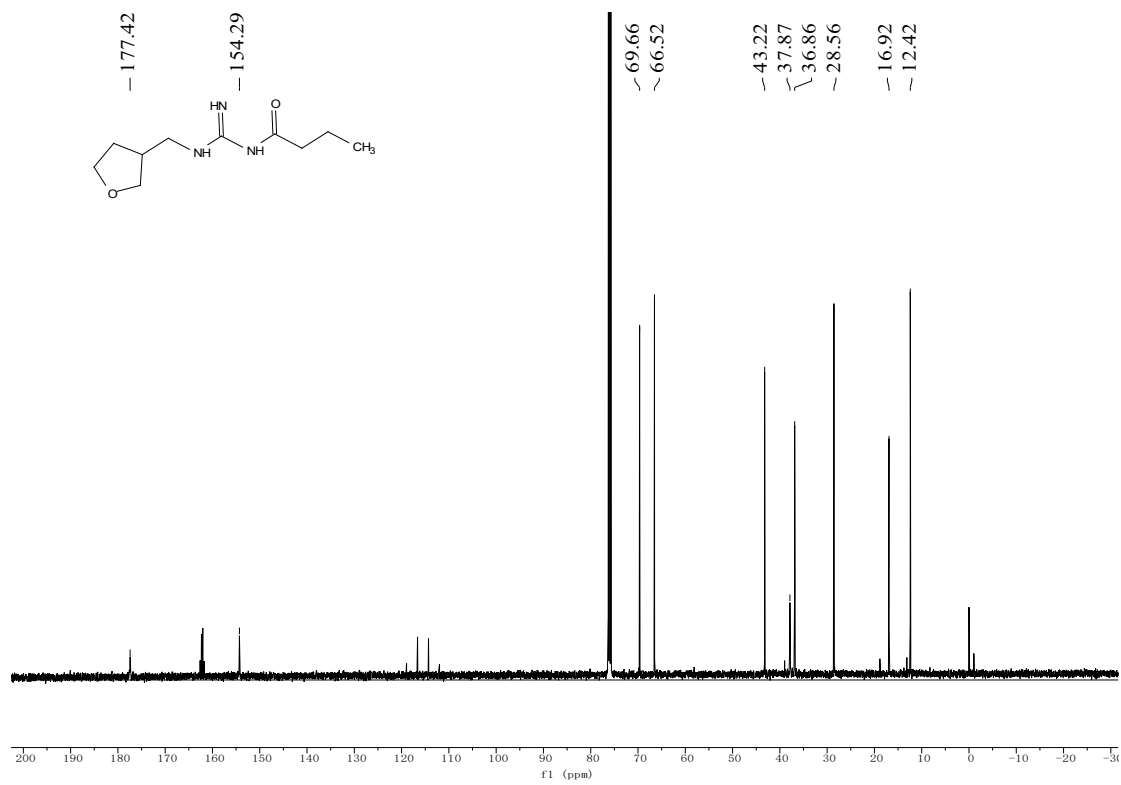
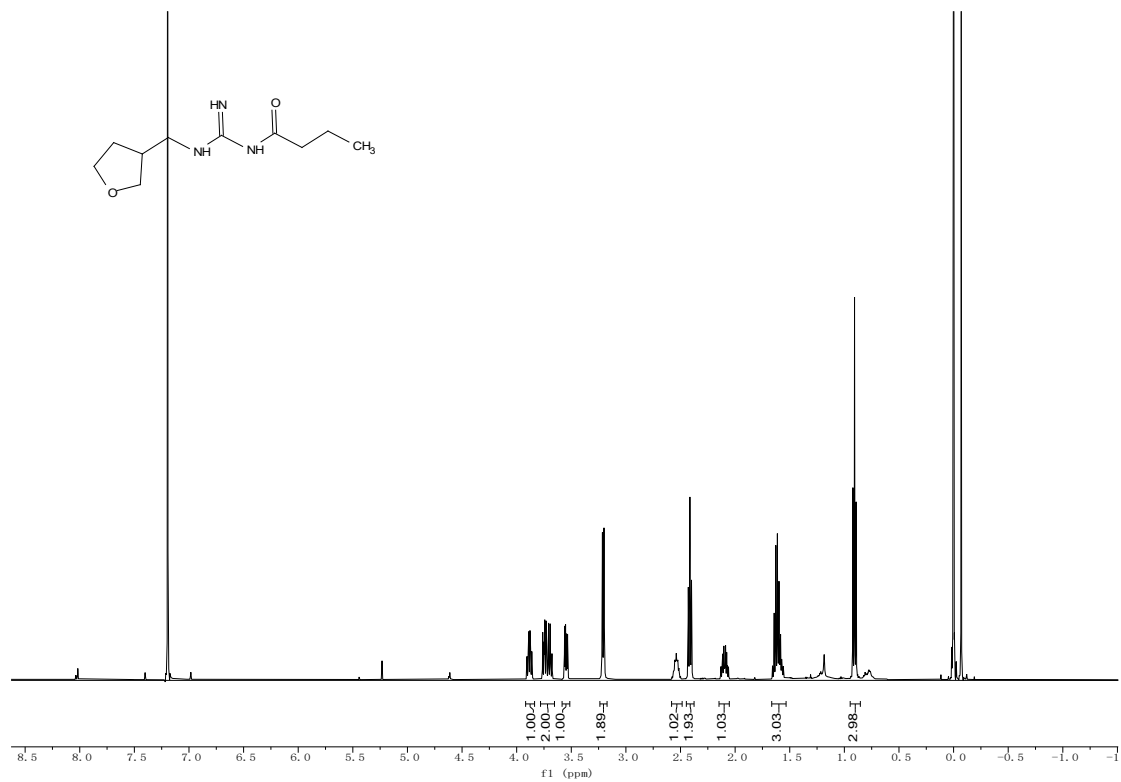


Fig S36.  $^1\text{H}$ ,  $^{13}\text{C}$  spectra of 7j





LJY-2 #59 RT: 0.57 AV: 1 NL: 3.25E9  
T: FTMS + p ESI Full ms [170.0000-2500.0000]

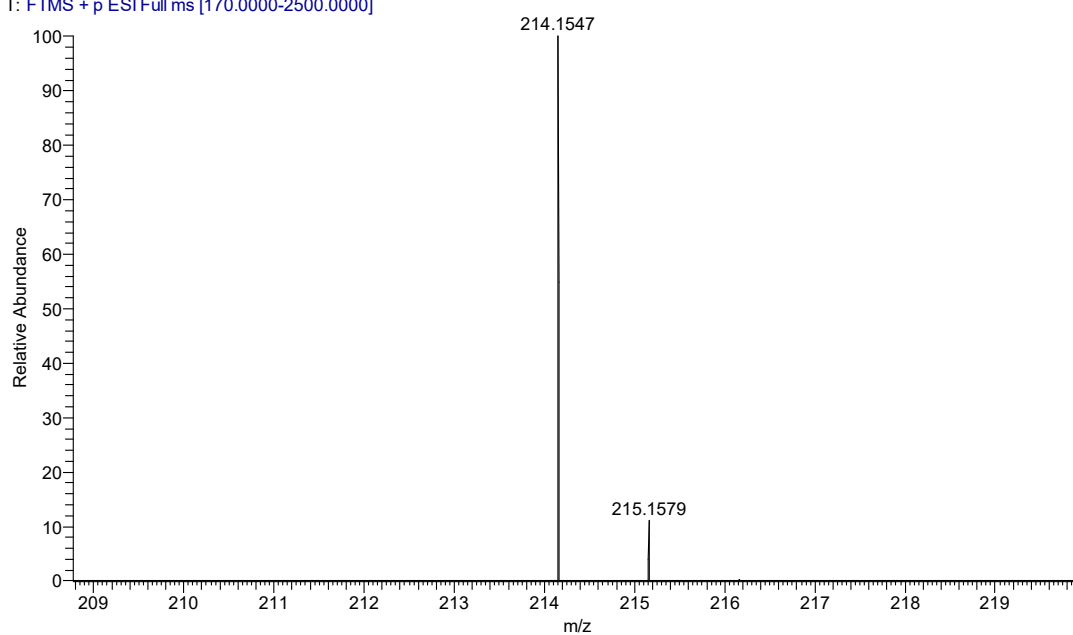
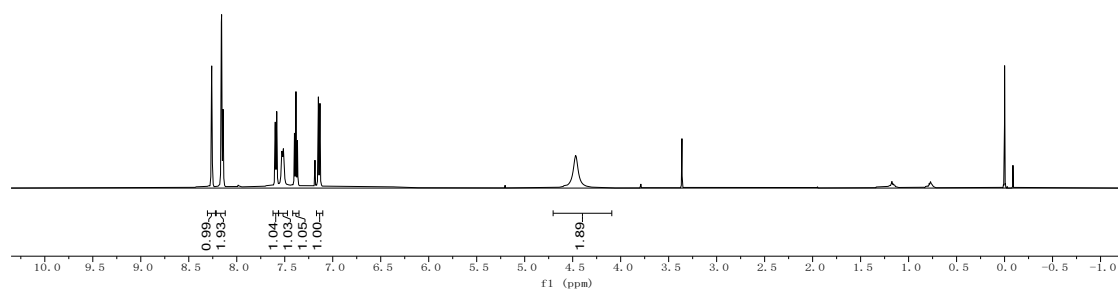
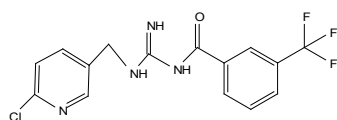
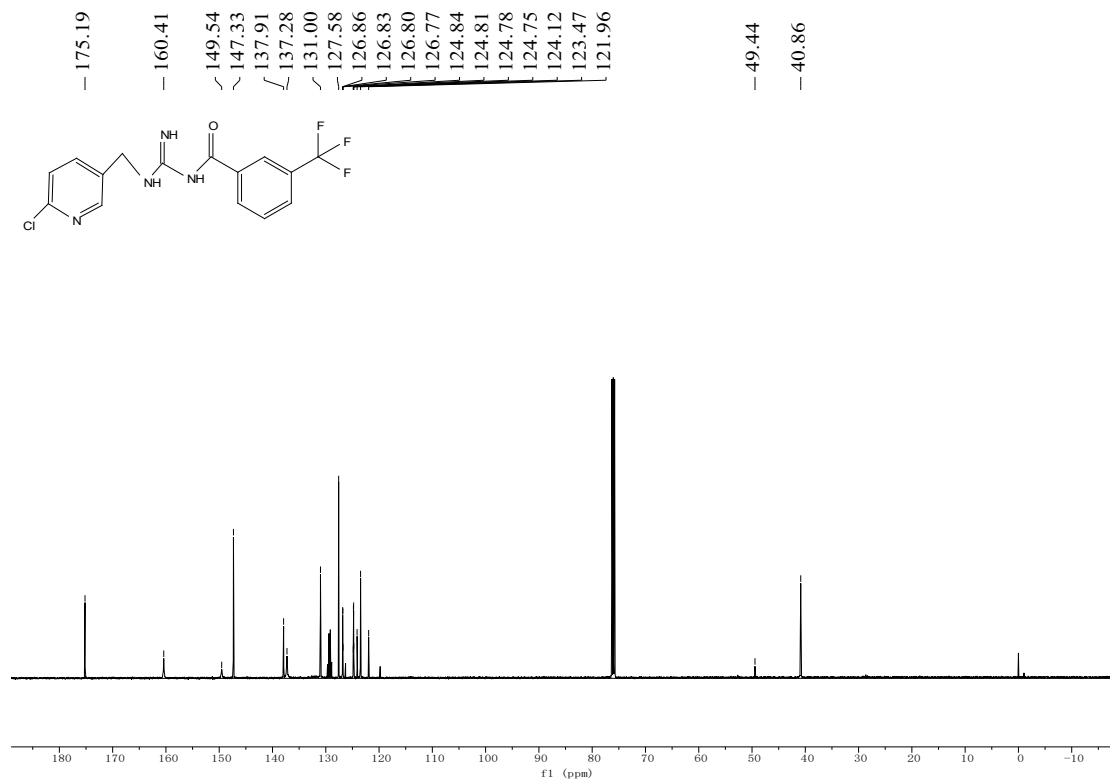


Fig S37.  $^1\text{H}$ ,  $^{13}\text{C}$  spectra of 7k





LJY-9 #57 RT: 0.57 AV: 1 NL: 1.10E10  
 T: FTMS + p ESI Full ms [170.0000-2500.0000]

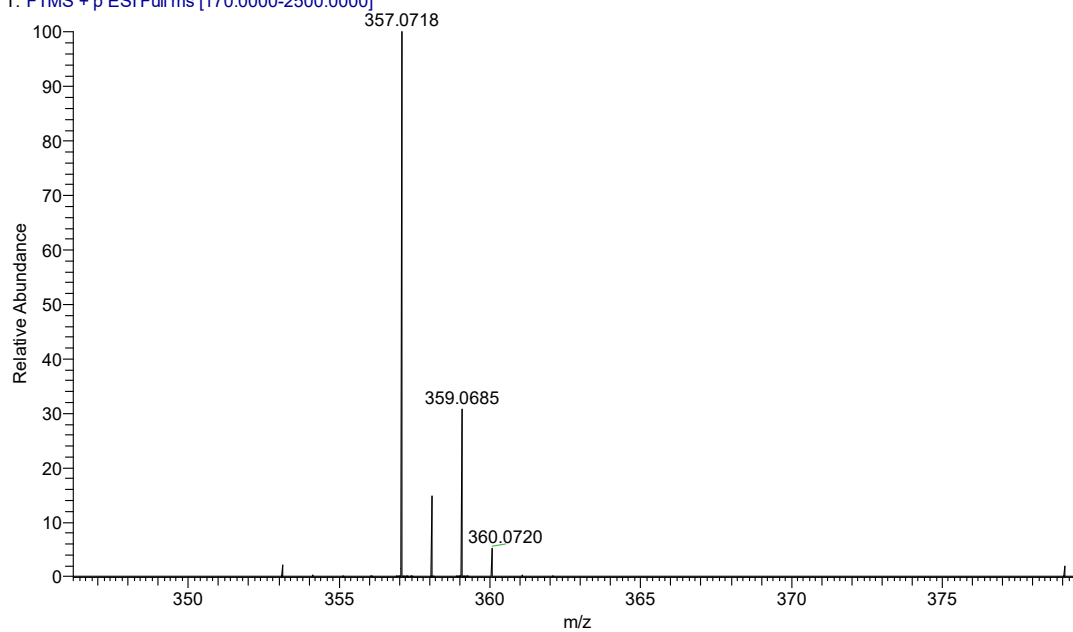
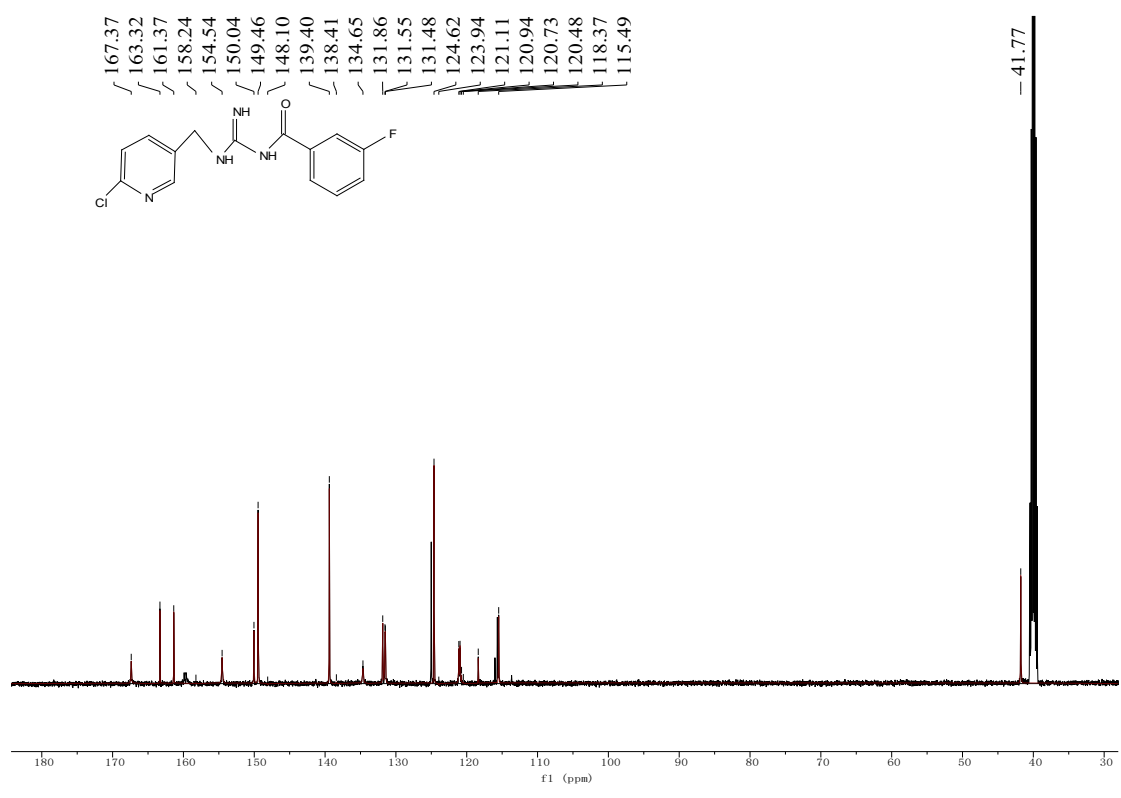
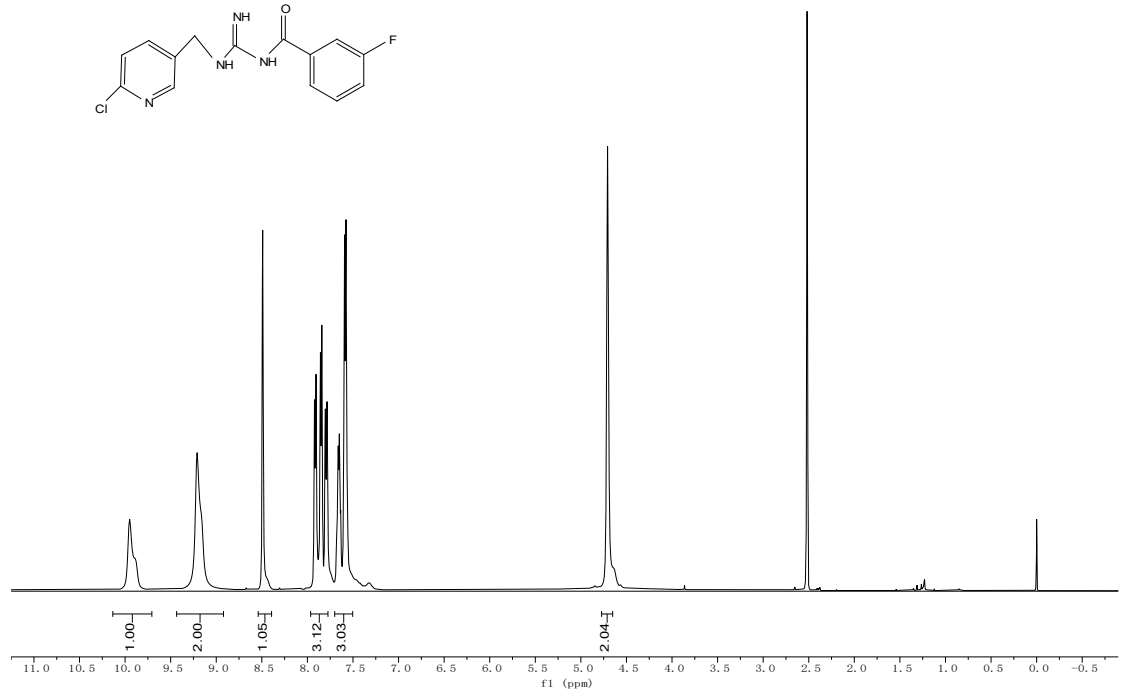


Fig S38.  $^1\text{H}$ ,  $^{13}\text{C}$  spectra of 71



LJY-13 #69 RT: 0.68 AV: 1 NL: 8.78E8  
T: FTMS + p ESI Full ms [170.0000-2500.0000]

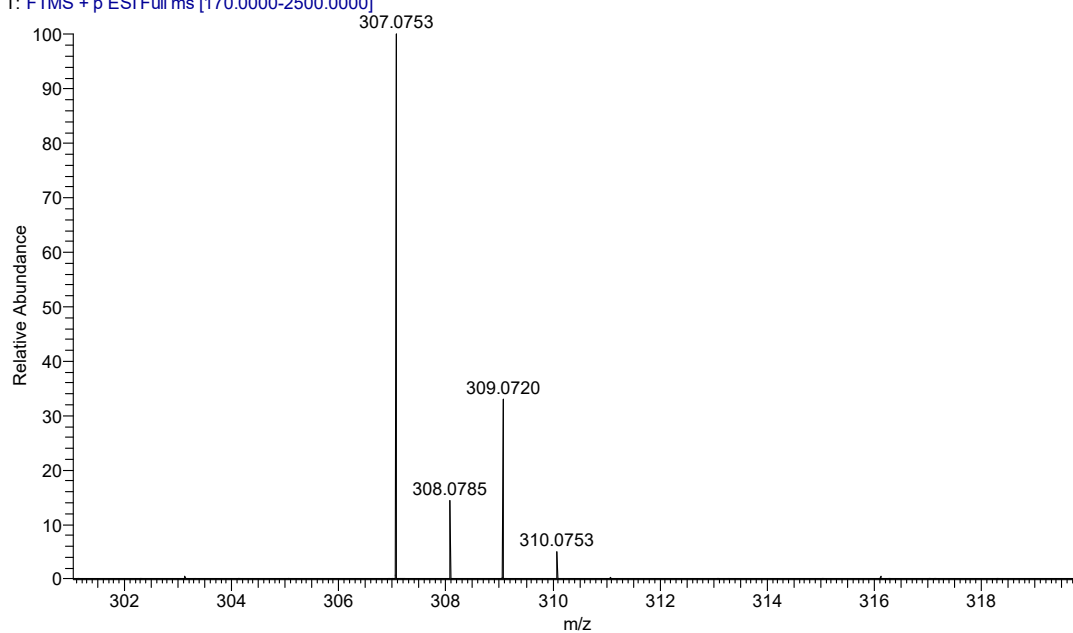
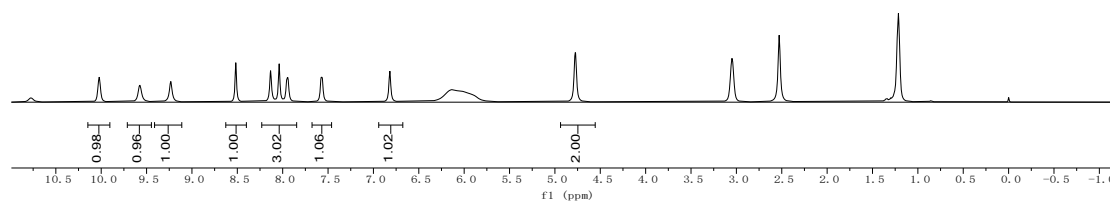
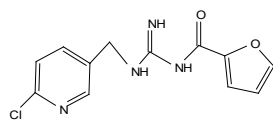
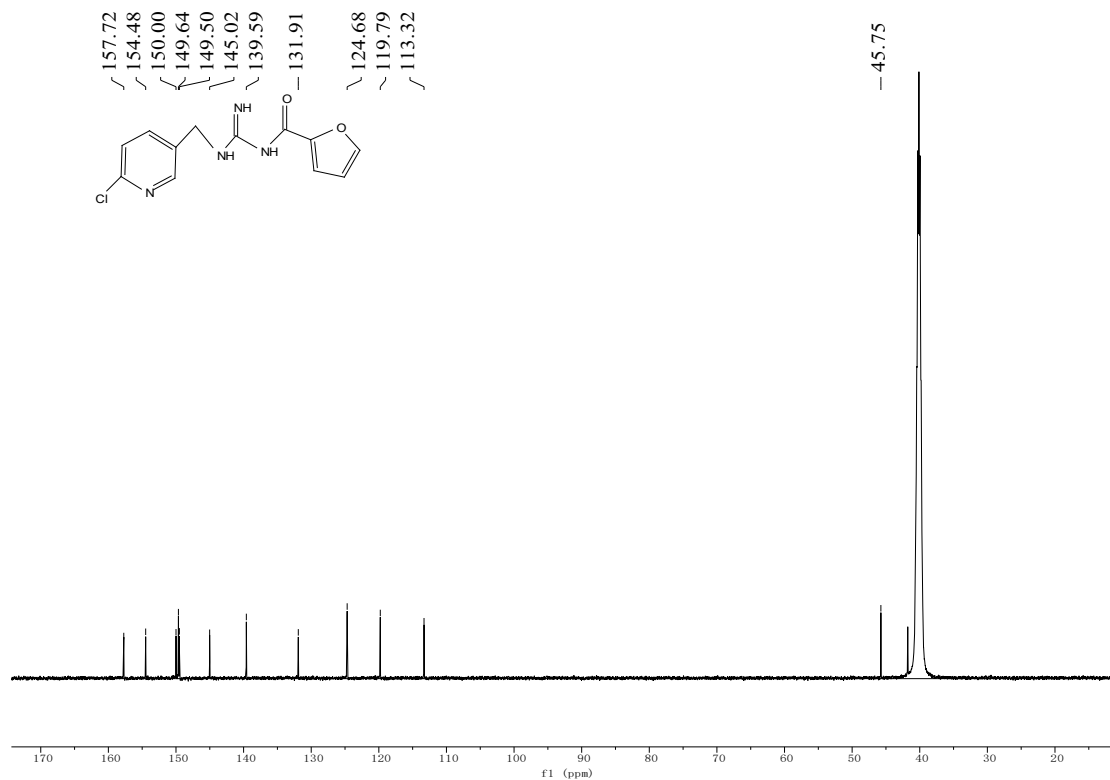


Fig S39.  $^1\text{H}$ ,  $^{13}\text{C}$  spectra of 7m





LJY-FN1

Pos\_LJY-FN1 249 (1.431) AM (Cen,4, 80.00, Ar,10000.0,0.00,0.00); Cm (249:251)

1: TOF MS ES+  
1.16e7

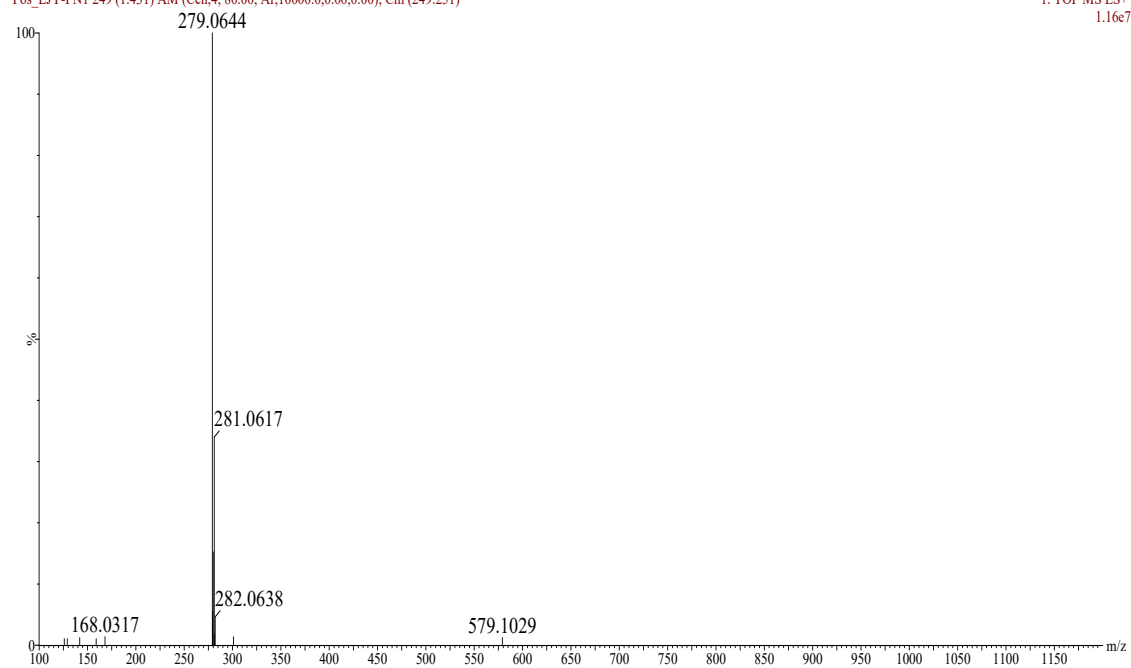
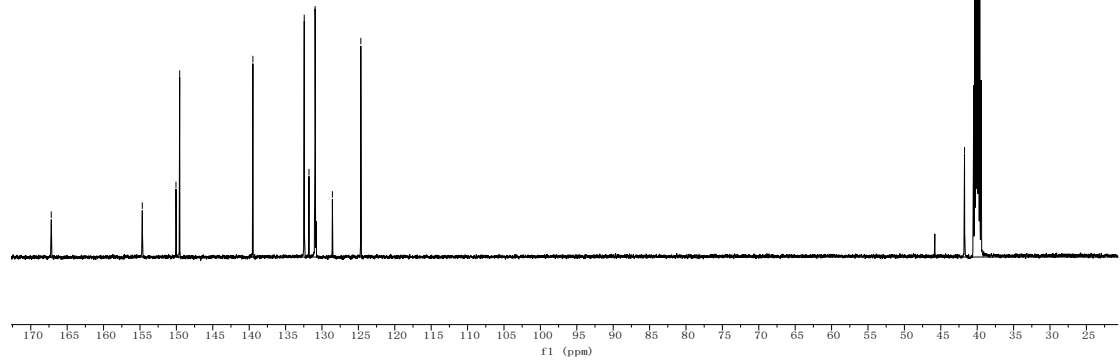
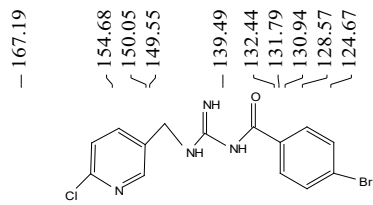
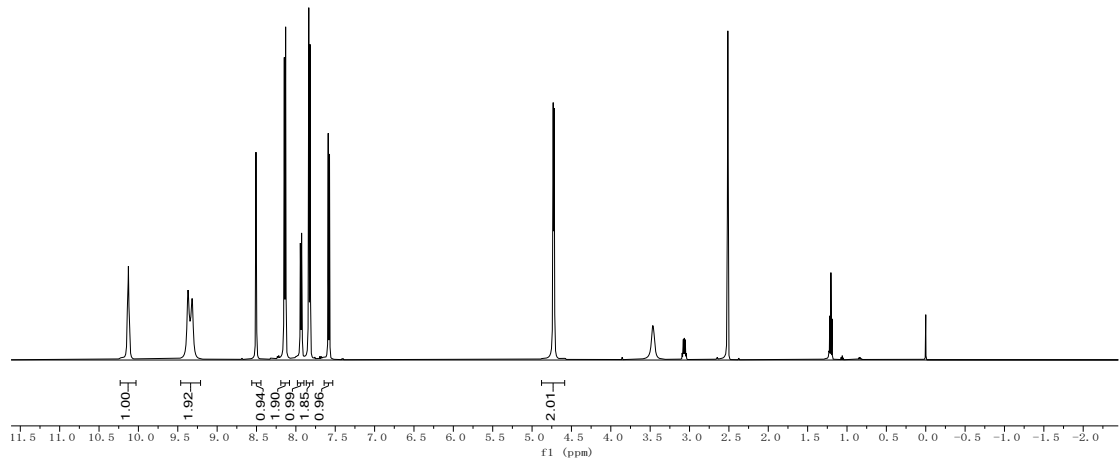
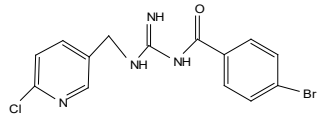


Fig S40. <sup>1</sup>H, <sup>13</sup>C spectra of 7n



LJY-BB

Pos\_LJY-BB 364 (2.061) AM (Cen:4, 80.00, Ar:10000.0,0.00,0.00); Cm (364:369)

1: TOF MS ES+  
6.90e6

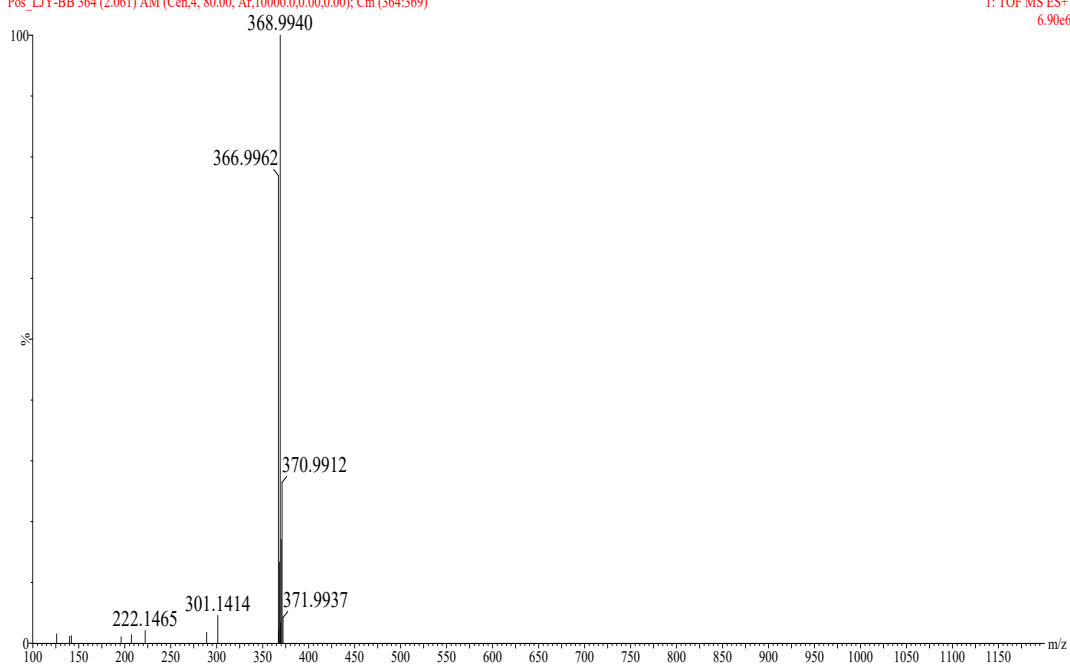
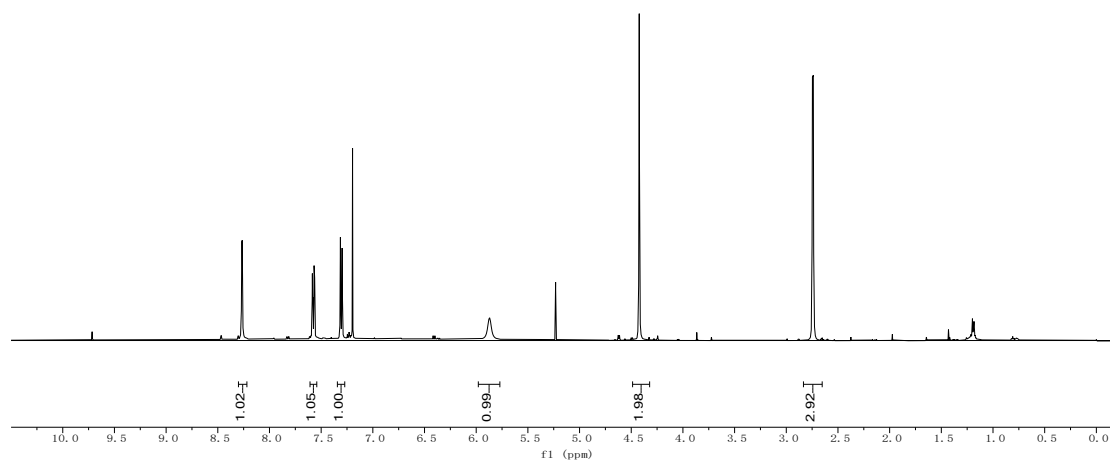
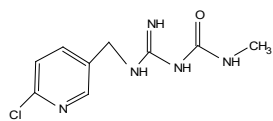
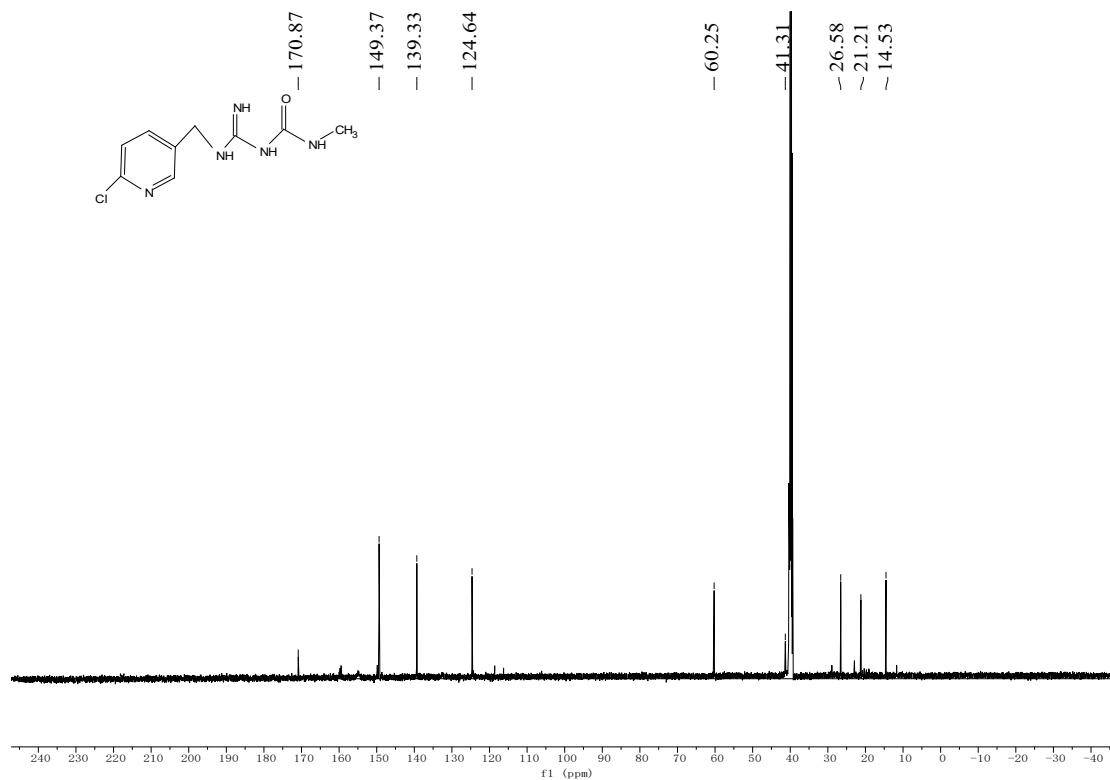


Fig S41.  $^1\text{H}$ ,  $^{13}\text{C}$  spectra of **7o**





LJY-16 #53 RT: 0.53 AV: 1 NL: 5.19E9  
T: FTMS + p ESI Full ms [170.0000-2500.0000]

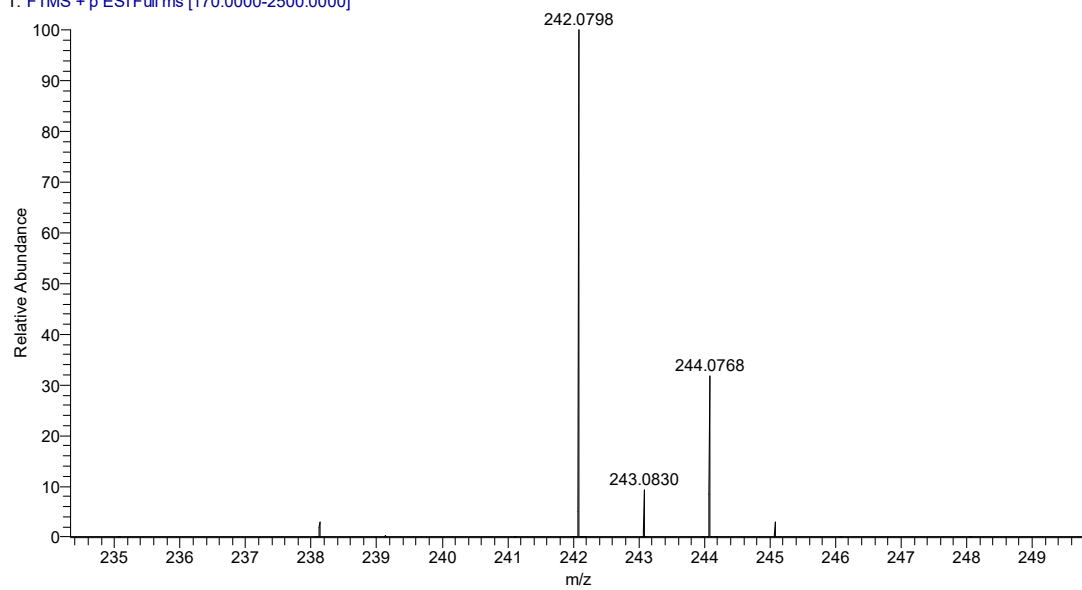
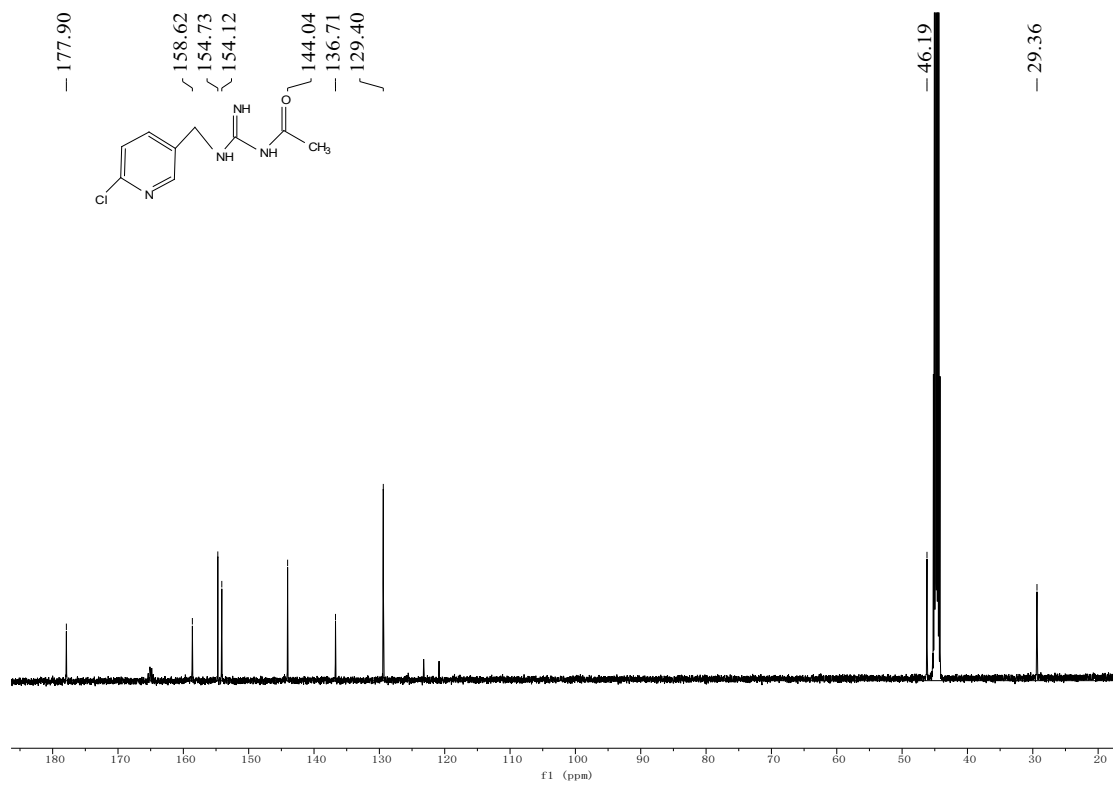
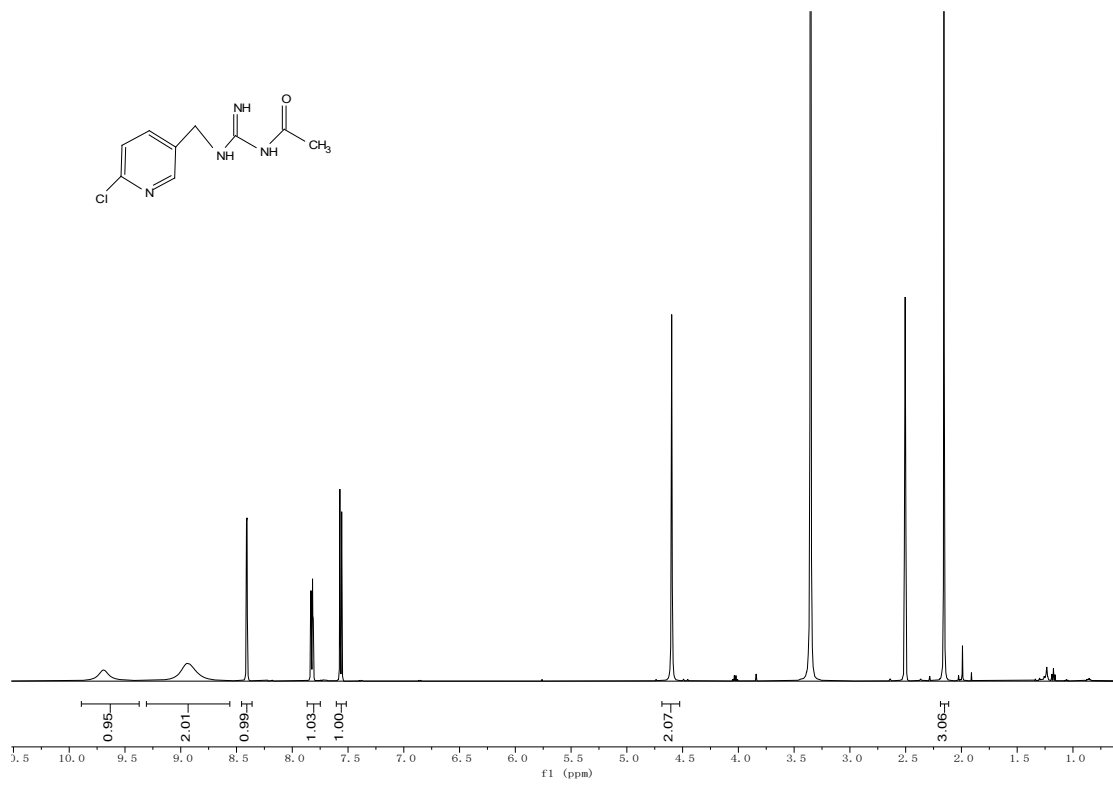


Fig S42.  $^1\text{H}$ ,  $^{13}\text{C}$  spectra of 7p





LJY-6 #55 RT: 0.54 AV: 1 NL: 4.15E9  
T: FTMS + p ESI Full ms [170.0000-2500.0000]

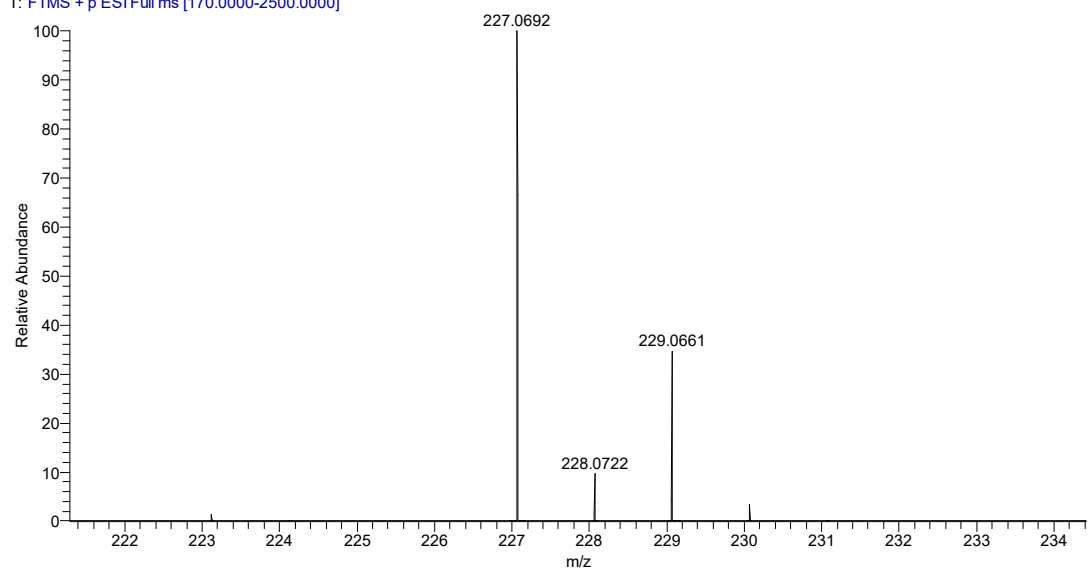
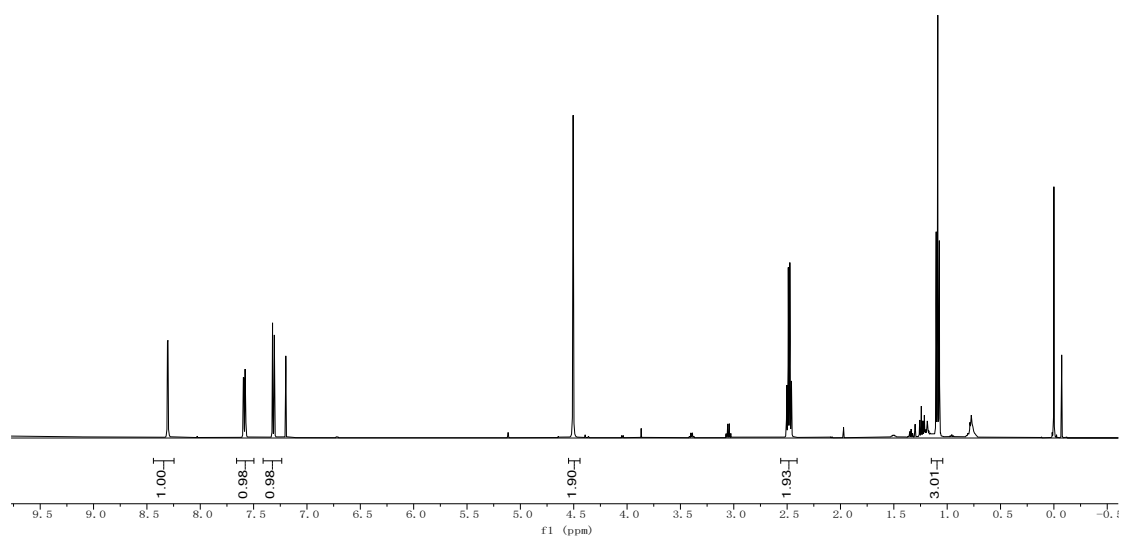
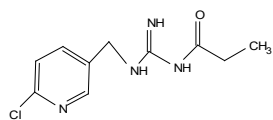
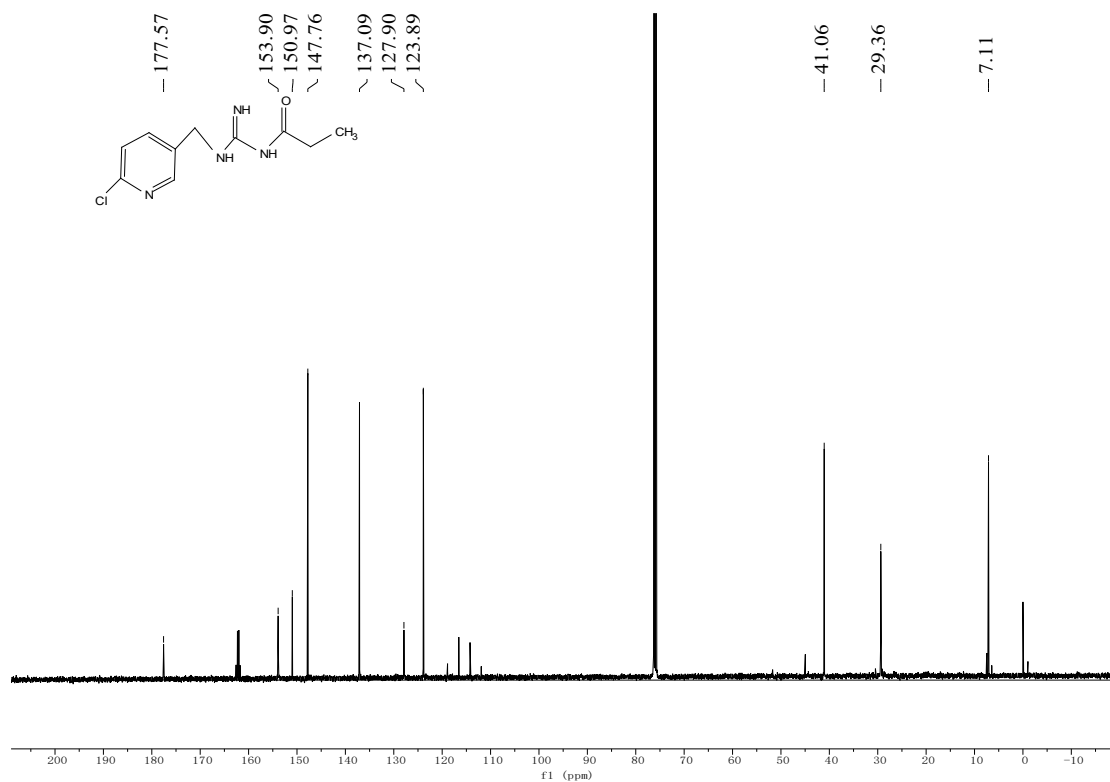
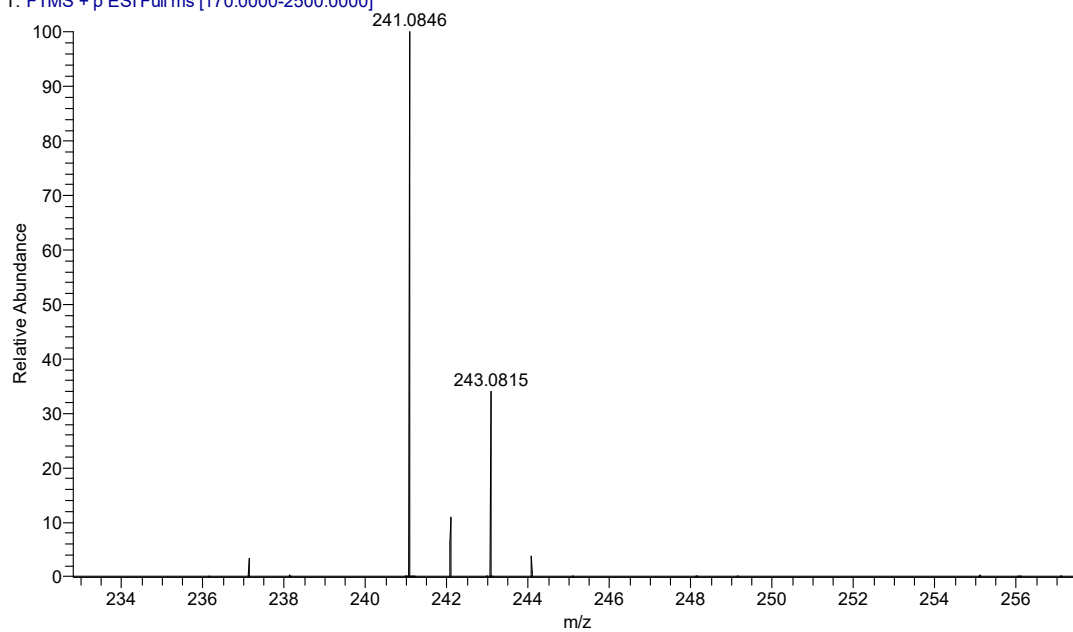


Fig S43.  $^1\text{H}$ ,  $^{13}\text{C}$  spectra of 7q

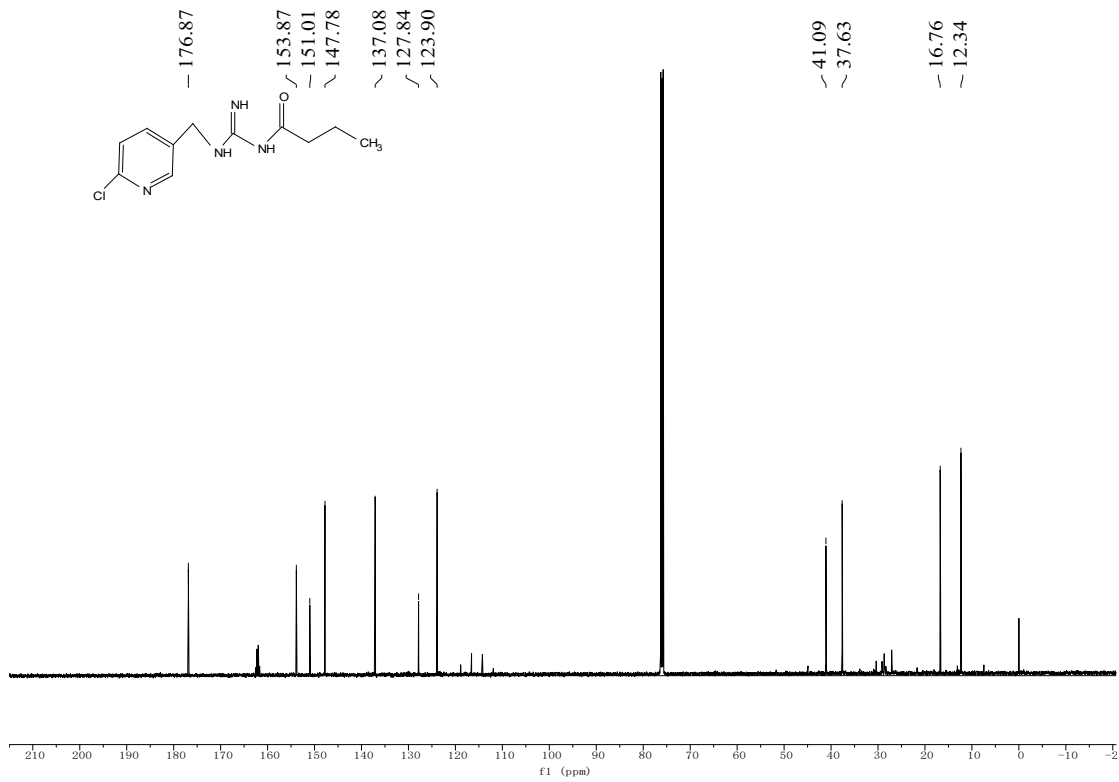
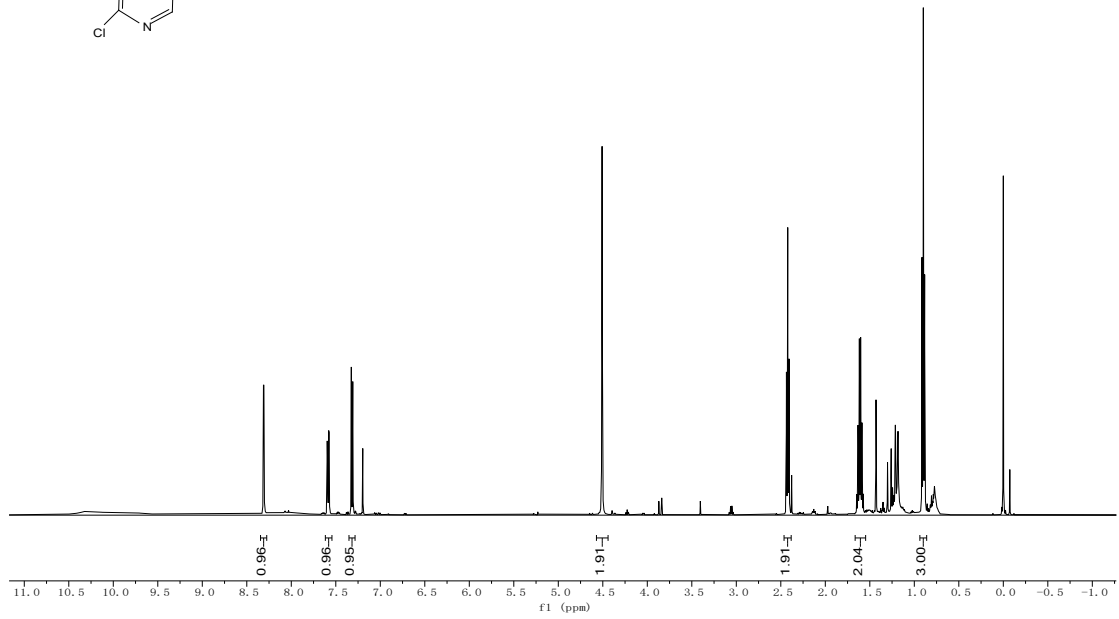
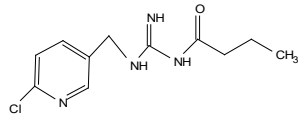




LJY-7 #55 RT: 0.55 AV: 1 NL: 4.18E9  
 T: FTMS + p ESI Full ms [170.0000-2500.0000]



**Fig S44.** <sup>1</sup>H, <sup>13</sup>C spectra of **7r**



LJY-8 #55 RT: 0.55 AV: 1 NL: 4.97E9  
T: FTMS + p ESI Full ms [170.0000-2500.0000]

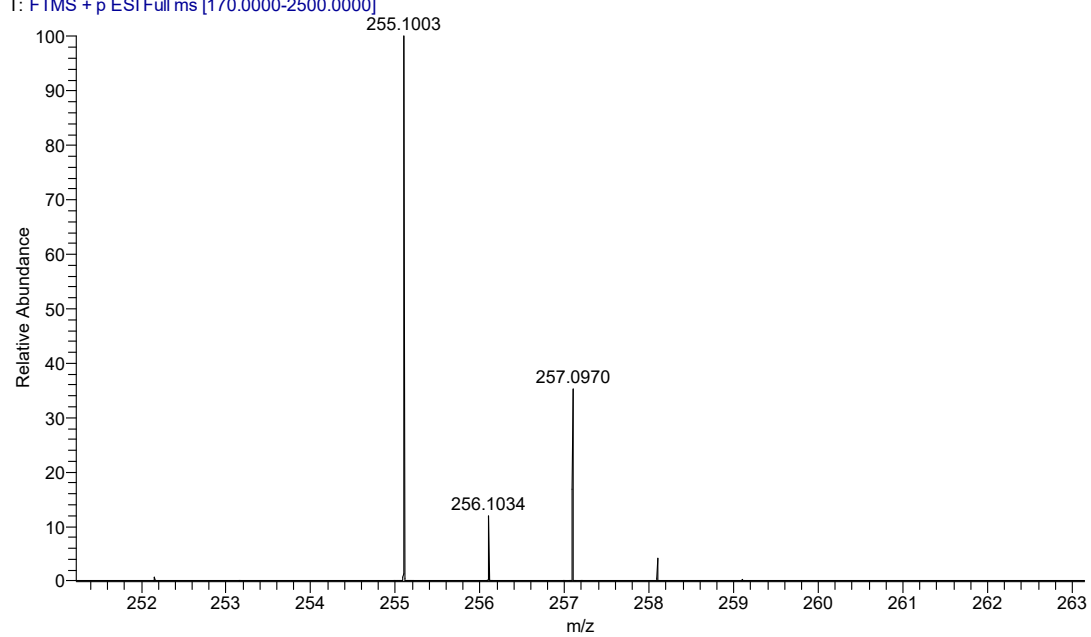
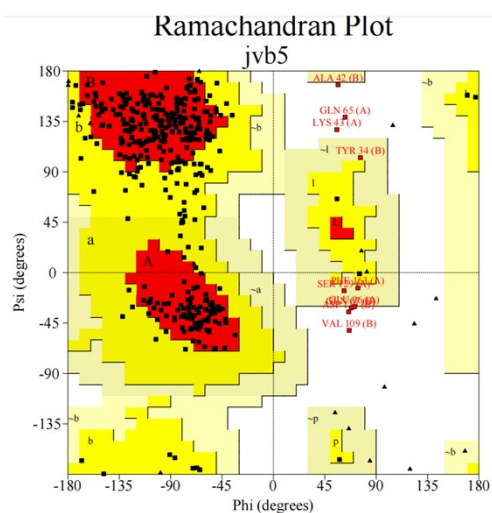
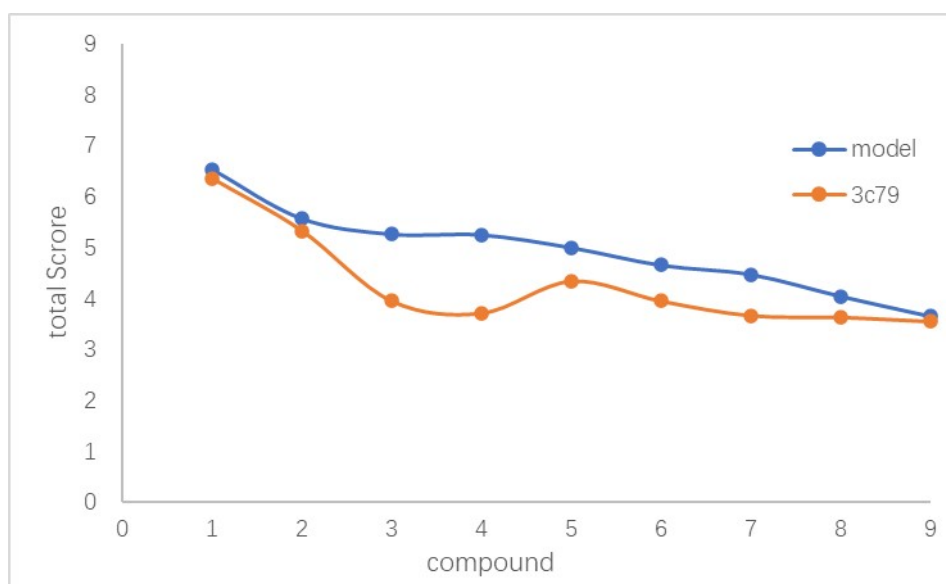


Fig S45.  $^1\text{H}$ ,  $^{13}\text{C}$  spectra of **7s**



**Fig S46.** The Ramachandran Plot to modelled proteins.



**Fig S47.** Scoring evaluation of commercial neonicotinoid insecticides with modeled proteins and 3C79(Compound name is consistent with **Table S1**)



**Fig S48.** Symptoms of *P. xylostella* larvae after 72 h treatment with DMSO and compounds **7a**,

**7i** at 30 mg/L.

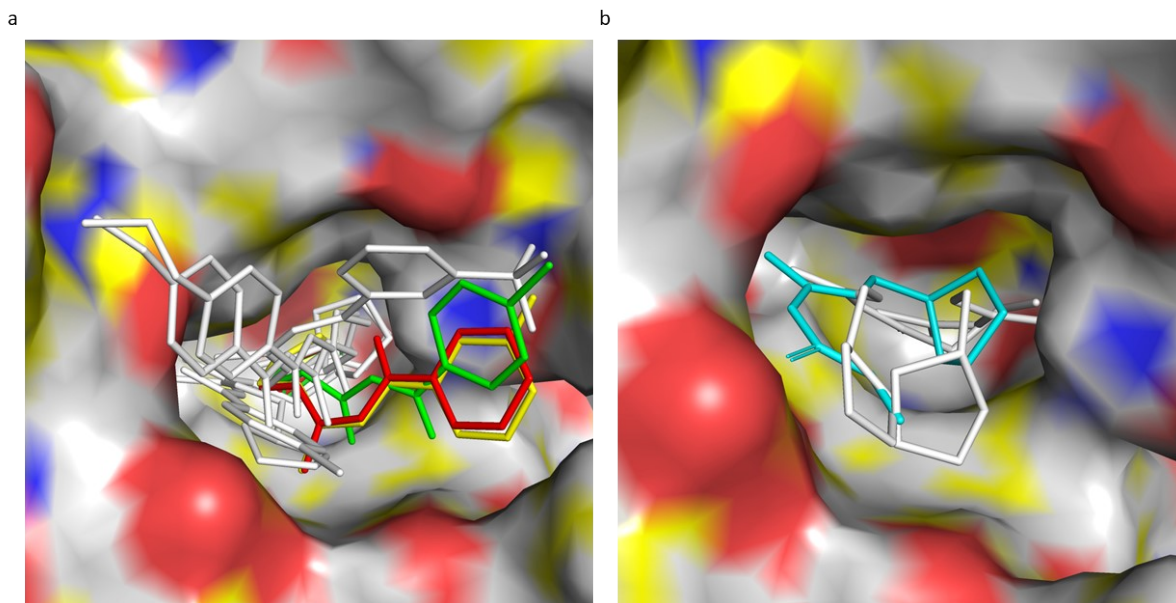


**Fig S49.** Stacked docking configurations of compounds **7a-k**. (a) Stacked docking configuration of compounds **a-h**, where **7a** is in red, **7d** is in green and **7e** is in yellow. (a) Stacked docking configuration of compounds **7i-k**, where **7i** is in blue.

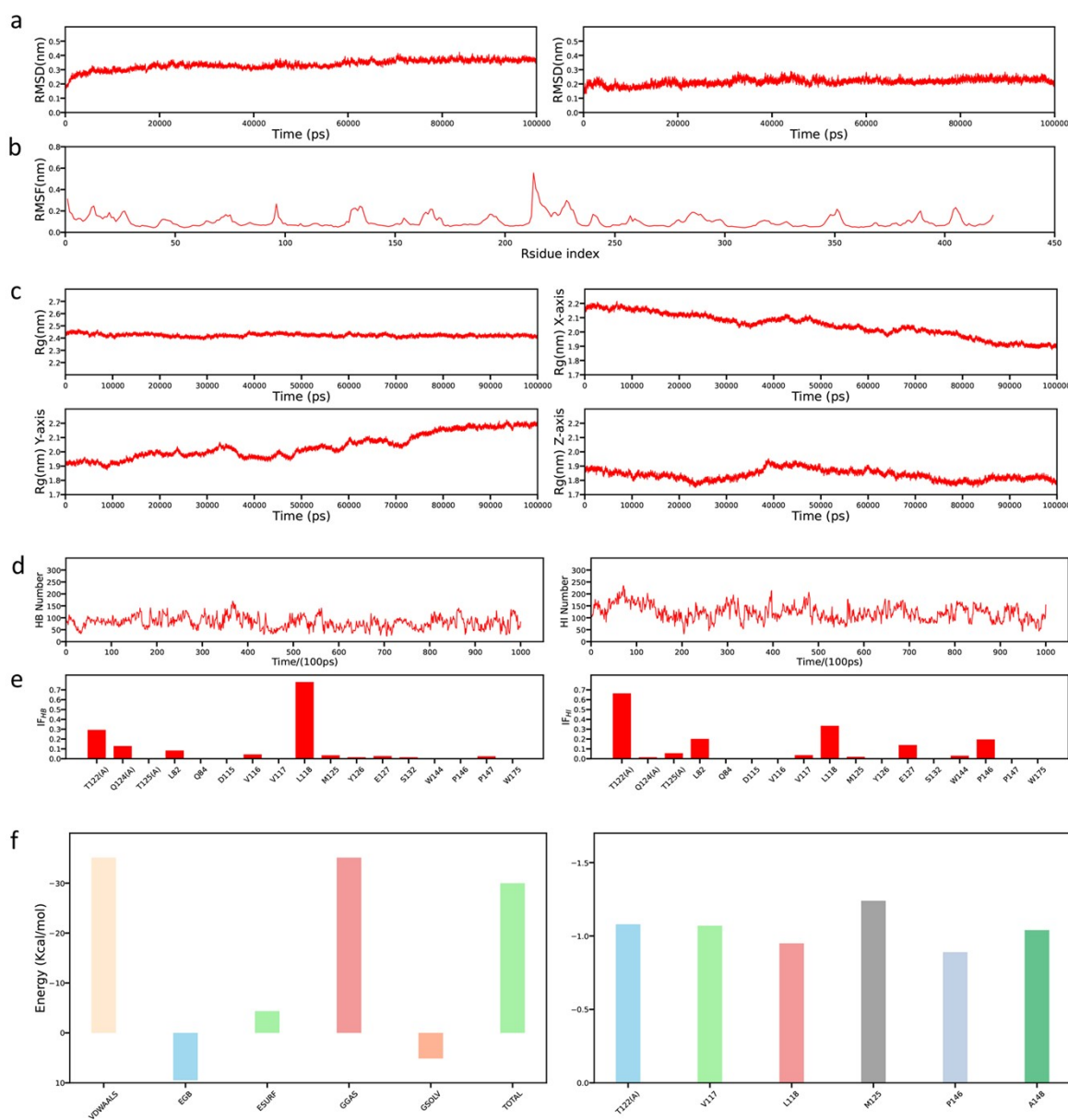


**Fig S50.** MD simulation analysis of compound 7e. (a) RMSD of the **7e** bound protein complexes over 100 ns MD simulations where the Y-axis represents RMSD value the X-axis represents the Time (PS). (b) RMSF changes of the proteins during 100 ns MD simulations. the Y-axis represents the RMSF value the X-axis represents the Residue index. (c) The four plots show the changes in overall protein Rg, X-axis Rg, Y-axis Rg, and Z-axis Rg during the 100 ns MD simulation. (d) Hydrogen Bond and Hydrophobic Interactions Formed by **7e** During 100 ns MD Simulation. (e) the H-bond (HB) and hydrophobic (HI) interaction fractions (IF) of the Inhibitors with protein during the last 50 ns MD Simulation. (f) Analysis of the Binding Free Energy Components and Residue Energy Decomposition for the **7e** Complexes with the Protein.



**Table S1.** Scoring evaluation of commercial neonicotinoid insecticides with modeled proteins and 3C79

NO	compound	model	3c79
1	Guadipyr	6.5352	6.3547
2	Nitenpyram	5.5692	5.3343
3	Dinotefuran	5.2625	3.9597
4	Thiamcthoxam	5.2486	3.7184
5	Cycloxaprid	4.9989	4.3421
6	Imidaclothiz	4.6569	3.9542
7	Acetamprid	4.4749	3.6701
8	Clothianiain	4.0503	3.6370
9	Sulfoxaflor	3.6582	3.5545